Analysis on division patterns and transcriptional activity in embryos from medaka "*Oryzias latipes*" before the midblastula transition

Dissertation zur Erlangung des naturwissenschaftlichen Doktorgrades der Bayerischen Julius-Maximilians-Universität Würzburg

Vorgelegt von

Michael Kräußling

Würzburg 2011

Eingereicht am: .....

Mitglieder der Promotionskommission:

Vorsitzender: .....

Gutachter: .....

Gutachter: .....

Tag des Promotionskolloquiums: .....

Doktorurkunde ausgehändigt am: .....

Ehrenwörtliche Erklärung

Hiermit erkläre ich ehrenwörtlich, dass die vorliegende Arbeit von mir selbständig und unter Verwendung der angegebenen Quellen und Hilfsmittel angefertigt wurde. Weiterhin habe ich noch keinen Promotionsversuch unternommen, oder diese Dissertation in gleicher oder ähnlicher Form in einem anderen Prüfungsverfahren vorgelegt

Würzburg, den

.....

Michael Kräußling

Table of contents

1. Introduction

1.1. Cleavage phase in embryos from zebrafish and medaka

Embryogenesis is the process of differentiation and maturation of an organism. It begins with fertilization and ends with hatching or birth, respectively. Furthermore, it involves different cellular events like proliferation, differentiation and maturation and it is initiated by the formation of a zygote upon fertilization of the egg. The cleavage follows directly on fertilization and egg activation. It is a sequence of cell divisions that subdivide the egg into a cluster of blastomeres without significant growth.

The cleavage can be either total, which means it completely divides the whole egg (holoblastic), or partial, dividing just the cells of the egg and leaving the yolk untouched (meroblastic). The meroblastic cleavage is typical for eggs that contain a large amount of yolk. Furthermore, it can be sub-divided into a superficial and discoidal form of the meroblastic cleavage.

Cells in superficial cleavages undergo a normal karyokinesis, but lack cytokinesis. This produces a polynuclear cell. The discoidal form instead cleaves the cell, separating nuclei and cell membranes, but does not penetrate the yolk and leaving it untouched.

The meroblastic discoidal cleavage is the typical cleavage form for fish, for example for *Danio rerio* (zebrafish) and *Oryzias latipes* (medaka). Here, the initial cell sits on top of the yolk, first as a small yolk-free region, and later as a multicellular blastodisc [1][2]. But although both species share the same general cleavage type, they also show some remarkable differences in cleavage occurrence and progression. For example, both species differ in their cleavage-timing. In zebrafish, the first cell forms within 10 minutes after fertilization and is cleaved about 30 minutes later. The subsequent cleavages occur in 15-minute intervals [1]. However, the formation of the first cell in medaka needs more time and takes about 1 hour. The subsequent cleavages also occur in a longer interval of 35- to 40-minutes between each division [2]. The first cleavages in both species progress highly synchronously and

symmetrically, either parallel or right-angled to the first cleavage, but differ in their spatial progression in later cleavages. During the first half of the cleavage phase, the symmetric cleavages separate the initial cell into symmetric and bilateral rows of blastomeres. At the 16-cell stages, the cells in zebrafish are still arranged in symmetric rows and they stay symmetric until the 128-cell stage. The cells in medaka embryos at the 16-cell stage instead are already in a more roundish orientation, as a precursor of the blastodisc that is about to be established in both species during the second half of the cleavage phase [1][2].

A further, and more important, difference between the cleavages of zebrafish and medaka is the fact that the cleavage in medaka totally divides the blastomeres, whereas cleavages in zebrafish only partially cut the cells. This leaves cytoplasmic bridges between the cells and the yolk. Only during the cleavage to the 16-cell stage are the first cells completely separated from the yolk [1].

The cleavage phase in both species ends with the occurrence of the first asynchronous cell divisions. For zebrafish, this event was determined to happen during cycle 10, at a high blastula stage containing about 1000 cells [1], and for medaka after the 13^{th} cycle at a late blastula stage of about 4000 cells [2]. Shortly after cleavage phase, embryos enter gastrulation, a time period of massive cell migration and reorganizations at which the three germ layers are formed by a combination of cell migration, ingression and invagination. Gastrulation again is followed by organogenesis. The fundamental body structures are determined and the organs are formed by cells from the three germ layers. In some cases, cells have to migrate over long distances to reach their determined destinations and several organs contain cells from more than on germ layer. The medaka larva hatches after a total of 9 days of development and reaches sexual maturity 6 to 8 weeks later [2][3].

A schematically illustration of the life cycle of medaka, as this is the model organism was the subject of investigations of this thesis, is shown in Figure 1.

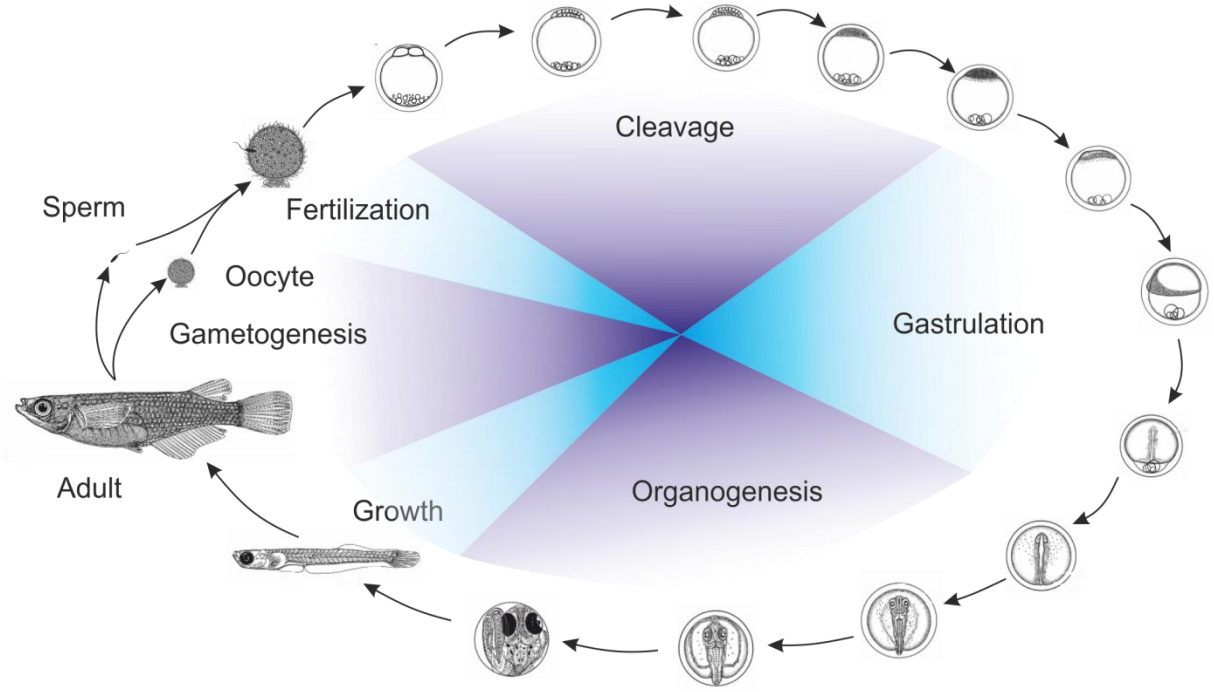

Figure 1: Schematic overview of the life cycle of medaka. Cleavage phase ends after growing for 10h20min at 26°C. Gastrulation ends 25hours post fertilization (hpf). The larva hatches after about 9 days and reaches sexual maturity about 6 to 8 weeks after hatching. Embryo sits on top of the yolk during cleavage phase (Data from Iwamatsu [2][4], Figure is a modification from Iwamatsu [2] and Gilbert [5]).

1.2. Biological function of the cleavage phase

Embryogenesis can occur either oviparous, with little or no embryonic development inside the mother, or viviparous, with the complete embryonic development inside the mother.

Eggs of oviparous organism, like frog, fly and fish, are often confronted with the challenge to fend for themselves from the time point of egg deposition until hatching. More precisely, the eggs have to produce a larva with just the reserves that were supplied within the egg during oogenesis without having access to other sources of supply. Also, those embryos often lack the protection of a parent animal and are at the mercy of the environment and predators.

To overcome these challenges, evolution has developed two simple strategies that are found in many oviparous species:

First one is the production of relatively large eggs that provide all the supply that is needed to develop a hatchling out of a single cell without further supply from outside [6]. This includes nutrients for the entire developmental process as well as maternally encoded gene products

and cytoplasmic components that supply the zygote with the necessary factors during the first rounds of cell divisions.

The second strategy is a fast embryogenesis and hatching at the fastest possible speed.

In mammals, which belong to viviparous organisms, the egg is confronted with a different situation. Here, the egg has to take advantage of the nutrient-rich uterus in which the embryo develops until birth. For this, the embryo develops a machinery of extraembryonic tissues that interact with the uterus and transport nutrients to the embryo. This kind of support makes it obsolete to supply the egg with the extensive amounts of maternal factors deposited in the eggs of oviparous species. Furthermore, the protective environment inside the uterus also allows a more leisurely pace of development that is mainly based on the zygotic production of components.

1.3. Features of the cleavage phase

Embryogenesis has been studied at different scales in different model systems, but especially in *Caenorhabditis elegans* (roundworm), *Drosophila* and *Xenopus laevis* (clawed frog) as well as *Danio rerio* (zebrafish). The data from these species have formed a general concept about the processes and events during cleavage phase in oviparous species.

Embryogenesis starts with a period of fast progressing, highly synchronous and transcriptional quiescent cell divisions with no cell migration. This period is generally called the cleavage phase and it has been reasoned that this phase of exponential cell number growth provides the amount of cells that is used as feeder for gastrulation and germ layer formation [7].

In most species, cell divisions during cleavage phase undergo normal karyokinesis, followed by a complete or nearly complete cytokinesis.

One explanation for how such fast cell cycles can be achieved is that the eggs are highly packed with maternal transcripts, proteins, nutrients and other factors that were stored in the egg during oogenesis. This supply makes it possible to run cellular processes in the absence of transcription of mRNAs from the zygotes genome.

Cell divisions during cleavage phase progress without cell growth between single divisions. In consequence, cells become progressively smaller with each division. This stands in contrast to normal somatic cell cycles where cells grow during the interphase to maintain a relatively constant cell volume [8].

Another factor that enables the fast progressing cell cycles is the relatively short S-phase. This is achieved by using more origins of DNA replication than for somatic cell cycles [9][10][11]. Also, cell cycles during cleavage phase only consist of M-phases and the relatively short S-phases. Both gap phases, the G1- and the G2-phases of the cell cycle are either very short or totally missing during cleavage [12][13][14][12][15]. With the lack of gap phases, cell cycles also lack checkpoint controls. Mitosis is usually followed by the G1-checkpoint that controls that cell division has proceeded correctly and that everything is ready for DNA replication at the subsequent S-phase. The S-phase again is followed by the G2-checkpoint that controls whether DNA replication has completed correctly and that everything is ready for mitosis [16]. These checkpoint controls are missing in early embryos of *Drosophila* and *Xenopus* and support the fast progression through the cell cycle [17][18][19].

The cleavage phase of *Drosophila*, *Xenopus* and zebrafish ends with a transition that is followed by the onset of gastrulation. During this transition, cell cycle lengthens, cell divisions become highly asynchronous, the cells gain motility and transcription of the zygotic genome is highly increased [20]. Finally, embryos enter gastrulation after they passed through these changes.

The exact temporal duration or number of cell divisions for how long the cleavage phase lasts differs between species. For *Drosophila*, cleavage phase lasts for 10 cell cycles until cell

cycle lengthening begins [21][22][23], 12 cycles for *Xenopus* [13][24][25] and 10 cycles for zebrafish [20][1].

1.4. The midblastula transition and maternal-to-zygotic transition

The time point at which cleavage phase ends and the fundamental changes, the cell cycle lengthening, desynchronisation, and transcriptional activation, occur, was named the "midblastula transition" (MBT). This term was originally coined by the work of Jacques Lefresne and Jacque Signore and their accurate description of the cleavage phase in axolotl [26]. After MBT, maternal factors have lost the control over the embryo's developmental fate, which now lies with the zygotic [27]. Shortly after MBT, embryos enter gastrulation.

However, the majority of these data was obtained from *Drosophila* and *Xenopus,* but several aspects were confirmed for other species, especially *C.elegans,* sea urchins and zebrafish as well. These observations in other species are far less detailed, but support the key data from *Drosophila* and *Xenopus*: the fast cell cycle speed at the beginning of cleavage, the decrease of cell size during cleavage, the transition from synchronous to more asynchronous divisions and the relative transcriptional quiescence.

For example, the desynchronisation and cell cycle lengthening to the end of cleavage phase has been shown for numerous different species: *Rana.temporaria* (Amphibia) [28], *Ciona.intestinalis* (Ascidiacea) [29], *Bufo.vulgaris* (Amphibia) [30], Misgurnus.fossilis (Actinopterygii) [31], loach (Actinopteriygii) [32], sea urchin (Echioidea) [33], *Ambystoma.mexicanum* (Amphibia) [34][35][36], and *Helobdella.triserialis* (Clitellata) [37].

Usually, this often observed cycle lengthening and desynchronisation at the late phase of the cleavage phase is taken as the mark for the beginning of MBT [20].

It is not perfectly clear why all these changes - the desynchronisation, cycle lengthening, cell motility, zygotic transcription - occur at the end of cleavage phase. It was argued that fast cell replication interferes with zygotic transcription, whereas cell cycle lengthening advances

transcription of zygotic genome [38][39]. Furthermore, a rapid succession of cell divisions is also incompatible with the aspects of cell movement [40][41]. In addition, it is supposed that a longer interphase and the introduction of gap phases provide time for cytoskeletal changes that enable cell movements upon gastrulation [7].

In this context, the term “maternal-to-zygotic transition” (MZT) is also used more and more often. But in contrast to the MBT, which is referring to a specific time point or a single cell cycle stage, the MZT describes processes that span a longer time period or several cell divisions, that usually also include the MBT. More precisely, MZT is used to describe the processes and events that hand over the developmental control of the embryo from maternal factors to the zygotic genome. This involves the processes that lead to degradation of maternal transcripts and proteins as well as the processes that initiate transcription of the zygotic genome, which is also called the zygotic genome activation (ZGA) [42].

1.5. Controlling the midblastula transition

A well established and approved hypothesis for how MBT timing is controlled is based on the nucleo-cytoplasmic ratio (N/C). It states that a repressor was stored in the egg during oogenesis and blocks the processes that lead to MBT-activation. This hypothetical factor is suggested to be titrated out by the increasing amount of chromatin during cell divisions, until it loses its repressing potential and MBT is initiated. This was hypothesized after observing that polyspermic embryos from *Xenopus* showed premature zygotic transcription which was early by two cell divisions [13].

The influence and controlling potential of the nucleo-cytoplasmic ratio has been verified extensively by different approaches for *Drosophila, Xenopus* and zebrafish:

Observations in haploid *Drosophila* eggs, which were derived from females homozygous for the female sterile mutation *maternal haploid* (*mh*) have demonstrated that cell cycle

lengthening occurs one cycle later than in normal diploid eggs. Furthermore, cellularization, the process at which plasma membranes are formed around the nuclei, separating the large syncytium into single cells, is also delayed by one cell cycle in haploid eggs [23].

MBT onset in *Xenopus* is not regulated by the number of cell divisions, which was demonstrated by cleavage-suppression with cytochalasin B. Although those embryos did not go through cytokinesis, the nucleo-cytoplasmic ratio in those embryos was unchanged nevertheless because the cytochalasin B treatment did not alter the rate of DNA replication. The amount DNA increased by every round of DNA replication into a large syncytium, and the timing of MBT initiation was thereby not changed in these embryos [13]. Blocking of RNA synthesis neither had influence on the cell cycle lengthening or desynchronisation in Xenopus [13]. MBT onset is also not regulated by the elapsed time, number of cell cleavages or DNA replications. This was demonstrated by blocking cell cleavage which led to syncytium-like Xenopus eggs in which cell cycle lengthening occurred at the same time as in untreated embryos. Moreover, alternating the cell volume by constricting the cytoplasm accelerated or delayed the onset [25]. More precisely, halving the cytoplasm resulted in early cell cycle lengthening by one cell cycle [43]. Also, constricting *Xenopus* eggs at the 1-cell stage and thereby reducing the cytoplasmic volume for the initial nuclei led to premature cycle lengthening in the progeny cells of this nucleus. Finally, a nucleus that migrated to the constricted side of the embryo produced cells that maintained rapid and synchronous divisions for two more rounds, demonstrating that MBT is not regulated by the number of cleavages [13][44]. Decreasing the cell volume by constricting the cytoplasm decreased the number of short and synchronous cell divisions [25].

In zebrafish cell cycle lengthening occurs one cycle earlier in tetraploid embryos and one cycle later in haploids, respectively [20]. Cell cycle desynchronisation and motility were also early or late by one cell cycle in tetraploid or haploid embryos, respectively. However, cycle lengthening is not controlled by the elapsed time or the total number of cell divisions, but by

nucleo-cytoplasmic ratio. This was demonstrated in experiments at which nuclei migrated into prior enucleated cells of the same embryo. Those cells maintained a rapid cell cycle for more cell divisions which were related to the cell volume [20]. Altogether, these data suggest that MBT starts in zebrafish at cycle 10 and is controlled by the nucleo-cytoplasmic ratio.

Different aspects of the N/C-ratio were also confirmed in other species like starfish [45], newt [43], or axolotl [26]. Overall, the different studies strengthen the hypothesis of a MBT that is controlled, whether directly or indirectly, by the nucleo-cytoplasmic.

1.6. Degradation of maternal factors and zygotic genome activation during MZT

The time period that covers the initiation of maternal factor degradation until the large scale initiation of zygotic transcription has been defined as the maternal-to-zygotic transcription (MZT).

Maternal transcripts guide the embryos' fate during the first rounds of rapid cell divisions. Before the cell cycle lengthens and the developmental control is handed over to the embryo, maternal transcripts are degraded. So far, the exact reasons for the degradation are unclear, but it has been suggested that the elimination of specific maternal mRNAs is required to prevent dosage defects upon zygotic transcription initiation. Furthermore, the elimination of ubiquitously distributed maternal mRNAs could be required for embryonic patterning. Alternatively, a gradual decrease of maternal transcript levels might be necessary to guide the gradual increase of the embryos cell cycle length [42].

The MZT consists of two general events, the degradation of maternal mRNAs and the activation of the zygotic genome [42].

The first event, the degradation of the maternal transcripts, is primarily contributed by maternal factors that are activated upon egg fertilization and enhanced by zygotic transcripts at later time points [42].

Gene expression profiling in *Drosophila* oocytes have demonstrated that about 55% of the *Drosophila's* genome are present as maternal transcripts [46]. From these maternal transcripts are about 20% destabilized upon egg activation, at which SMAUG (SMG) alone, a multifunctional posttranscriptional regulator, is responsible for the degradation of 2/3 of the mRNAs targeted upon egg activation [46]. In zebrafish, the microRNA miR-430 was demonstrated to be initially expressed at about 50% epiboly [47], an early gastrula stage, and being responsible for the subsequent degradation of over 750 maternal mRNAs of which more than 300 are direct targets of miR-430 [48].

The second event of the MZT is the activation of the zygotic genome which leads to the subsequent activation of transcription. As studies in *Drosophila* and zebrafish have shown, this process is no "all or nothing"-event at which the whole genome starts to be transcribed at once. Instead, the transcriptional activation occurs in waves of increasing degree at which different subsets of genes are transcribed. For *Drosophila*, the first wave of transcription occurs at cycle 8/9 and a second, larger wave at cycle 14 [15]. A similar observation was made for zebrafish in which a first wave of transcription occurred after cycle 6/7 and a second wave at the sphere stage of the blastula [49].

The mechanisms behind the activation of zygotic transcription are still poorly understood. However, different hypotheses on the regulation of the zygotic genome activation at MZT have been proposed. Those are the nucleo-cytoplasmic ratio, a maternal clock and transcriptional abortion [42].

The nucleo-cytoplasmic ratio model has already been shown to be most likely responsible for MBT regulation. It suggests that a maternal factor in the egg blocks zygotic genome activation and is titrated out with every cell division. This is supported by the fact that DNA, which is added to the egg, is transcribed for a short period after injection, but becomes deactivated shortly after injection, but becomes reactivated again upon ZGA. This demonstrates that proteins and factors of the transcription-machinery are already present and

fully functional in the fertilized egg. In turn, this also suggests that transcription is blocked on the DNA level [50]. The functional translation machinery for instance is used to inject in-vitro transcribed mRNAs into eggs at the 1-cell stage if pre-ZGA translation of a certain protein is needed.

However, the amount of added DNA has an influence on the ZGA timing and the ZGA can be initiated prematurely by increasing the amount of DNA content. Also, ZGA activation is not based on the exact number of cell divisions or rounds of DNA replications, nor on the time elapsed since fertilization, but it depends on reaching a critical ratio of DNA to cytoplasm. So the first detectable transcription in Xenopus is early by two cell divisions in polyspermic embryos and corresponding late in monispermic embryos [13].

Further support for the concept that the nucleo-cytoplasmic ratio is controlling the timing of ZGA comes from a zebrafish mutant, in which the chromosome segregation but not cell division is blocked. This segregation blocking in the zebrafish mutant leads to polyploid cells and an early transcription start by several cell cycles before wild type [51].

Although the influence of the nucleo-cytoplasmic ratio has been known for almost 30 years, relatively little is known about how the DNA in pre-MZT embryos is blocked for transcription and by which factors this transcription blockade is achieved.

However, it is known that DNA methylation near promoters or enhancer elements inactivates the respective gene [52][53][54] and that the DNA methylation is processed by the enzyme DNA methyltransferase, known as Dnmt1, that targets CpG pairs [55]. In this context, the *Xenopus* homolog of the mammalian Dnmt1, the xDnmt1, has been identified as a possible candidate for a dilutable repressing factor of zygotic transcription. Depletion of the maternal mRNA by antisense RNA led to hypomethylation of the genome and to premature zygotic transcription [56].

Furthermore, it has been shown that tramtrack (Ttk) is a dilutable repressing maternal factor that regulates the transcriptional initiation of a subset of early expressed genes in *Drosophila*

[15]. In *Drosophila*, the first waves of detectable zygotic transcripts appear after cycle 8. For Ttk has been shown that it is a repressor for the segmentation gene *fushi tarazu* (*ftz*) and *even-skipped* (*eve*) [57]. Alternations of the Ttk concentration in early Drosophila embryos resulted in a change of *ftz* expression timing [15]. This clearly demonstrated that Ttk specifically regulates the activation of transcription of specific genes in a concentration depending manner as it is guided by the nucleo-cytoplasmic ratio [15].

However, this kind of regulation could only be confirmed for a small subset of genes. The majority of genes in *Drosophila* seem to be regulated by the absolute time and developmental stage, and not by the nucleo-cytoplasmic ratio [58].

In consequence, a transcriptional regulation by the absolute developmental time was hypothesized in the model of a regulating maternal clock.

It has been shown for haploid embryos from *Drosophila* that the initiation of maternal transcript degradation is not depending on the DNA content, but on the elapsed time since fertilization or rather on the number of cell divisions [58]. However, expression level analysis showed that the timing of expression initiation of many genes changed from diploid to haploid embryos, arguing for the nucleo-cytoplasmic regulation model [23]. This is contradictory with the majority of the overall investigated zygotic genes in *Drosophila*. They showed the same transcription level at different time points in diploid and haploid embryos, arguing for a mechanism controlled by the time or number of cell cycles [58]. Also, the multifunctional posttranscriptional regulator SMAUG (SMG) is translated upon egg activation and is essential for the destabilization of most of the maternal transcripts [46] as well as for the numerous transcriptions upon zygotic genome activation [59]. Thereby, the degradation of maternal mRNAs could be regulated by SMG.

A third model that tries to explain the maternal-to-zygotic transition is the transcript-abortion model. It postulates that zygotic transcription is not present during early cleavage phase because the DNA replication machinery aborts transcription during the rapid progressing cell

cycles. This theory is strengthened by experiments in which the cell cycle was blocked. This led to subsequent premature zygotic genome activation during the extended interphase in *Drosophila* [39] and *Xenopus* [60]. Relatively large transcripts are aborted during mitosis [38] and smaller transcripts are enriched. This is confirmed by the fact that the first wave of transcripts in *Drosophila* embryos lacks introns and encodes small proteins and encode for proteins that are involved in degradation of maternal transcripts and the corresponding activation of zygotic transcription [61].

1.7. Aim of the thesis

The MBT and linked stages during animal embryogenesis were the targets for intense investigations over several decades. In consequence, the occurring changes in cell division, embryo morphology and transcriptional activity were well described, but still not fully understood. This is especially true for the mechanism that controls the onset of the MBT.

So far, the nucleo-cytoplasmic ratio has been demonstrated to be responsible for regulating cycle lengthening and desynchronisation at MBT onset. This is putatively achieved by a factor that was stored in the egg during oogenesis. It was hypothesized further that this hypothetical factor is titrated out by the ongoing cell divisions and the constantly increasing amount of DNA, although the nature of this factor and its mode of action were not identified until now [13][20].

In medaka so far the MBT was only investigated by determining the earliest time point during embryogenesis at which a certain subset of paternal transcripts could be detected. This was achieved by crossing two different inbred strains, which were obtained from two natural occurring medaka populations and that show polymorphisms for certain expressed sequence tag (EST) markers. In this study, it was observed that paternal ESTs are not transcribed before stage 11, an early-late blastula stage of around 2000-4000 cells, and the start of MBT in medaka was thereby determined to stage 11 [62].

The medaka fish represents a useful complementary model system that is comparable to zebrafish [4], which was used to verify the fundamental aspects of MBT for fish [20].

The aim of this thesis was to expand the knowledge of the processes that lead to MBT onset in general, and to obtain a better understanding of MBT activation in medaka in particular. For this, the timing of cell cycle desynchronisation was investigated by modern confocal microscopy techniques. Also, the exact cell volumes and their individual influence on MBT onset were subjects for investigation at single cell resolution.

Furthermore, the earliest time point for any zygotic transcriptional activation in medaka was aimed to be determined, since this has not yet been performed in a global, genome-wide manner.

Finally, previous work in the lab has revealed that STAT3 is translocated to the nucleus at specific stages before MBT in medaka embryos. Therefore it was interesting to investigate the influence of STAT3 on zygotic transcription and MBT regulation itself.

2. Results

In the literature, the cleavage phase is described as a sequence of rapid, synchronous and transcriptionally quiescent cell divisions. Cell cycle lengthening, desynchronisation as well as transcriptional activation of the zygotic genome at large scale occurs only at the initiating midblastula transition and in return, those events are taken as a sign for the beginning MBT [13][63][26][62]. Although numerous models try to explain the mechanism controlling MBT onset, the best established one suggests MBT regulation via the nucleo-cytoplasmic ratio [13][20][25].

2.1. Asynchronous cell divisions in early embryos

2.1.1. Confocal imaging of distinct developmental stages reveals cell cycle desynchronisation before MBT

In order to investigate the duration of synchronous cell divisions of even cycle lengths in pre-MBT medaka embryos, a confocal imaging approach was chosen instead of conventional light microscopy time lapse observations that have been usually used [20].

For this, medaka embryos at different time points between the 2-cell stage and the 512-cell stage were fixed in PFA. After physical preparation, DNA staining and mounting on a microscope slide, they were scanned under a confocal microscope. Subsequently, the raw data from the confocal scans were software processed and analyzed. This revealed that the cell cycle in early medaka embryos is only synchronous for the first 4 cell divisions during which the embryos develop from the 1-cell stage to the 16-cell stage. However, a minor temporal spacing could already be detected during cycle 4, the division from 8 to 16 cells, which might be taken as a first sign or indication for an upcoming cell cycle desynchronisation. The first clear temporal discrepancy is detectable during the next cycle, cycle 5, the division from 16 to 32 cells. Here, a clear temporal spacing by different ana-/telophase progression levels of the cell cycles between single cells within the same embryo could be observed. This

desynchronisation increased during the following cycles until total synchrony was lost at latest at cycle 7, 64 to 128 cells (Figure 2).

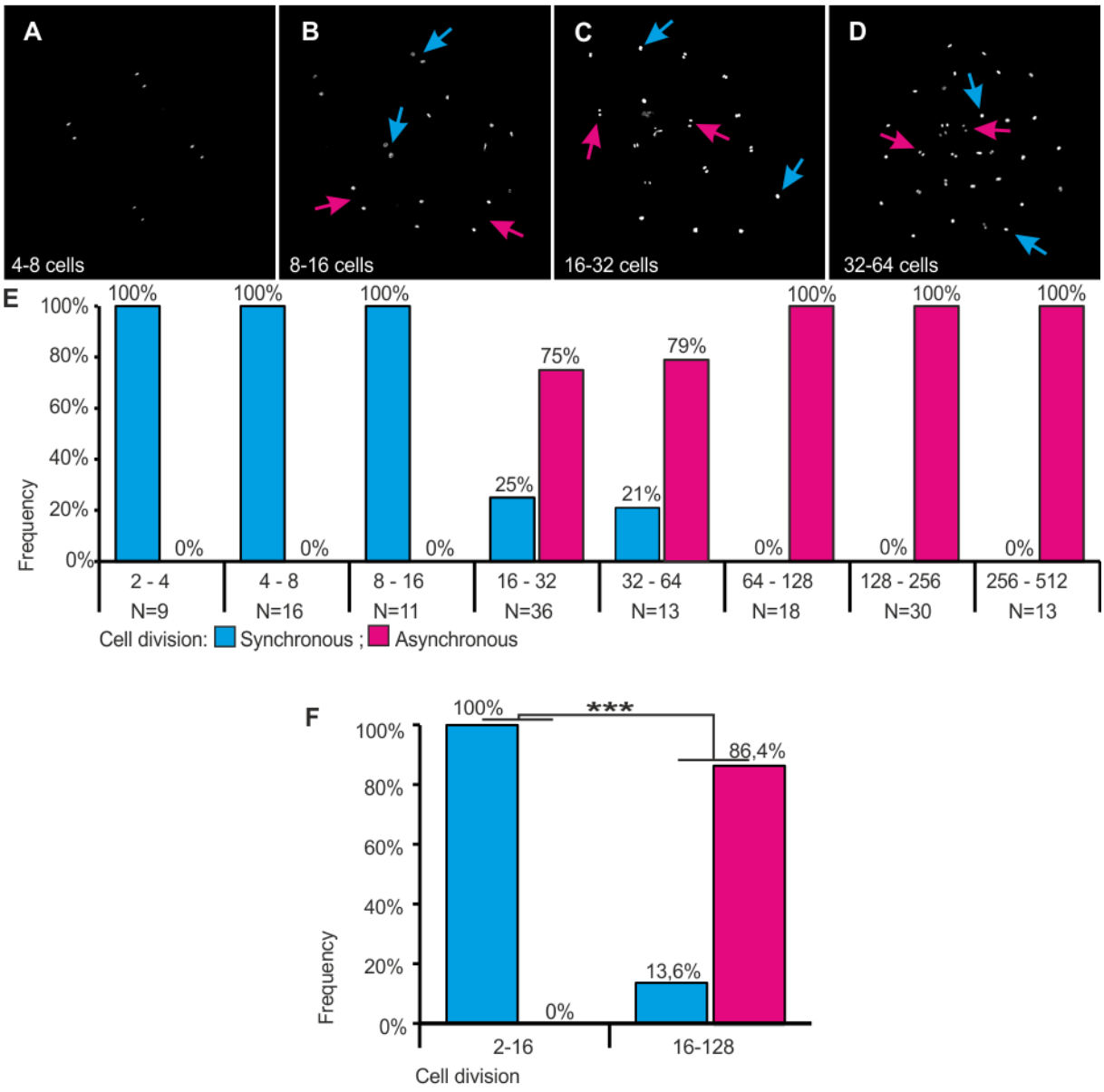

Figure 2: Progression from synchronous to asynchronous cell division in early medaka embryos. (A-D) Medaka embryos during the cell divisions 3 to 6. (A) Cell division is highly synchronous in embryos that divided from 4 to 8 cells. Cells are all in telophase (B) Cell division is synchronous in embryos at cell divisions 4, 8 to 16 cells. Cells are all in telophase. The daughter chromosomes in some cells are more apart from each other (Red arrows) than in other cells (Blue arrows). (C and D) At later divisions, cell cycles in embryos are asynchronous as some cells are still in interphase (Blue arrows) while other cells within the same embryo are already at late ana-/telophase of the cell cycle (Red arrows). (E) Progression of synchronous to asynchronous cell division from cell division 2 (2 to 4 cells) to cell division 9 (256 to 512 cells). Synchronous dividing embryos are represented by blue bars; asynchronous dividing embryos are represented by red bars. (F) Distribution of synchronous to asynchronous cell division in embryos between the 2- to 16-cell stages and between the 16- to 128-cell stages. Cell division is synchronous (Blue bars) until embryos have reached the 16-cell stage and asynchronous (Red bars) during the following cell divisions (Chi-square test, $p<0,001$) (Figure modified from Kraeussling et al. [64]).

However, instead of totally dividing randomly and with no clear structured division pattern after cycle 7 and during the following divisions until the end of cleavage phase, medaka embryos establish a specific and highly directed cell division pattern that is called "metasynchronous cell division". This term describes a division pattern in which cell divisions take place in guided intervals. The occurring cell divisions describe clear waves in which division starts first in cells at the center of the embryo and later, with a temporal delay in cells that are located more distant from the center and closer to the embryos' periphery.

Early embryos consist only of a small number of cells, and as a result of symmetric cleavages along the X-/Y-axis, these cells are usually arranged in a rectangular or elongated manner until the 16-cell stage. From the 32-cell stage onwards and until the initiation of gastrulation, the structure of the embryos becomes more and more rounded in the form of a multilayered disc.

Beginning with cycle 6, dividing from 32 to 64 cells, more and more embryos were found in which a temporal spacing of cell division initiation between cells at central, and more and more peripheral positioning were detected. This temporal spacing continuously increased during the following cell divisions. However, at the latest with division 8, while dividing from 128 to 256 cells, the spacing has reached a level and extend at which the metasynchronous cell division wave was clearly detectable. Mitosis is initiated first central positioned cells and later in peripheral cells. More precisely, in the early phase of division 8, the very central cells were already at late ana-/ or telophases, whereas the peripheral cells were still clearly at interphase stage. At the late phase of division 8, central cells had completed mitoses and proceeded to interphase stage, whereas peripheral cells were still in mitotic phases (Figure 3). The metasynchronous division pattern was maintained until the onset of MBT when cell cycle lengthens and synchrony is lost.

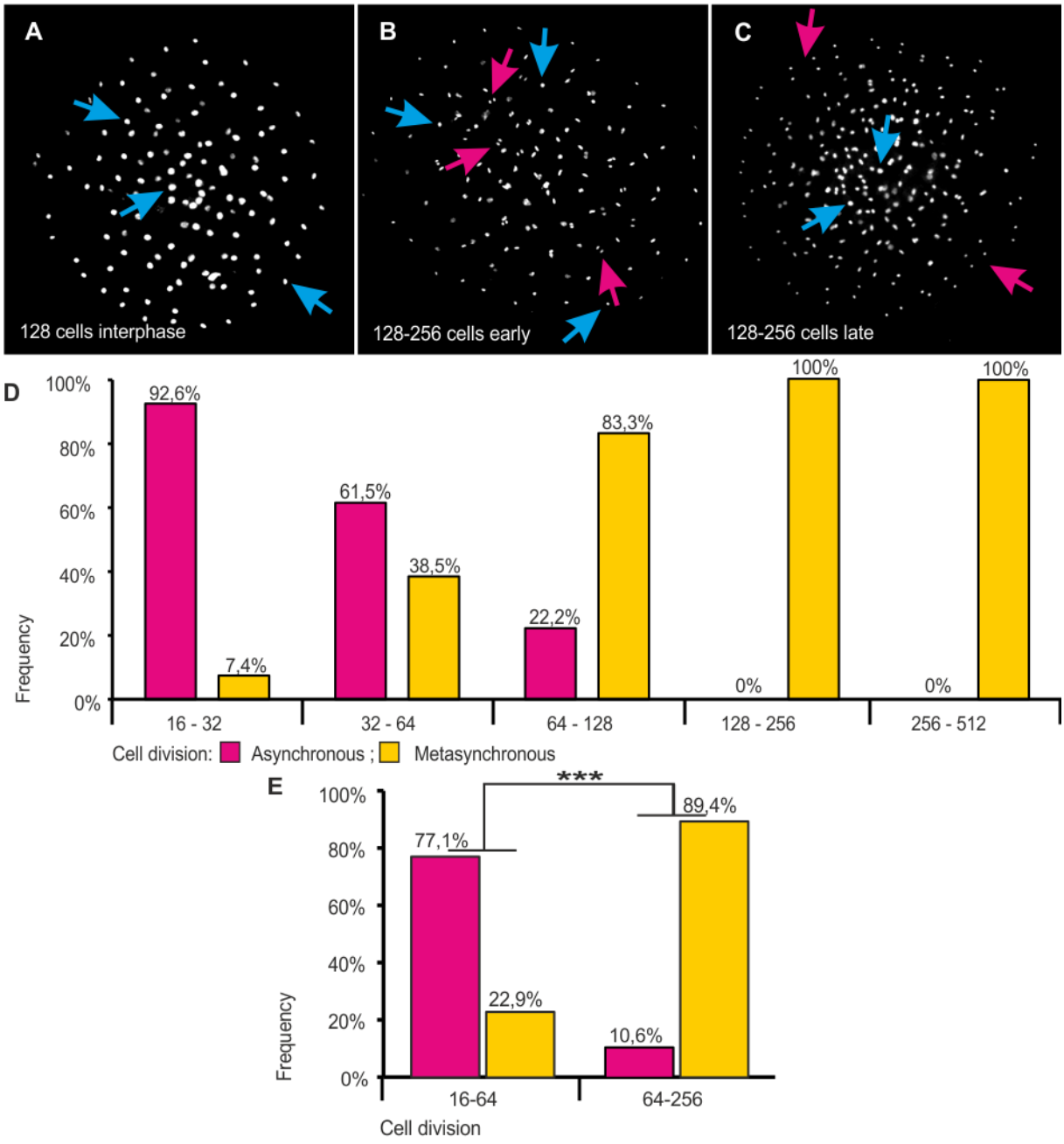

Figure 3: Progression from asynchronous to metasynchronous cell division in early medaka embryos (A-C) Different time points during cell division 8, 128 to 256 cells: interphase, early mitosis, late mitosis. (A) All cells are at clear interphase state (Blue arrows), no mitotic cells are detectable. (B) Early division. Central positioned cells are in mitosis and show clear characteristics for an ana-/telophase stage (Red arrows). More peripheral positioned cells still show interphase characteristics (Blue arrows). (C) Late division. Central positioned cells are already at interphase (Blue arrows), whereas peripheral cells still are at late ana-/telophase (Red arrows). (D) Distribution of randomly asynchronous to directed metasynchronous cell division between cycle 5(16 cells to 32 cells) and cycle 9 (256 to 512 cells). Randomly asynchronous dividing embryos are represented by red bars; metasynchronous dividing embryos are represented by yellow bars (E) Distribution of randomly asynchronous to clearly metasynchronous cell division in embryos between the 16- to 64-cell stages and between the 64- to 256-cell stages. Cell division is randomly asynchronous (Red bars) until embryos have reached the 64-cell stage and metasynchronous (Yellow bars) during the following cell divisions (Chi-square test, $p<0,001$) (Figure modified from Kraeussling et al. [64]).

2.1.2. Metasynchronous division pattern formation in living medaka embryos

To confirm the findings from the observations on fixed embryos, time-lapse observations on living embryos were performed. For this, medaka embryos at the 1-cell stage were injected with mRNA encoding an eGFP-tagged Histone2B protein (H2B-eGFP). After transcription, these proteins tag the cells' chromosomes by integration into the chromatin after DNA replication. Subsequently, these embryos were scanned using a standard confocal microscope and imaged continuously throughout the cleavage phase.

Again, the cell cycle in medaka embryos was found to be highly synchronous until the 16-cell stage. Also, a clear minor temporal spacing of cell cycle initiation between single cells within the same embryo clearly emerged during the division from 16 to 32 cells. This temporal spacing of cell division initiation increased with every cell division. At the earliest with division 6 (cycling from 32 to 64 cells) cell division initiated clearly first in cells positioned centrally and later in more peripheral cells. Also, at the latest with cell division 8, 128 to 256 cells, this temporal spacing separated cell cycle initiation between central and peripheral positioned cells, so that cell divisions occurred in clearly visible waves (Figure 4).

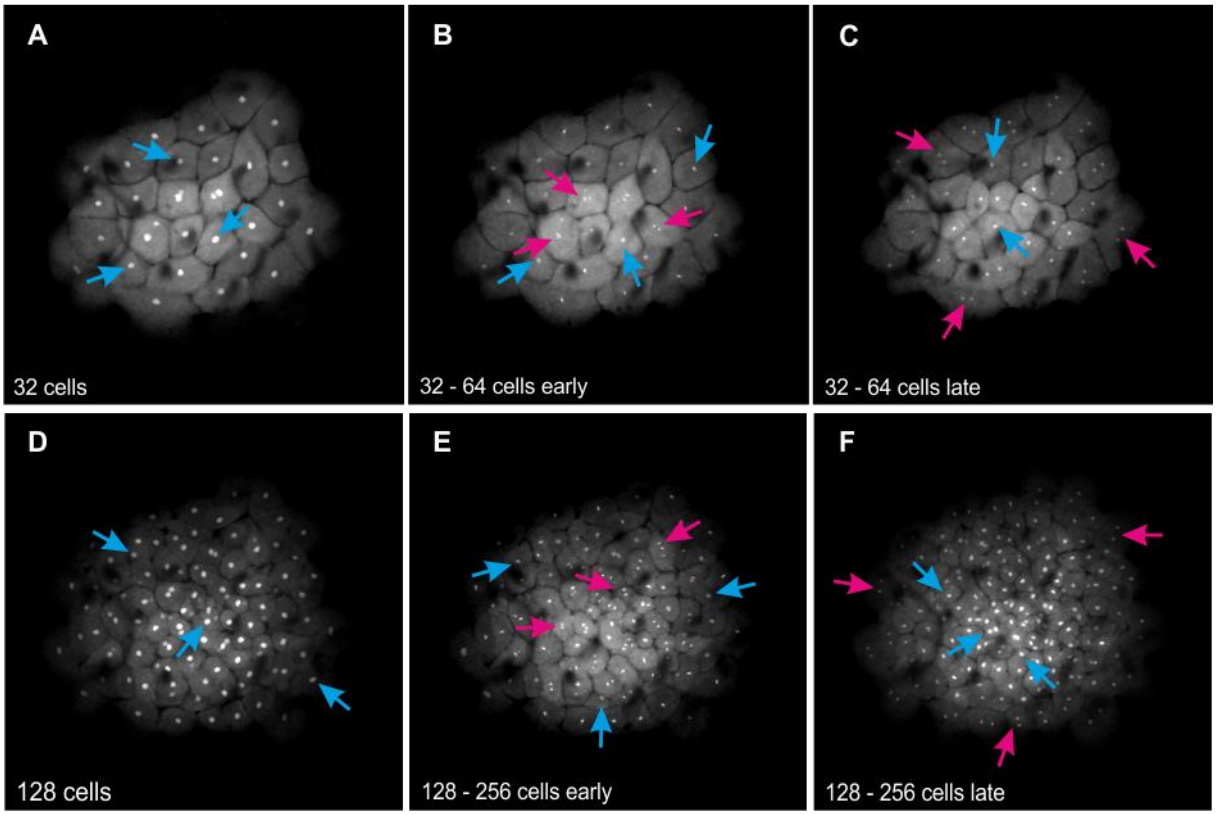

Figure 4: Different time points during cell division 6, 32 to 64 cells (A-C) and division 8, 128 to 256 cells (D-F): interphase, early mitosis, late mitosis. (A) At 32 cells, all cells are at interphase (Blue arrows), no mitotic cells are detectable. (B) Early division 6. Central positioned cells are in mitosis and show clear characteristics for an ana-/telophase stage (Red arrows). More peripheral positioned cells are still at interphase (Blue arrows). (C) Late division 6. Central positioned cells are already at interphase (Blue arrows), whereas peripheral cells still are at late ana-/telophase (Red arrows). (D) At 128 cells, all cells are at interphase (Blue arrows, no mitotic cells are detectable. (E) Early division 8. Central positioned cells are at late ana-/telophases of mitosis (Red arrows). Peripheral positioned cells are still in interphase (Blue arrows). (F) Late division 8. Central positioned cells are at interphase (Blue arrows), whereas peripheral cells still are at late ana-/telophase (Red arrows) (Figure modified from Kraeussling et al. [64]).

2.1.3. Cell cycle desynchronisation is reflected in nuclear size

Both, the general loss of cell cycle synchrony and the correlation between desynchronisation and cell positioning could also be detected if cells were tracked throughout several cell divisions with respect to their nuclear size. For this, medaka embryos again were injected with mRNA encoding for H2B-eGFP and scanned continuously under a confocal microscope at a constant time interval. Afterwards, the nuclear sizes of single a cell and its resulting daughter cells after each cell division were determined as the area of the H2B-eGFP signal in the confocal scans.

The observation of an embryo between the mid 8-cell and late 64-cell stage showed that the sizes of the nuclei had their greatest extension in cells during interphase. This nuclear area/size decreased when cells advanced to metaphase and chromosomes condensated in preparation for the next cell division. In consequence, the smallest nuclei were found in anaphase cells, shortly after chromosome separation. Afterwards, the nuclear sizes increased again (Figure 5).

Focusing on the most centrally positioned cell of the 4 tracked daughter cells at the 32-cell stage, it became obvious that this cell showed condensed chromatin one time point prior to all other cells. Again, at the next cell stage, 64 cells, the two daughter cells from the same "early"-cell at the 32-cell stage showed condensed chromatin one measurement point before the other tracked cells. Furthermore, they also entered mitosis two measurement points before the remaining cells. Moreover, the most peripherally positioned cell of all daughter cells at division 32 to 64 cells showed a minor delay in cell cycle. More precisely, the daughter chromosomes in this cell did not show the clear separation like the other cells and could only be detected as distinct spots one time point later (Figure 5).

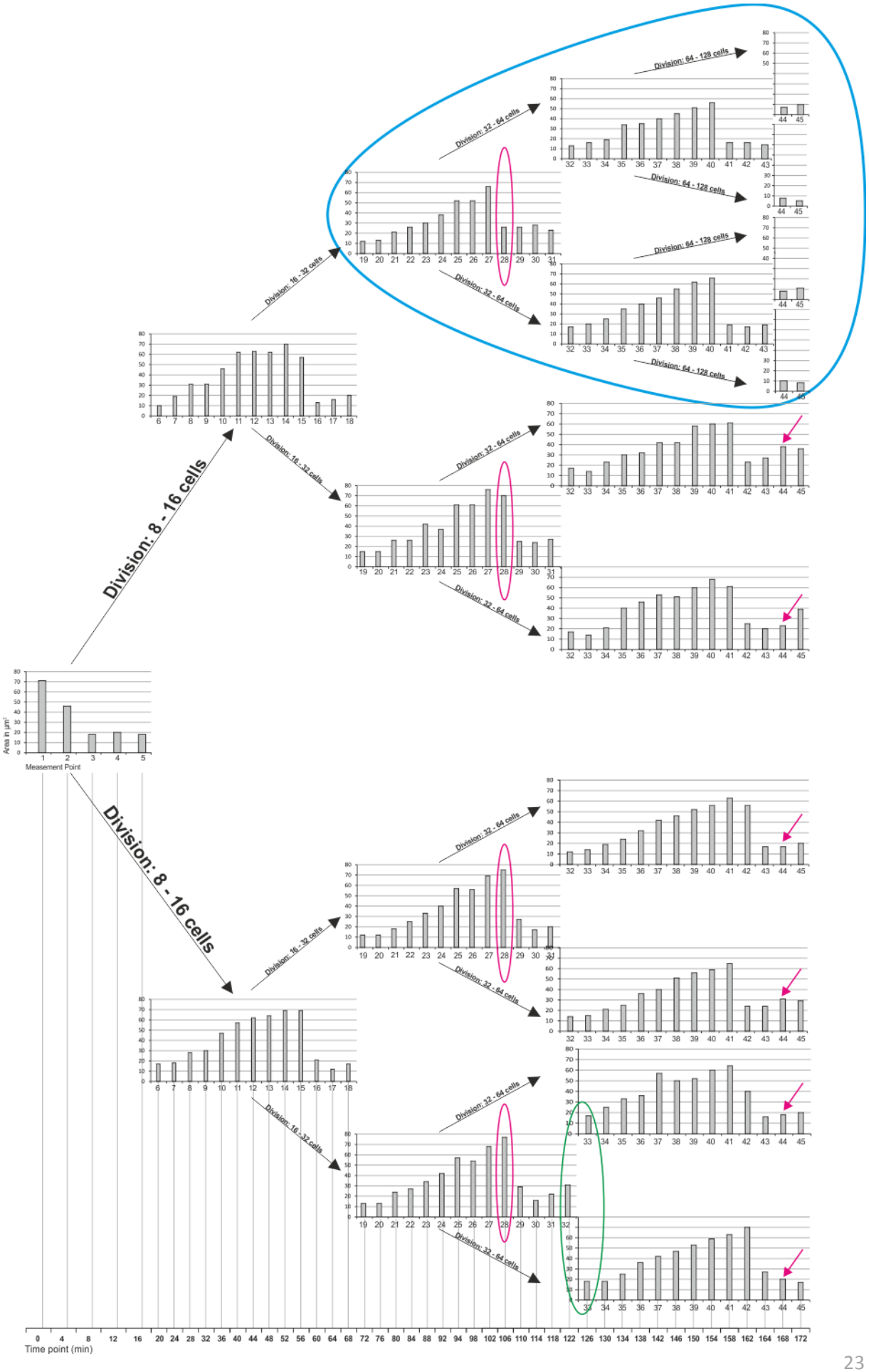
Division: 8 - 16 cells
Division: 16 - 32 cells
Division: 32 - 64 cells
Division: 64 - 128 cells
Area in µm²
Measement Point
Time point (min)

Figure 5: Progression of nucleus sizes between the 8 and 64-cell stage. Changes in nucleus size (as a determined area) of a cell at the mid 8-cell stage (far left) and of its daughter cells until the late 64-cell stage (far right) are shown. Black arrows lead to the graphs of the daughter cells. Chromosomes are condensed 1 time point before the other cells (Red circles) in the most central positioned cell at the late 32-cell stage (Blue circle). The 2 most central cells during the 64-cell stage have separated their chromosomes 2 time points before the other cells (Red arrows). Overall, mitosis is early in more central cells (Blue circle). Cell division is late in the most peripheral cell at the late 32-cell stage (Green circle) (Figure from Kraeussling et al. [64]).

2.1.4. Asymmetric cell division affects the metasynchronous division pattern

An additional interesting observation that was made during the time lapse experiments was that some embryos did not divide symmetrically from the 2-cell to the 4-cell stage. In symmetrically dividing embryos, the cells until the 32-cell stage were arranged in a rectangular way and progressed towards a circular pattern at 32 cells and especially at later cell stages of the cleavage phase.

Cells in asymmetrically dividing embryos were not arranged in a rectangular but in a highly asymmetric manner. The degree of asymmetry depended of where the cleavage furrows have run during the division to the 4-cell stage.

However, in asymmetrically divided embryos, the cell cycle also de-synchronized with cycle 5, the division from16 to 32 cells. But compared to symmetrically divided embryos, the percentage of embryos that developed a clear metasynchronous division pattern was significantly lower in embryos that divided asymmetrically (Figure 6).

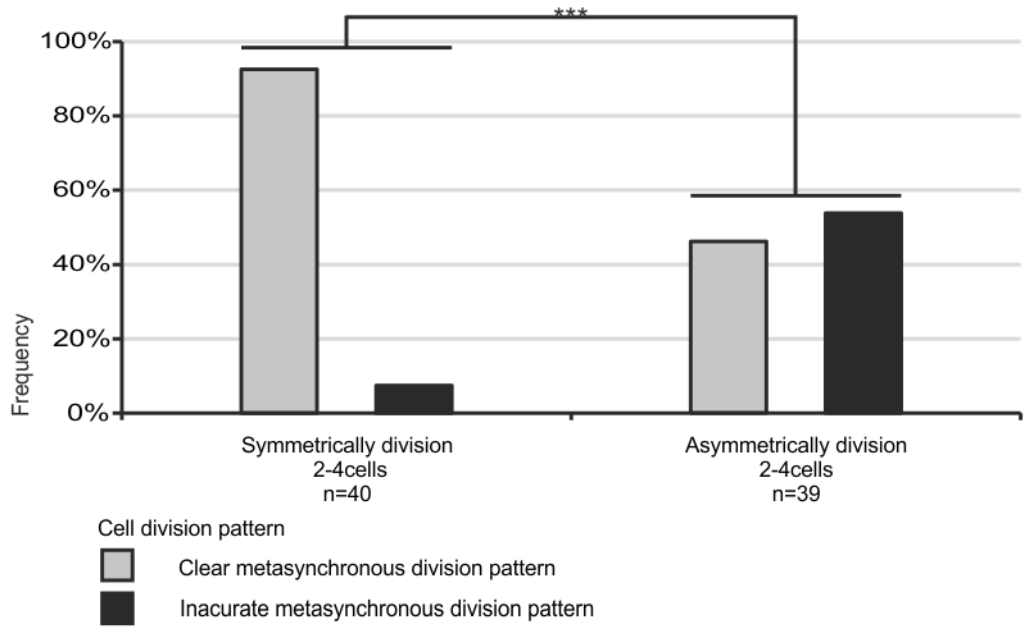

Figure 6: Frequency for a clear metasynchronous division pattern in embryos that were injected with mRNA encoding for H2B-eGFP and that divided symmetrically (left columns) or asymmetrically (right columns) from the 2-cell to the 4-cell stage. Symmetric embryos showed more often (37/40; 92,5%) a clear metasynchronous division pattern than asymmetric embryos (18/39; 46,2%) (Chi-square test; $p<0.001$) (Figure modified from Kraeussling et al. [64]).

Although some of the asymmetric embryos did not establish the typical metasynchronous division pattern, cell divisions still occurred in a structured and organized way. In the given example, the cells of the embryo were arranged in a more elongated manner and the cell divisions progressed in waves that ran from one pole of the embryo to the opposite pole (Figure 7).

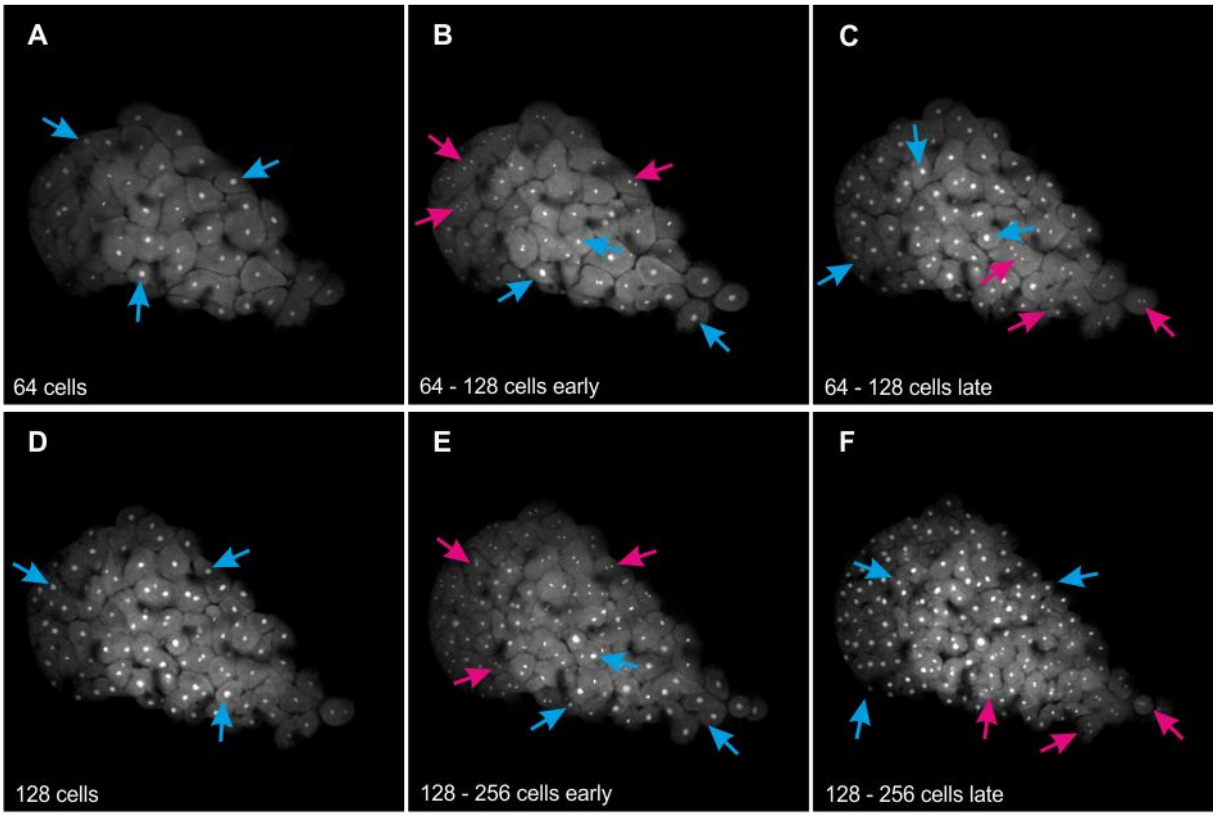

Figure 7: Different time points during cell division 7, 64 to 128 cells (A-C) and division 8, 128 to 256 cells (D-F): interphase, early mitosis, late mitosis. (A) At 64 cells, all cells are at interphase (Blue arrows), no mitotic cells are detectable. (B) Early division 7. Cells at the left side of the embryo are in mitosis and show clear characteristics for an ana-/telophase stage (Red arrows). Cells at the opposite right side are still at interphase (Blue arrows). (C) Late division 7. Cells at the left side are now at interphase (Blue arrows), whereas cells at the opposite right side cells still are at late ana-/telophase (Red arrows). (D) At 128 cells, all cells are at interphase (Blue arrows, no mitotic cells are detectable. (E) Early division 8. Cells at the left side of the embryo are at late ana-/telophases of mitosis (Red arrows Cells at the opposite right side are still in interphase (Blue arrows). (F) Late division 8. Cells at the left side are now at interphase (Blue arrows), whereas cells at the opposite right side cells still are at late ana-/telophase (Red arrows) (Figure modified from Kraeussling et al. [64]).

2.2. Asymmetric cell divisions from 2 to 4 cells in medaka embryos

2.2.1. Classification of medaka embryos

The mRNA injections in medaka embryos and the subsequent time-lapse observation showed that embryos can divide in a highly asymmetrically manner from the 2-cell to the 4-cell stage. This resulted occasionally in malformed embryos that lacked the typical cell arrangement of an embryo at cleavage-phase. Moreover, they also often lacked the organized division pattern of the typical metasynchronous division.

To determine if this observation was a naturally occurring phenomenon, or just a direct result of the mRNA-injection, which represents a massive interference and manipulation with the cell, untreated medaka embryos were investigated for asymmetric cell divisions. More precisely, it was looked for cleavage furrows orientation and the cell-cell arrangements at the 4-cell stage.

This examination revealed that medaka embryos showed a broad spectrum of cleavage symmetries and cell-cell arrangements. However, although the spectrum spanned from highly symmetric cleavages to highly asymmetric cleavages, three distinct classes of cleavage types were determined: type I, type II and type III.

Embryos that were classified as type I showed a high level of symmetry along the X-/Y-axes with four uniform cells whose cleavage furrows formed a perfect or almost perfect 90° intersection point in the center of the four cells. As consequence of this symmetry, each cell in a type I embryo had only contact to its two neighboring cells (Figure 8A).

The type II embryos did not have the strict axial symmetry along the X-/Y-axes as type I embryos. Although the intersection point between their four cells still showed the 90° angle and was still located in the center of all four cells, the cleavage furrows no longer formed the cross like structure of type I embryos. Consequently, two of the four cells still only had contact to their two neighboring cells, but the other two also had contact to their opposing cell and formed a structure that looked like an hourglass (Figure 8B).

The four cells in both, the type I or type II embryos were arranged in a manner that showed similarities to a cloverleaf.

However, type III embryos finally did not show any kind of axial symmetry and/or a clearly organized structure. The clear cloverleaf-like cell arrangement of type I and type II embryos was also lost. Cells in type III embryos were often arranged in an elongated manner, but lacked a distinct pattern (Figure 8C-F).

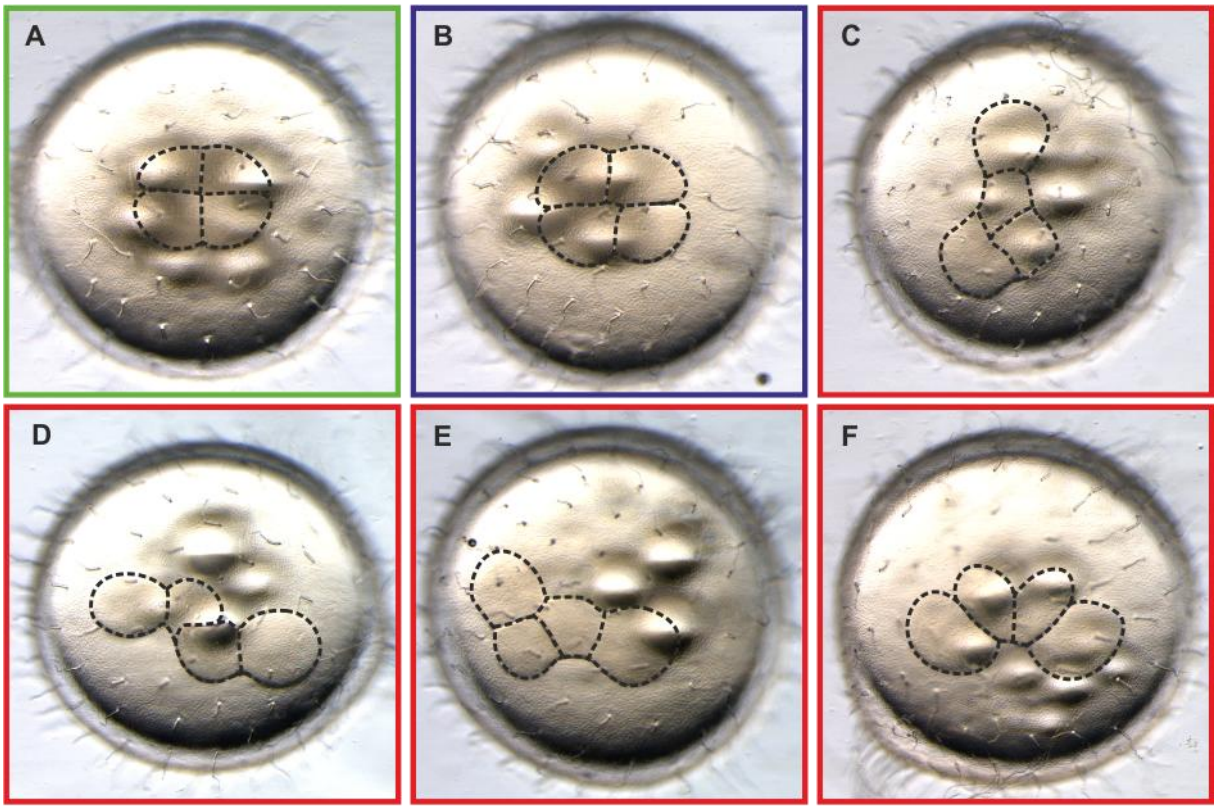

Figure 9: Classification of the three embryo types in medaka at the 4-cell stage. Cell boundaries were highlighted for better visualization (A) Type I embryo with high levels of symmetry along the cleavage furrows and a central intersection point with right-angled cells at the interception point. (B) Type II embryo with still right-angled cells at the central positioned intersection point, but clearly affected symmetry on the X-/Y-axes. (C-F) Showing different examples for type III embryos. Embryos have almost totally lost symmetry on the X-/Y-axes and no clear intersection point is found (Figure modified from Kraeussling et al. [64]).

2.2.2. Asymmetric cleavages do not affect correct embryo development

If the morphology of type III is compared of those of type I or type II embryos, it is obvious that type III were highly unstructured and unorganized.

This posed the question if this high grade of asymmetry has a negative effect on embryo development. To address this question, the survival rates of the three embryo/cleavage types were determined. Altogether, 774 embryos from a large random mating colony of medaka fish were classified according to their cleavage type. From these embryos 171 were classified type I (22%), 424 type II (55%) and 179 type III (23%) (Figure 10).

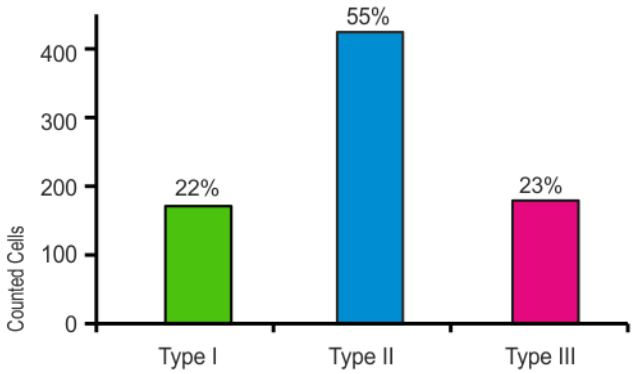

Figure 10: Frequency of type I, type II and type III embryos at the 4-cell stage. Type I embryos occurred with a frequency of 22% (171/774) of total embryos (Green bar), type III embryos with 23% (179/ 774) (Red bar). Type II embryos represent the largest group of the three types with 55% (424/774) of all embryos (Blue bar) (Figure modified from Kraeussling et al. [64]).

After classification, those embryos were raised under standard conditions and monitored for early embryonic death.

Surprisingly, only one of the 774 monitored embryos died before hatching and this individual one was scored as type II. The remaining embryos showed normal developmental outcomes and hatched on time around day 9-10 post fertilization.

2.2.3. Morphogenic and developmental differences between the embryo types

For further investigations of morphogenetic differences between the three medaka cleavage types and their possible influence on early embryonic development, time lapse observations on the three cleavage types were performed. More precisely, embryos of all three cleavage types were investigated at the interphase of each cell stage between the 4-cells (at classification) up to the 1024-cell (pre-blastula stage) shortly before MBT. Afterwards, the morphologies of the single embryos were evaluated compared to an idealized embryo, which was originally described in detail by Iwamatsu [2].

From the three embryo types the type I embryos demonstrated the highest similarity to this idealized development. They start with the typical cell arrangement in a rectangular cloverleaf at the 4-cell stage. This high level of symmetry and the homogenous embryo morphology were maintained throughout the entire cleavage phase until stage 10, which is at 1024 cells. At this time point the embryos have established the typical roundish and multi-layered disc of the early blastula stage and are just around to enter the mid blastula transition (Figure 11).

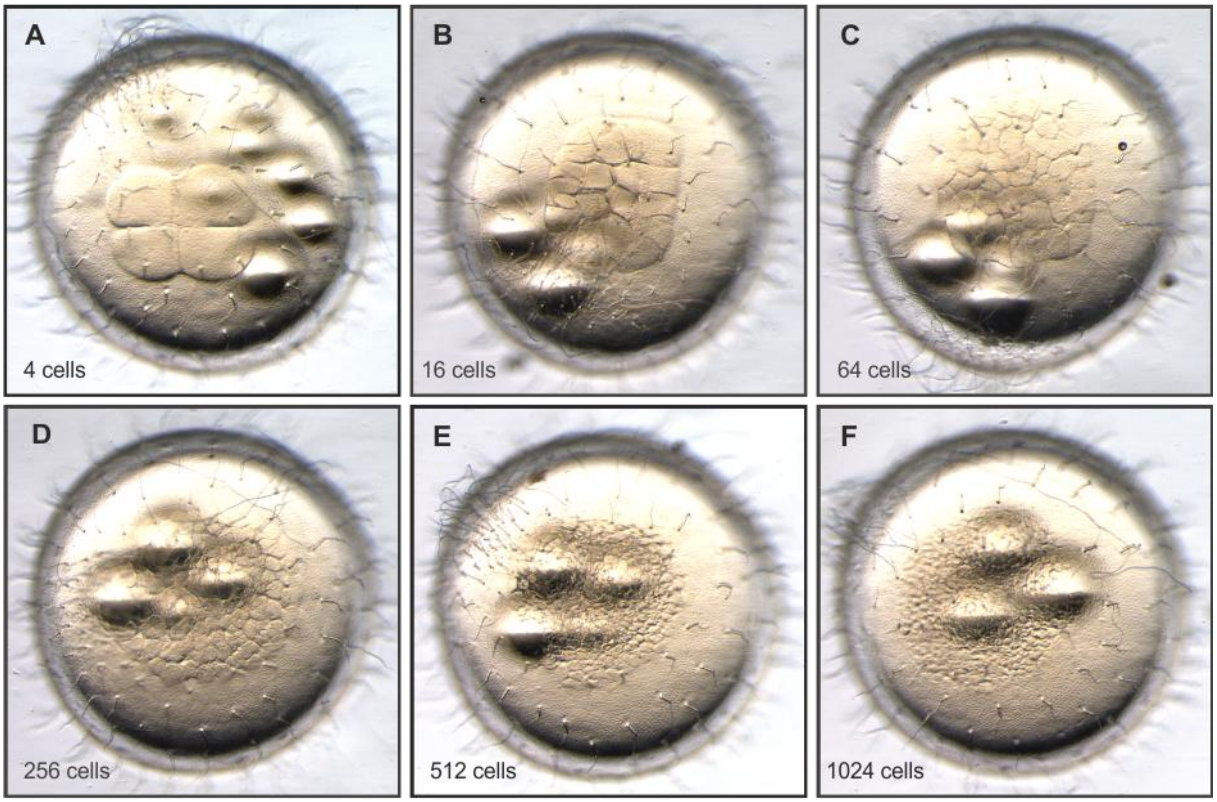

Figure 11: Distinct time points during the cleavage phase of a type I embryo. Embryos are highly symmetric along the X-/Y-axes throughout the cleavage phase. (A) A type I embryo at the 4-cell stage showing the typical cloverleaf-like structure and an overall rectangular shape of the embryo. (B) At the 16-cell stage, embryos still possess the rectangular shape. (C) Embryos start to get more and more roundish at around the 64-cell stage. (D) Embryos at the 256-cell stage have established a roundish shape and the maximal extension of the pre-MBT embryo. (E-D) Embryos do not show any further morphological changes between the 512-cell stage and the 1024-cell stage, but have established the typical pre-MBT embryo disc at 1024 cells (Figure modified from Kraeussling et al. [64]).

Type II embryos showed only minor differences to type I embryos and differ only during early stages from the idealized medaka embryo. Sometimes they had slightly shifted shapes at the 8-cell stage or the 16-cell stage as the cells of the embryos were not arranged in a perfectly symmetric, but in a slightly elongated manner. These minor differences were compensated until the 32-cell stage or the 64-cell stage, respectively.

In contrast, type III embryos clearly showed major morphological differences to type I and type II embryos, as well as to the idealized medaka embryo from Iwamatsu. They displayed a broad spectrum of different shapes often being elongated, bent or both.

The individual shape was the direct result of the progression of the cleavage furrows at the division from 2 to 4 cells. However, also type III embryos were able to re-establish the typical shape of the multilayered cell-disc of the early blastula stage. But compared to type II embryos, this process took considerably longer. The respective duration was again directly connected to the level of asymmetry of the cell division from the 2 to the 4-cell stage.

In the given example, the embryo was not able to fully compensate before stage 10 (1024 cells) (Figure 12).

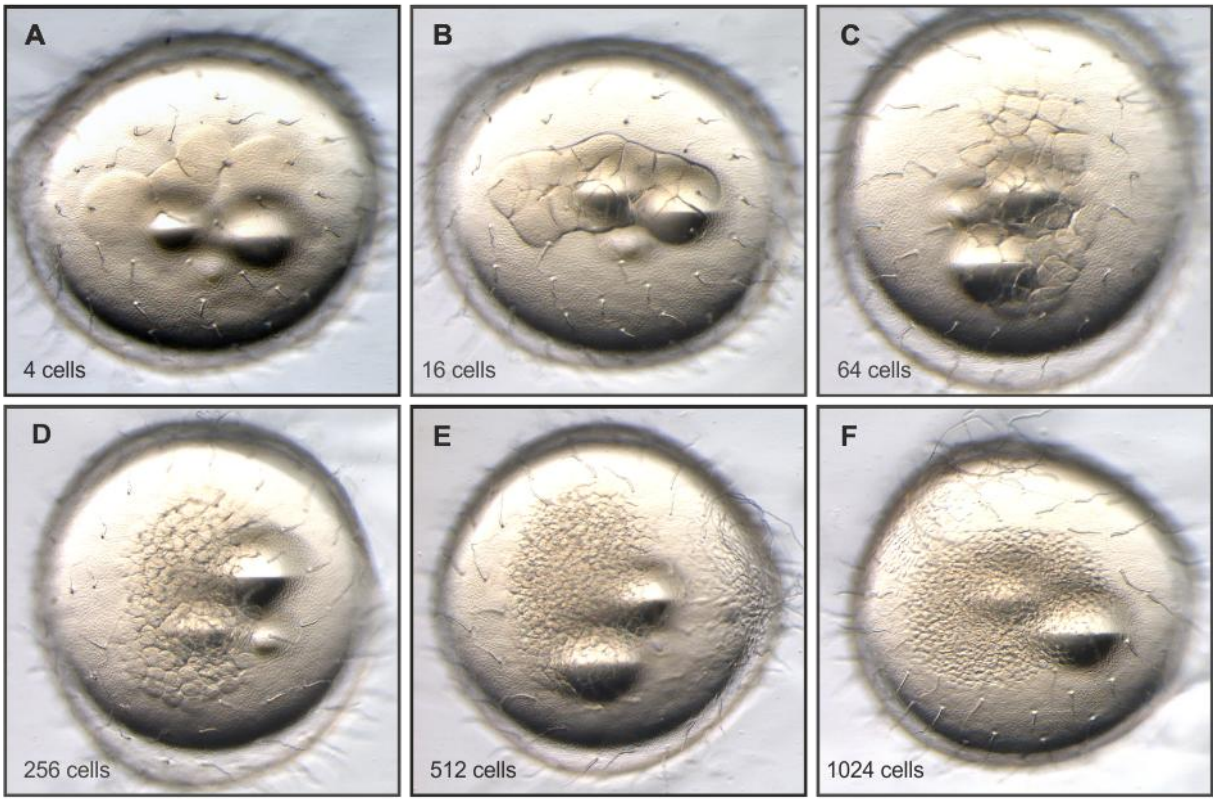

Figure 12: Distinct time points during the cleavage phase of a type III embryo. The embryo is highly asymmetric along the X-/Y-axes until stage 10 at the end of cleavage phase. (A) Cells ate the 4-cell stage are orientated in an elongated manner (B) At the 16-cell stage, the embryo still show the elongated form that resulted from the elongated cell-orientation at the 4-cell stage. (C-E) The embryo starts to get more and more roundish at around the 64-cell stage, but still has a clearly elongated shape at the 64-, 512- and 256-cell stage respectively. (F) The type III at stage 10, 1024 cells, has established an almost perfect roundish shape and shows high similarity to a type I or type II embryo (Figure modified from Kraeussling et al. [64]).

2.3. Measurement of cell volumes in medaka embryos at the 4-cell stage

2.3.1. Determination of cell volumes with fluorescent dyes and confocal imaging

The nucleo-cytoplasmic ratio is evidently the major mechanism that controls MBT activation [13][20][25]. This has been proven via cell volume manipulations or nuclear transplantations which then resulted in early or late MBT activation, respectively [12][22][43][45][65]. However, cell volumes for the nucleo-cytoplasmic ratio have only been estimated and precise volumes for single cells have never been determined in a comparative way.

Since medaka embryos showed large differences in morphology, which were the result of misplaced cleavage furrow progression, this raised the question if asymmetric cell cleavage also affects equal distribution of cytoplasmic material.

Again, a confocal imaging approach was chosen to address this problem as it allowed the precise determination of cell shapes in all 3 dimensions and thereby provided a source for more detailed information that allowed an exact cell volume determination.

For pilot experiments and establishing the required techniques, embryos were treated with different fluorescent dyes that stained for cell membranes. Afterwards, these embryos were scanned with a confocal microscope and analyzed with a 3D reconstruction software to measure individual cell volumes. For this, several dyes were tested to identify the most suited one: Bodypi Green, Bodypi Red, CellMask Orange, CellMask DeepRed (all Invitrogen). Although they all stain plasma membranes, the staining patterns showed considerable differences between the dyes (Figure 13).

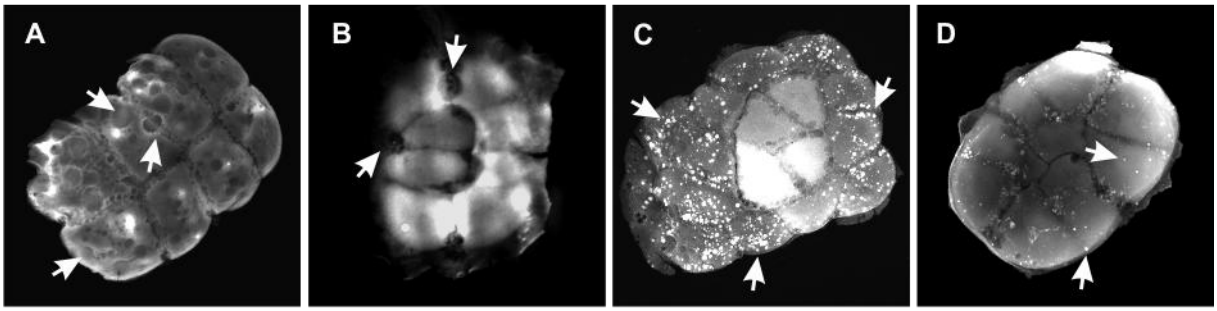

Figure 13: Maximum intensity collapsed Z-stacks of confocal scans of membrane stained medaka embryos. (A) Staining with Bodypi Green shows a clear and sharp signal of the cell surface. (B) Staining with Bodypi Red shows a diffuse and blurred signal on the cell membrane. (A, B) Generally, Bodypi staining is imperfectly as small dents in the cell surface remain unstained (arrows). (C) Staining with CellMask Orange accompanies small spherical aggregates on the cell surface (arrows). (D) Staining with CellMask DeepRed results in a sharp and homogenous staining of the cell with only a very small number of spherical aggregates (arrows).

These tests demonstrated that staining with CellMask DeepRed offers the highest potential to fulfill the requirements for measuring cell volumes.

Fluorescent staining and confocal imaging of embryos at the 1- and 2-cell stage showed that it was not possible to measure cell volumes at these two stages by this technique. The boundary between the cell membrane of the embryo and the yolk membrane was not contrasted enough to clearly determine the cell shape. Especially at the 1-cell stage it was not possible to identify the exact cell shape. This situation greatly improved with reaching the 2-cell stage, but cellular boundaries were still not clear enough for a correct and fair detection with software protocols. Only after reaching the 4-cell stage the cellular boundaries between the cells, as well as to the yolk, had reached a contrast-level that allowed the discrimination of single cells and performing exact measurements (Figure 14).

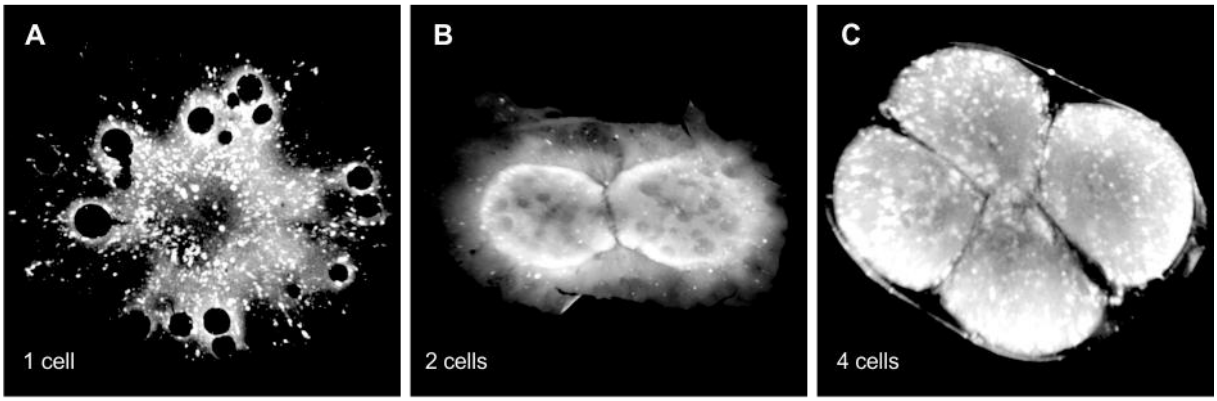

Figure 14: Maximum intensity collapsed Z-stacks of confocal scans of medaka embryos at three different time points: 1-cell stage, 2-cell stage, 4-cell stage. (A) Cell boundary at the 1-cell stage is diffuse. The cell is flattened and the membrane has many large and unguided outgrowths on top of the yolk. (B) Outgrowths at the 2-cell stage are smaller and more specific compared to the 1-cell stage. Cell boundary is clear at the center between both cells and at the collateral sides of the cells but becomes more and more diffuse again near the most outward edge of the cells. (C) Boundaries of single cells are sharp and clearly detectable (Figure modified from Kraeussling et al. [64]).

Furthermore, after scanning various embryos at 4-cell stage, it became clear that numerous embryos change the X-/Y-positions of their cleavage furrows and of the intersection points along the Z-axis. As the measurement protocol isolates the single cells by an optical dissection, it is strictly required for a fair volume determination that the positioning of the cell boundaries remains constant and unchanged. Whenever this requirement did not apply, the respective embryos were excluded from the measurement (Figure 15).

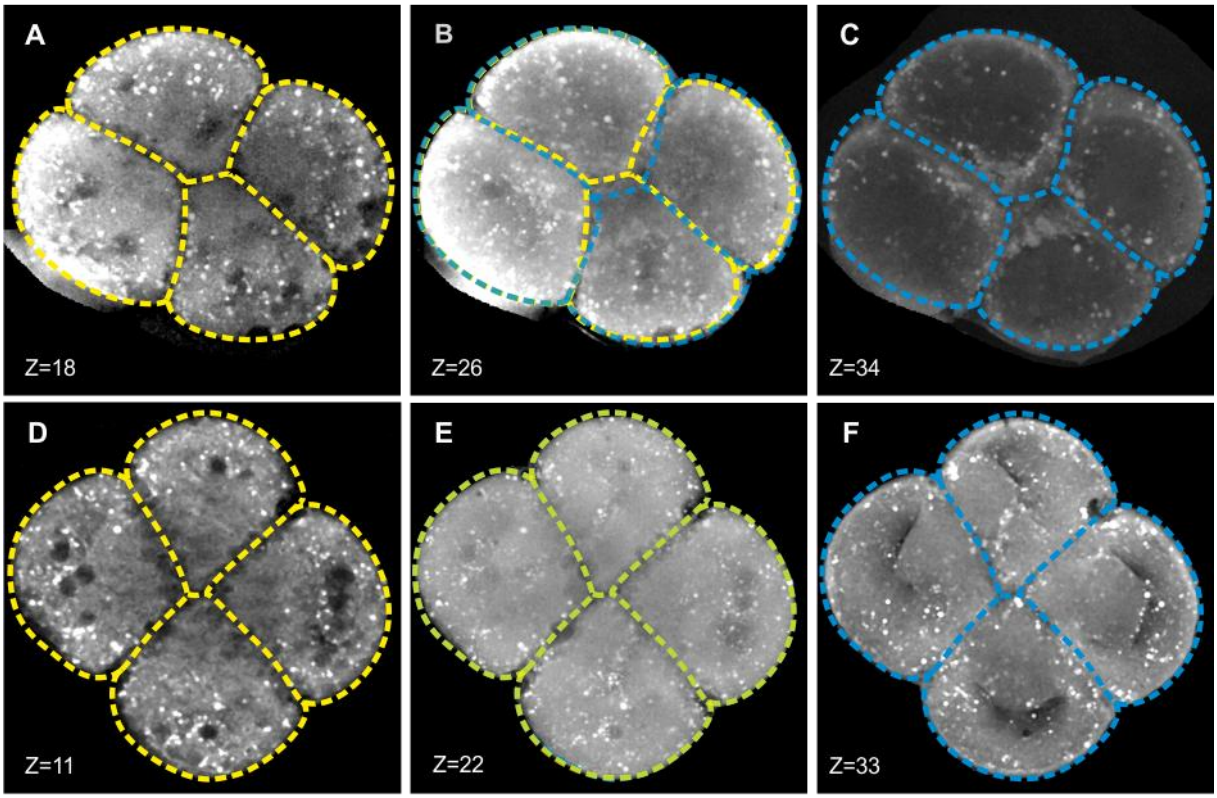

Figure 15: Highlighted cell borders in a confocal stack at three positions along the Z-axis (top, middle, bottom) in two different embryos. (A, D) Cell borders in the bottom position are highlighted in yellow. (C, F) Cell borders in top position are highlighted in blue. (B, E) Overlap of the top and bottom cell borders are projected on the middle position. (B) Cell borders of the top and bottom position do no overlap as the position of the cleavage furrows differ between top and bottom. (E) Cell borders of the top and bottom position overlap as the position of the cleavage furrows do not differ between top and bottom (Figure modified from Kraeussling et al [64]).

2.3.2. Cell volumes differences in medaka embryos at the 4-cell stage

In theory, if all cells within an embryo would possess the same cell volume, they would also possess the same amount of relative volume from the total embryo's volume. For an embryo at the 4-cell stage, this would mean that the cells in an "ideal" embryo would all occupy 25% of the total volume.

The investigation of a total of 33 medaka embryos at the 4-cell stage showed that only 2 embryos were close to this ideal value. Of the 33 measured embryos only 5 embryos consisted of four cells of similar or equal cell volumes, if a relative volume difference of maximally 5% between the largest and the smallest cell of an embryo was taken as threshold. The majority of embryos consisted of three cells that showed a relative similar volume, and a fourth cell showing a relatively larger or smaller volume respectively (20/33) as long as the differences between the relative volumes' differences of the smallest and the largest cells to the embryos mean relative volume did not exceed at factor 2.

Overall, the cell volumes within individual medaka embryos at the 4-cell stage spanned large differences (Figure 16A). These differences became even more obvious if the fold-change differences between the largest and the smallest cells within the same embryos were compared with each another (Figure 16B). This revealed for the embryo with the most similar cell volumes between all cells, that the volume of the largest cell was only 1.05 times larger than the volume of its smallest cell. In contrast, in the embryo with the most dissimilar cell volumes, the volume of the largest cell was 2.69 times larger than the volume of the smallest cell. However, most embryos (15/33), showed fold differences between 1.3 and 1.5 times between the largest and the smallest cell.

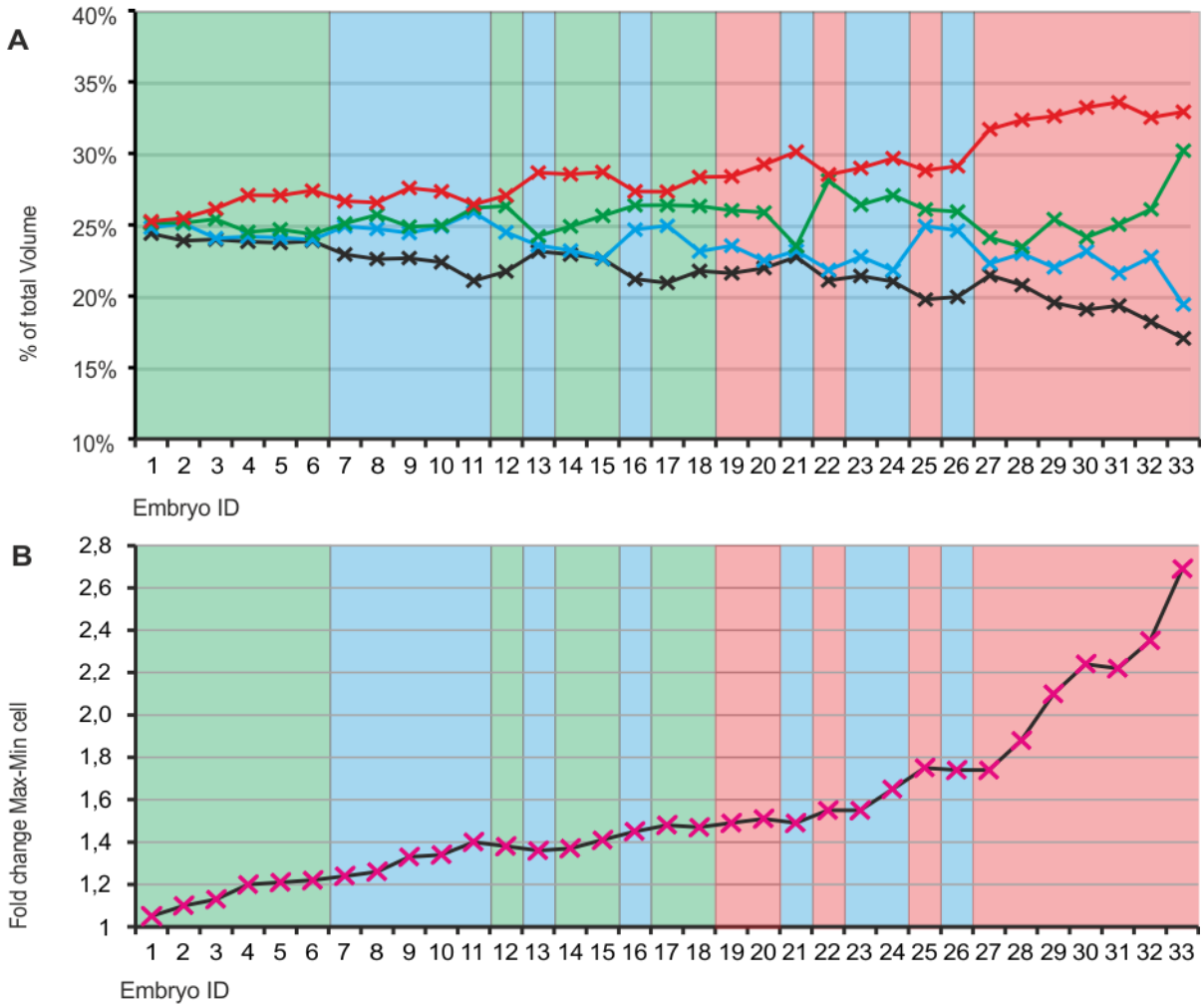

Figure 16: (A) Cell volume differences in medaka embryos at the 4-cell stage. Values on the y-axis represent the percentage of each cell from individual embryos relative to the combined volume of all 4 cells. Embryos are listed on the y-axis with increasing differences between the largest and the smallest cell of individual embryos, increasing from the left to the right. Graphs represent single cell volumes of each embryo: smallest cells (black line), second smallest cells (blue line), second largest cell (green line) and the largest cells (red line). (B) Fold changes between the largest and the smallest cells of individual embryos. Fold change values are shown on the y-axis. Embryos that are listed on the x-axis are equal to embryos in (A). (A-B) Background colors represent the corresponding embryo type; type I in green, type II in blue, type III in red (Figure modified from Kraeussling et al. [64]).

The measurements depicted in figure 16 already gave indication that there might be a connection between the level of asymmetry and the cell volume differences. In consequence, when cell volumes were correlated to the level of asymmetry, it became apparent that embryos with higher levels of asymmetry were more likely to show larger cell volume differences than embryos with lower levels of asymmetry (Figure 17).

However, the correlation between asymmetry and cell volume differences is no strict rule since per se since some type I embryos were identified that differed more in cell volumes than type II embryos. Also, some type III embryos differed more in cell volumes than type II embryos (Figure 16B).

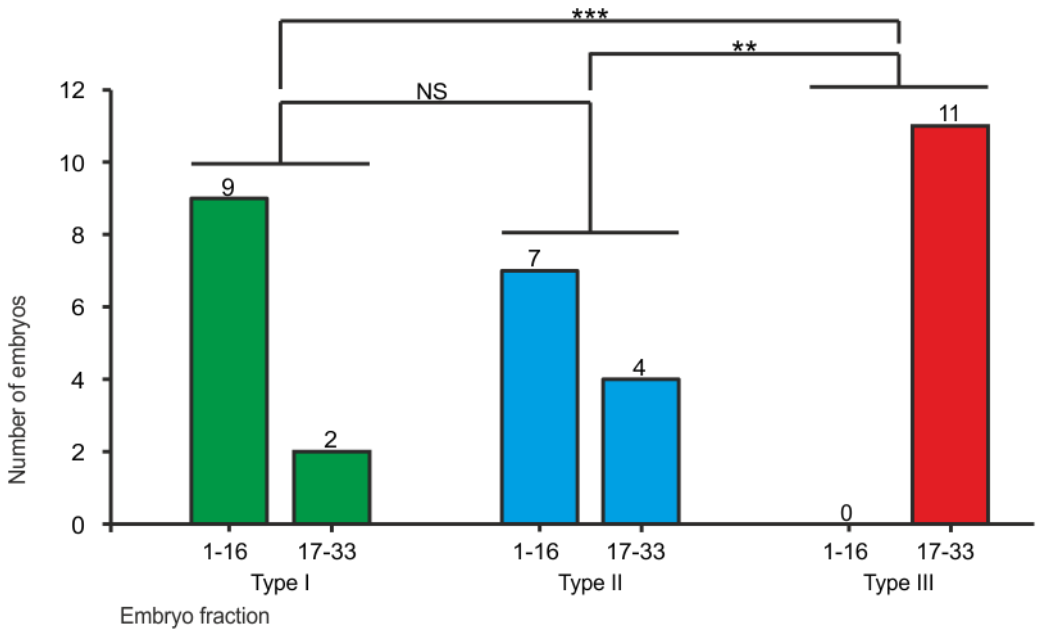

Figure 17: The occurrences of each embryo type among the first fraction of embryos representing the most similar embryos (embryos 1 to 16) and the second fraction representing the most dissimilar embryos (embryos 17 to 33) were correlated with each other. Type I embryos are represented by green bars, type II embryos by blue bars, and type III embryos are represented by red bars. No significant difference in the occurrence of type I and type II embryos ($p=0.3382$). Type III embryos are significantly more often found in the dissimilar fraction than type II embryos ($p=0.00135$) and especially than type I embryos (Chi-square test ; $p<0.001$) (Figure modified from Kraeussling et al. [64]).

2.4. Early transcriptional activity before MBT

2.4.1. RNA Polymerase II in pre-MBT medaka embryos

The activation of transcription is generally believed to an event that occurs not before the midblastula transition, although evidence for ongoing transcription at low levels before MBT already exist in several species [15][49][61]. In order to explore the actual situation in pre-MBT medaka, embryos were investigated for an active mRNA transcription machinery. This was done by analyzing RNA polymerase II (RNAPII) for phosphorylation, an accepted indicator for active transcription [66][67][68][69]. For this, embryos between the 2-cell and the 1024-cell stage were subjected to immunofluorescence staining.

Surprisingly, cells showing positive staining for polymerase II phosphorylation were already detected in early medaka embryos at the 16-cell stage (Figure 18A).

Also, the location of positive cells seemingly did not follow a specific pattern during the 16-cell and 32-cell stages as phosphorylation was found at multiple positions in different embryos in both stages.

At the 64-cell stage, p-pol II positive cells located predominantly in or near the center of the embryos, whereas peripheral cells mostly remained phosphorylation negative. By the next stage, at 128 cells, almost all peripheral cells were still negative for RNAPII phosphorylation. Additionally, phosphorylation-negative cells in more central positions were also found at this stage (Figure 18B).

Positive and negative cells were mixed in embryos at the 256-, 512- and 1024-cell stage. Furthermore, RNAPII phosphorylation was now also found in cells at the periphery of the embryo (Figure 18C-D).

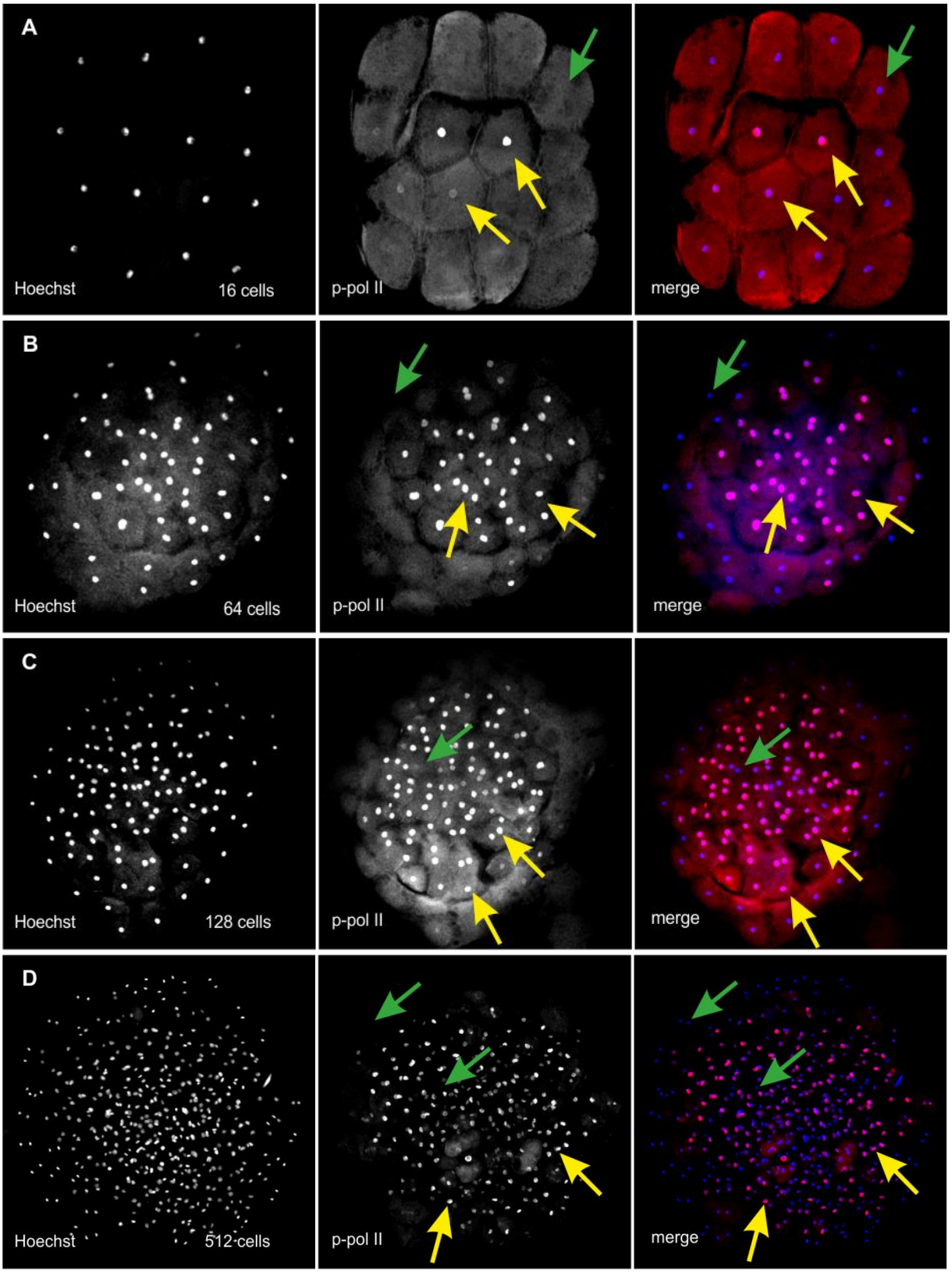

Figure 18: Polymerase II phosphorylation in medaka embryos at three different time points: 16 cells (A), 64 cells (B) and 128 cells (C). Figures show staining for DNA (Hoechst) phosphorylated polymerase II (p-pol II) and the overlay of both (merge; Hoechst is shown in blue, p-pol II is shown in red). (A) The 16-cell stage is the earliest stage at which phosphorylation was detected. Phosphorylation is rare and random at this stage. (B) At the 64-cell stage, positive cells are almost exclusively in the center in a uniformly distribution. (C) Most peripheral cells at the 128-cell stage are still negative for pol-II phosphorylation as well as some additional cells in more central

position. (D) Phosphorylation positive and negative cells are mixed in the center at 128 cells. Rim zone is free of p-pol II positive cells (Figure modified from Kraeussling et al. [64]).

However, as already mentioned, no phosphorylation was detectable between the 1- and 8-cell stages and polymerase II phosphorylation was first detectable in cells at the 16-cell stage. Furthermore, the level of p-RNAPII positive cells at the 16-cell stage was relatively low with an average of only 17% of all embryos (n=7). The number of positive cells then raised at the 32-cell stage to an average of 30.5% of all embryos (n=26) being p-RNAPII positive. After reaching the 64-cell stage, the number of p-RNAPII positive cells increased significantly to a level of 73% (n=18) and of 68% at 128 cells (n=7) (Figure 19).

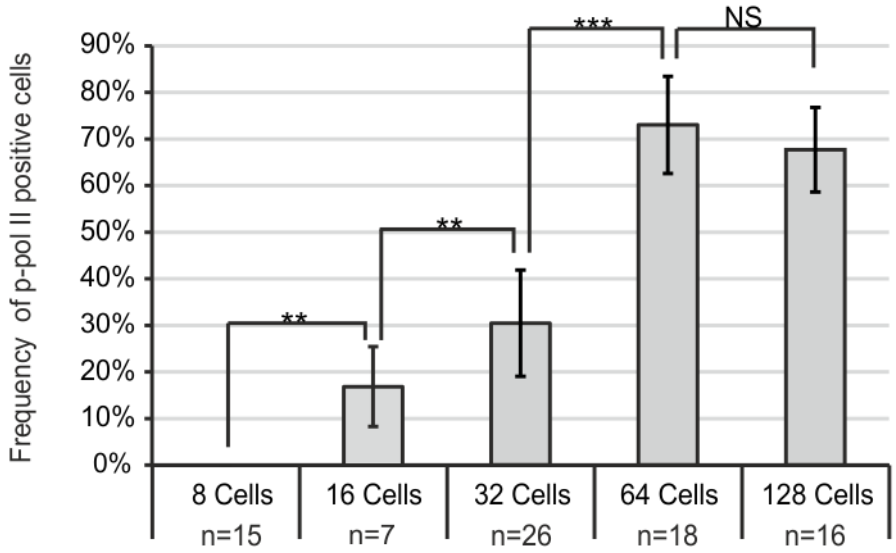

Figure 19: Polymerase II phosphorylation levels in medaka embryos between the 8-cell and the 128-cell stage. Polymerase II is unphosphorylated in embryos until the 8-cell stage but embryos start to show phosphorylation with 17% of all embryos cells being p-pol II positive ($p=0.002$). Phosphorylation levels have increased to the 32-cell stage ($p=0.0024$), but stay relatively low with 30.5%. The percentage of p-pol II positive cells increases at the 64%-cell stage to 73% ($p<0.001$) and remains close to this level at the 128-cell stage with 67.7% (Welch's test, $p=0.1186$; error bars are standard deviations) (Figure modified from Kraeussling et al. [64]).

However, none of the 154 analyzed embryos showed polymerase II phosphorylation in all cells.

2.4.2. Transcription of target genes before MBT

The transcriptional activity in pre-MBT medaka embryos, as it was indicated by the early RNA polymerase II phosphorylation, was confirmed on mRNA levels. This was achieved by investigating a selection of target genes for transcriptional up-regulation at specific time points. These were stages 0-2 (0-2cells), stages 8-10 (64-1000cells), stage 11 (early-late blastula), and stage 14 (pre-mid gastrula).

Among the target genes is *Ccnb1*, a member of the AB subfamily of cycline proteins that control the G2/M transition. For this gene a strong upregulation was found between the stages 8 to 10 and stage 11. Another gene, *RPS12*, which encodes for a member of the 40S ribosomal subunit, showed robust expression at stage 14.

However, *PSM1*, a protease, (and four other genes that are not further described here), showed no detectable up-regulation during the four investigated time points (Figure 20).

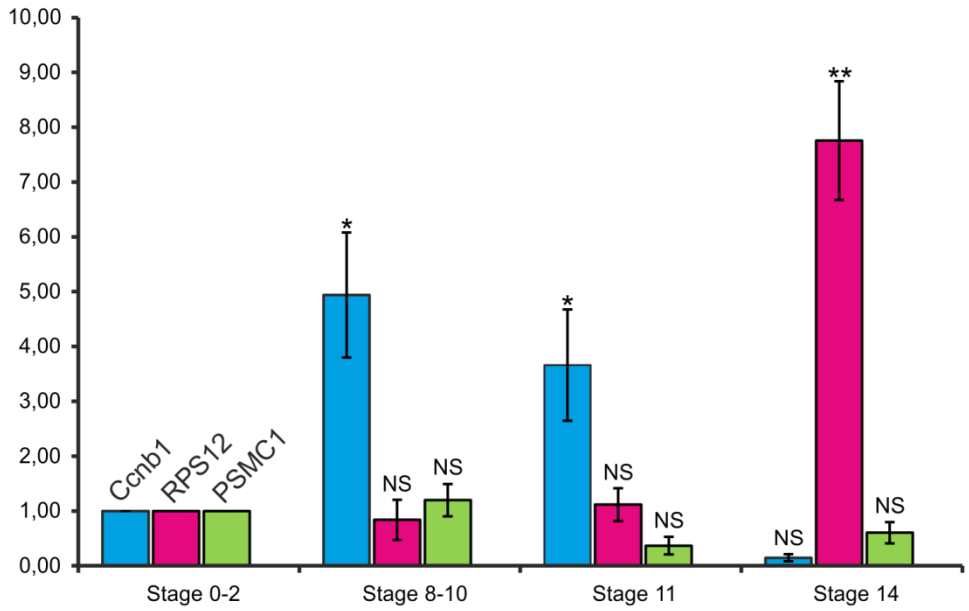

Figure 20: Expression levels of the three investigated genes *Ccnb1*, *RPS12* and *PSMC1* during four distinct time points (Stages 0-2, stages 8-10, stage 11, and stage 14). Expression of *Ccnb1* is represented by the blue bars. Expression is strong during stages 8-10 ($p<0.0268$) and stage 11 ($p<0.0452$). Expression of *Rsp12* is represented by the red bars. Expression shows induction at stage 11 and robust up-regulation at stage 14 ($p<0.0042$). Expression of *PSMC1* is represented by the green bars. Expression is not up-regulated. Expression levels at stages 0-2 were set as 1. Significances are relative to the expression level of stage 0-2. (Students t-test, error bars are standard deviations) ((Figure modified from Kraeussling et al. [64]).

2.4.3. STAT3 in early medaka embryos

STAT3 is involved in various processes that are, amongst other things, related to proliferation and stem cell-ness. Previous work in our laboratory has indicated that the transcription factor STAT3 is signaling strongly to the nucleus in pre-MBT medaka embryos (see Diploma thesis "Analysis of STAT3-activity during early development of *Oryzias latipes*"; M.Kräußling). Specifically, STAT3 protein is evenly distributed between the cytoplasm and the nucleus in embryos between the 1-cell and the 32-cell stages but after reaching the 64-cell stage, STAT3 proteins showed a strongly enhanced localization to the nucleus in a high percentage of the cells.

Since the time point of STAT3 localization to the nucleus coincidences with the strongly increasing number of cells being positive for phosphorylated RNA polymerase II, this raised the question if STAT3 has a specific role at this time point.

To determine the possible function of the early localization of STAT3, two mutated versions of STAT3 were generated to investigate the influence on early development in medaka. These mutated STAT3 forms are (1) a constitutively active form which constantly signals to the nucleus without stimulation, and (2) a dominant negative form, which not only cannot be activated to its biological function, but also blocks functional wild type STAT3 proteins.

2.4.4. Generation of mutated medaka STAT3

Mutated versions of STAT3 have already been generated for the murine STAT3 and the functionalities of these mutations were well established for both, the constitutively active and the dominant negative form [70][71][72][73][74]. The generation of the medaka mutations was performed using the wild type medaka STAT3 sequence that had been cloned previously in our laboratory [75].

The generation of the constitutively active STAT3 (MF-STAT3-CA) was achieved by substituting the alanine residue at positions 661 and the asparagine residue at position 663 within the COOH-terminal loop of the SH2 domain of STAT3 (both positions are counted for the murine STAT3 sequence) by cysteines (Figure 21). The same approach was previously successfully used to generate a constitutively active from of the murine STAT3 (mSTAT3-C). For this protein, it had been shown that it was capable of bypassing the usual STAT3 activation and dimerization, which is initiated through tyrosine kinase phosphorylation, by a permanent dimerization of two mSTAT3-C monomers at the C-C loop [70].

The dominant-negative form of medaka STAT3 (MF-STAT3-DN) was generated by substituting the tyrosine at position 705 by phenylalanine. This not only blocks the activation of STAT3 via tyrosine phosphorylation, but also inhibits active endogenous STAT3 proteins [72][73]. The negative effect was also enhanced by substituting serine at position 727 with alanine which is required for maximal transcriptional activity [74][76][77][78] (Figure 21).

All three medaka STAT3 variants, the wild type, the constitutively active and the dominant negative form were cloned into the pEGFP-C1 plasmid (Clontech).

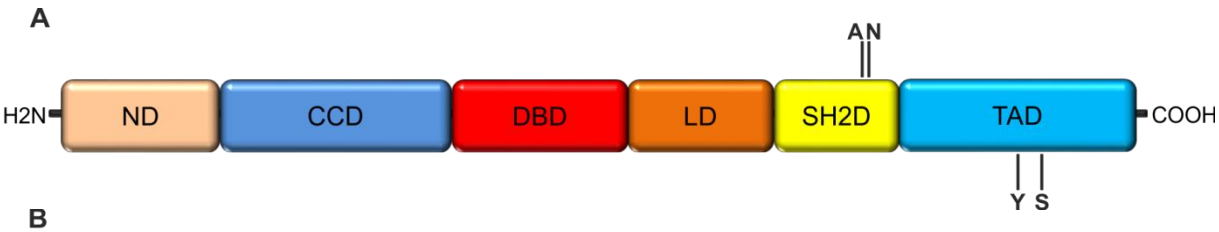

B

```
                1                                                                   70
MF_STAT3_WT     MAQWNQLQQL ETRYLEQLYH LYSDSFPMEL RQFLAPWIES QDWAYAANKE SHATLVFHNL LGEIDQQYSR
MF_STAT3_CA     .......... .......... .......... .......... .......... .......... ..........
MF_STAT3_DN     .......... .......... .......... .......... .......... .......... ..........
  Consensus     .......... .......... .......... .......... .......... .......... ..........
               71                                                                  140
MF_STAT3_WT     FLQENNVLYQ HNLRRIKQHL QSKYLEKPME IARIVARCLW EEQRLLQTAT STSQDGSAAH PTGTVVTEKQ
MF_STAT3_CA     .......... .......... .......... .......... .......... .......... ..........
MF_STAT3_DN     .......... .......... .......... .......... .......... .......... ..........
  Consensus     .......... .......... .......... .......... .......... .......... ..........
               141                                                                 210
MF_STAT3_WT     QILEHNLQDI RKRVQDMEQK MKMLENLQDD FDFNYKTLKS QGELNQDLNG NSQAAATRQK MAQLEQMLSA
MF_STAT3_CA     .......... .......... .......... .......... .......... .......... ..........
MF_STAT3_DN     .......... .......... .......... .......... .......... .......... ..........
  Consensus     .......... .......... .......... .......... .......... .......... ..........
               211                                                                 280
MF_STAT3_WT     LDQLRRQIVT EMGGLLTAMD YVQKNLTDEE LADWKRRQQI ACIGGPPNIC LDRLETWITS LAESQLQIRQ
MF_STAT3_CA     .......... .......... .......... .......... .......... .......... ..........
MF_STAT3_DN     .......... .......... .......... .......... .......... .......... ..........
  Consensus     .......... .......... .......... .......... .......... .......... ..........
               281                                                                 350
MF_STAT3_WT     QIKKLEELQQ KVSYKGDPII QHRPALEEKI VDLFRNLMKS AFVVERQPCM PMHPDRPLVI KTGVQFTNKV
MF_STAT3_CA     .......... .......... .......... .......... .......... .......... ..........
MF_STAT3_DN     .......... .......... .......... .......... .......... .......... ..........
  Consensus     .......... .......... .......... .......... .......... .......... ..........
               351                                                                 420
MF_STAT3_WT     RLLVKFPELN YQLKIKVCID KESGDVAAIR GSRKFNILGT NTKVMNMEES NNGSLSAEFK HLTLREQRCG
MF_STAT3_CA     .......... .......... .......... .......... .......... .......... ..........
MF_STAT3_DN     .......... .......... .......... .......... .......... .......... ..........
  Consensus     .......... .......... .......... .......... .......... .......... ..........
               421                                                                 490
MF_STAT3_WT     NGGRTNSDAS LIVTEELHLI TFETEVYHQG LKIDLETHSL PVVVISNICQ MPNAWASILW YNMLTNHPKN
MF_STAT3_CA     .......... .......... .......... .......... .......... .......... ..........
MF_STAT3_DN     .......... .......... .......... .......... .......... .......... ..........
  Consensus     .......... .......... .......... .......... .......... .......... ..........
               491                                                                 560
MF_STAT3_WT     VNFFTKPPVG TWDQVAEVLS WQFSSTTKRG LTIEQLTTLA EKLLGPSVNY SGCQITWAKF CKENMAGKGF
MF_STAT3_CA     .......... .......... .......... .......... .......... .......... ..........
MF_STAT3_DN     .......... .......... .......... .......... .......... .......... ..........
  Consensus     .......... .......... .......... .......... .......... .......... ..........
               561                                                                 630
MF_STAT3_WT     SFWVWLDNII DLVKKYILAL WNEGYIMGFI SKERERAILS PKPPGTFLLR FSESSKEGGI TFTWVEKDIS
MF_STAT3_CA     .......... .......... .......... .......... .......... .......... ..........
MF_STAT3_DN     .......... .......... .......... .......... .......... .......... ..........
  Consensus     .......... .......... .......... .......... .......... .......... ..........
               631                                                                 700
MF_STAT3_WT     GKTQIQSVEP YTKQQLNSMS FADIIMGYKI MDATNILVSP LVYLYPDIPK EEAFGKYCRP EAAHEPEAGG
MF_STAT3_CA     .......... .......... .......... ..C.C..... .......... .......... ..........
MF_STAT3_DN     .......... .......... .......... ..a.n..... .......... .......... ..........
  Consensus     .......... .......... .......... ..a.n..... .......... .......... ..........
               701                                                            765
MF_STAT3_WT     DSASITQPYL KTKFICVTPT NSGNTSDLFP MMSPRTLDSL MHNEPEAHSG HLDSITLDMD VASPM
MF_STAT3_CA     .......... .......... .......... ..A....... .......... .......... .....
MF_STAT3_DN     .......F.. .......... .......... ..A....... .......... .......... .....
  Consensus     .......y.. .......... .......... ..s....... .......... .......... .....
```

Figure 21: (A) Schematic illustration of the domain structure of the STAT3 protein. Abbreviations of each domain are indicated in the figure. ND: N-terminal domain (0-130 Amino acids); CCD: coiled-coil domain (131-320 AA); DBD: DNA-binding domain (321-465 AA); LD: linker domain (466-585 AA); SH2D: SH2 domain (586-688 AA); TAD: transactivation domain (689- 770 AA) [79].
(B) Alignment of the amino acid sequence of the wild type (WT) medaka STAT3 Protein (MF_STAT3_WT) and the two mutated forms, the constitutively active (CA) form (MF_STAT3_CA) and the dominant negative (DN) form of STAT3 (MF_STAT3_DN) respectively. The colored boxes mark the exchanged amino acids; green box for the CA form, blue boxes for the DN form. The residues Alanine at position 661 and Asparagine at position 663 (both positions are mouse-counted) were substituted with cysteine to generate the constitutively active form of STAT3.

2.4.5. Injection of MF-STAT3 mutants into medaka embryos

To investigate a putative role of early STAT3 signaling, medaka embryos were first injected with plasmids coding for the three different forms of medaka STAT3, the wild type, the constitutively active and the dominant negative form. For this, embryos at the 1-cell stage were injected with a mix containing one of the MF-STAT3 versions in a concentration of 20ng/µl together with mRNA encoding H2B-eGFP as an injection control. Embryos were first analyzed 24h after injection (Figure 22). Embryos injected with MF-STAT3-WT did not show developmental alterations and reached early neurula (stage 17), typical for this duration of development (Figure 22A). Embryos that were injected with MF-STAT3-CA appeared to be arrested in a pre-gastrula stage. The cells were arranged similarly to a blastodisc, typical for the late blastula or early gastrula stage, although the discs rim did not show the distinct boundary typical for a WT embryo (Figure 22B). The embryos that were injected with the plasmid carrying MF-STAT3-DN showed a relatively normal, but delayed development. Those embryos were still in a stage 15 like configuration, which is an about 7-8 hours retardation compared to normal development (Figure 22C).

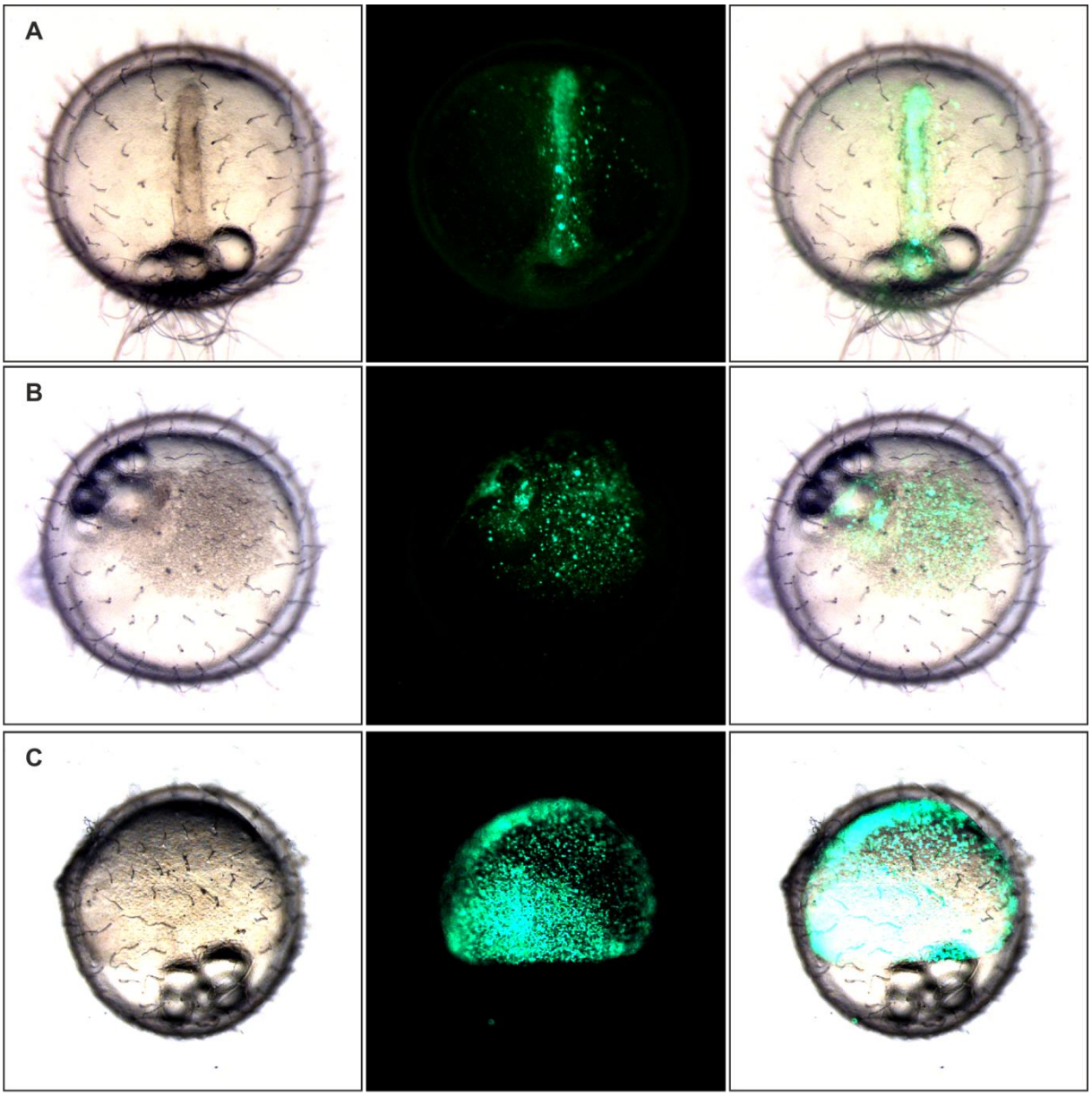

Figure 22: Effects of plasmids carrying different versions MF-STAT3 on medaka fish development after co-injection with H2B-eGFP_mRNA (green channel) into medaka embryos at the 1-cell stage after 24h of development; all dorsal views. (A) Control embryo injected with H2B-eGFP; embryo is at around stage 17. (B) Embryo injected with MF-STAT3-CA; embryo has not entered gastrulation. Cells are still arranged in a blastodisc-like structure and are arrested at a pre-gastrula stage. (C) Embryo injected with MF-STAT3-DN; embryo showing morphology typical for stage 15.

After 48hours of growth the embryos that that were injected with MFSTAT3-WT still showed normal development and reached stage 30, typical for this physiological embryogenesis (Figure 23A). However, most of the MF-STAT3-CA injected embryos had died (28/35). The remaining embryos demonstrated different attempts for a normal development. In the given

example, the majority of cells formed a-streak like structure of cells at the developmental stages 16/17, late gastrula or early neurula stage (Figure 23B).

Also, the majority of embryos injected with MF-STAT3-DN did show severe developmental deformations (24/30). They usually had atrophied trunks that were less developed than those of WT embryos, or they were generally arrested back in development. Especially the head formation was heavily affected (Figure 23C).

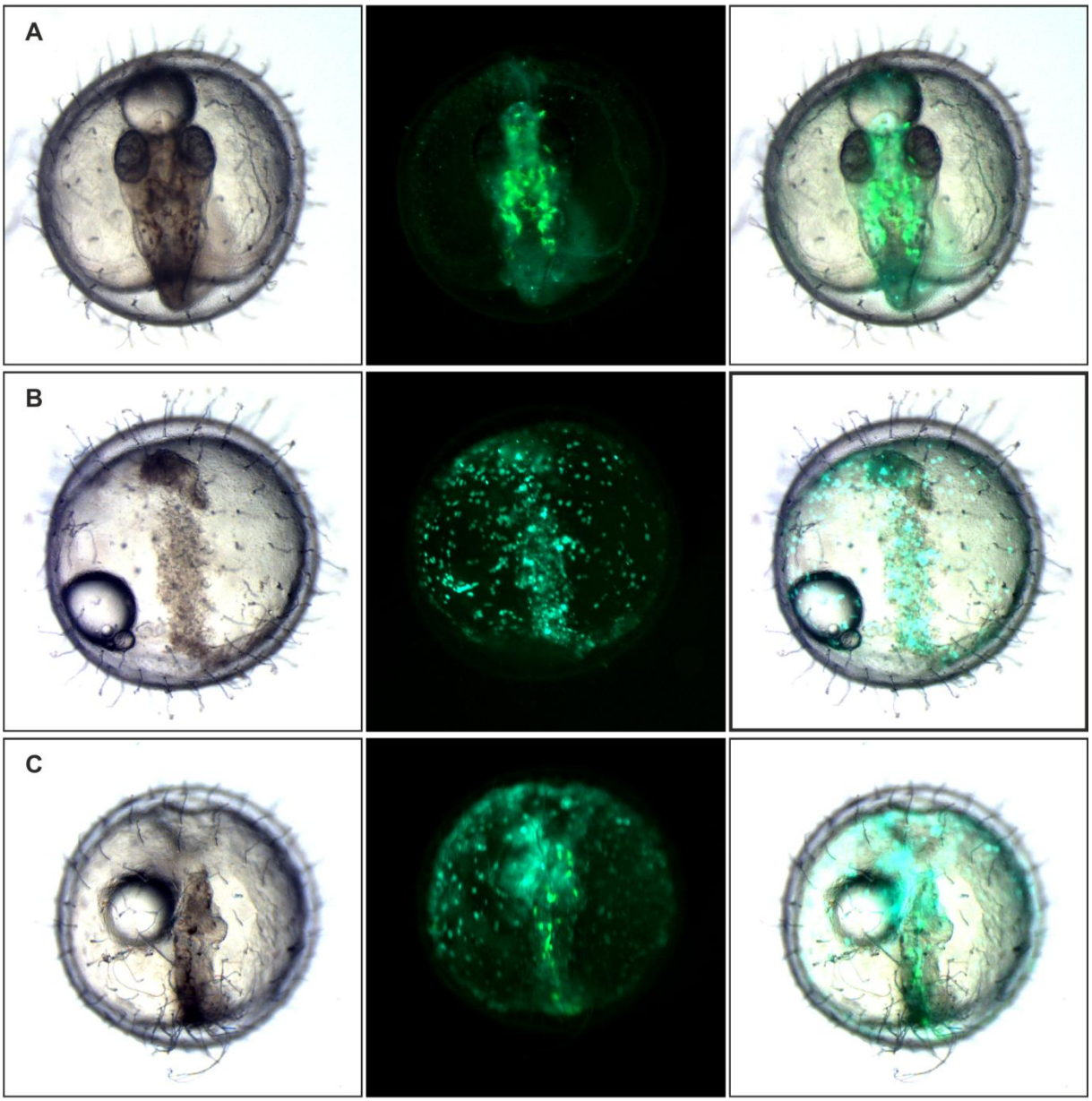

Figure 23: Effects of plasmids carrying different versions MF-STAT3 on medaka fish development after co-injection with H2B-eGFP_mRNA (green channel) into medaka embryos at the 1-cell stage after 72h of development; all dorsal views. (A) Control embryo injected with H2B-eGFP; embryo is at around stage 30. (B) Embryo injected with MF-STAT3-CA; single cells covering the yolk in a smooth formation, majority of cells forming a narrow streak. (C) Embryo injected with MF-STAT3-DN; embryo showing configuration of a stage 22 medaka WT, head structure is heavily deformed, eyes are missing.

In summary, embryos that were injected with the mutated MF-STAT3 forms and showed developmental defects and did not develop into viable larvae. The CA injected embryos displayed more severe effects and embryonic lethality while from the DN several were able to develop until hatching, but also died shortly after (6/53).

To investigate the effects of STAT3 on very early development, mRNAs of the three STAT3 variants were injected into medaka embryos at the 1-cell stage.

Unfortunately, the mRNA injections could not confirm the data from the plasmid treated embryos since no effects were detectable in the mRNA injected embryos. Only after injecting high dosages of mRNA (~1µg/µl) defects were detected, but those could not be distinguished between the CA and DN injected embryos.

3. Discussion

3.1. Loss of cell cycle synchrony in pre-MBT embryos of medaka

In this study, confocal microscopy on fixed medaka embryos at distinct stages has revealed that embryos lose cell cycle synchrony several stages before MBT.

In classical studies, cell cycle durations and synchronous divisions of embryonic development were mostly studied via conventional time-lapse cinematography [23][63][43][80]. There, the time spans between each cell division were determined by relatively easily detectable changes of the morphology, which were associated with a specific stage during cell cycle. For example, the brake-down of the cellular envelope during cytokinesis was used as marker for determining the cell cycle length in zebrafish [20]. In contrast to that, only very few studies used fluorescent dyes to determine cell cycle stage, for example incorporation of BrdU [37].

For determining the earliest time point of cell cycle desynchronisation in medaka, confocal imaging of fixed embryos at different developmental and cell cycle stages was used. Cell cycle synchrony in these embryos was determined by looking at single nuclei. If they showed differing chromosome morphology they were scored as being at different steps of the cell cycle [81] [82]. Hence, it was possible to detect the first cycle irregularities and clear asynchronies at cycle 5, the division from 16 cells to 32 cells. First, it was unclear if this desynchronisation was truly caused by cell cycle lengthening or if it was an effect of PFA-fixation and preparation for the confocal imaging. Only by investigating embryos of later stages it became clear that this desynchronisation was not the cell cycle desynchronisation associated with MBT onset, but the beginning of a metasynchronous cell divisions pattern. This kind of division pattern was characterized by cell divisions that occurred in clear spatial and temporal waves that start in the middle of an embryo and spread out to the embryos' rim. Wave-like cell divisions had already been reported for other species like *Xenopus* [63][27][83] and zebrafish [84][20][1][85], which divided in metasynchronous waves after cycle 5 and cycle 6 respectively, as well as for *Drosophila*, in which the waves progress in a

symmetrical wave from the anterior and posterior poles after cycle 9 [21][27]. In those species, the wave-like progression of cell division was not the result of a significant cycle lengthening and hence there is no indication of a MBT initiation [63][13][20].

My time lapse observations of the H2B-eGFP injected embryos, which were primarily performed to confirm the division pattern change, also did not provide reliable data about cell cycle durations and cycle lengthening. This is due to the limited temporal resolution of standard confocal microscopy. In zebrafish, cells divide with a 14 to 15 minutes interval during cleavage phase up until cycle 9 at 28°C. Afterwards, cell cycle lengthens by 2 minutes in cycle 10 and by an additional 5 minutes for each of the next 2 cycles. This leads to a cell cycle length of about 33 minutes at cycle 12, the time point of MBT start [20] [20]. Unfortunately, no reliable data corresponding the precise cell cycle duration are available for medaka, but Iwamatsu described the early medaka development with 35 minutes for one round of cell divisions at a temperature of 26°C [2].

Unfortunately, it was not reported at which temporal resolution the time laps observations in zebrafish were performed [20]. However, in this thesis continuous confocal scanning of injected medaka embryos was performed with a delay of 4 minutes between each confocal stack. This long interval makes it impossible to determine the exact duration of a cell cycle as well as to detect duration changes. However, this experiment has confirmed the loss of total cycle synchrony by cycle 5 and the establishment of the metasynchronous division pattern afterwards. This observation correlates with data from Xenopus and zebrafish in which cell divisions are metasynchronous by cycle 5 [27] and cycle 6 [86] respectively.

The mechanism underlying the metasynchronous cell division progression itself is still unknown [63]. A hypothetical explanation could be the differing access and supply of cells to maternal compounds in relation to their position in the embryo [87].

However, this theory is put in question by the observations made in asymmetrically dividing embryos after injection with H2B-eGFP mRNA. Although particular embryos showed highly

distorted embryonic shapes and also lacked the typical embryonic morphology, they were still able to maintain a highly structured cell division pattern. Instead of progression in waves that started in the middle of the embryos, for example cell divisions in these embryos occurred in waves that progressed from one pole to the other.

Further contradictory data came from studies on Xenopus, which showed that the cell cycle control in post-MBT embryos no longer depends on the nucleo-cytoplasmic ratio, but henceforward on cell contacts and external factors [44][88]. More precisely, isolated blastomeres in a dish maintained the same cell cycle duration and cell synchrony (~30min at 21°C; [44]) as blastomeres in the embryo (~35min at 23°C; [13]), but stopped cell proliferation after the 12^{th} division [88]. Culturing isolated blastomeres on different substrata instead was able to maintain cell proliferation for several additional cycles, but this did not last past the 16^{th} or 17^{th} cycle. Therefore appear blastomeres to be highly depending on factors from the outside at the latest after this time point [88].

Both, the rudimental wave-like divisions in asymmetrically cleaved medaka embryos, as well as the discrete division of isolated Xenopus blastomeres indicate that the metasynchronous division pattern is not controlled by differing access to yolk-factors.

3.2. Cell cleavage asymmetry and cell volume diversity

3.2.1. Asymmetric cell cleavage in early medaka embryos

The results in this thesis demonstrate that a noteworthy number of embryos show high levels of asymmetric cell cleavage at a very early developmental stage which impairs the homogeneous distribution of cellular material.

During the time lapse observations of H2B-eGFP mRNA injected embryos, an asymmetric division profile when dividing from 2 to 4 cells was occasionally observed. These kinds of embryos stand in contrast to the idealized development of medaka as meticulously reported by Iwamatsu [2]. For this ideal medaka embryo, he reported that cells are arranged in squares or rows during the first 4 cycles (1 to 16 cells), forming rectangular-like embryos. Later, upon the 32-cell stage and until the initiation of gastrulation, cells are arranged in a roundish and multi-layered disc.

However, this thesis has demonstrated that a noteworthy percentage of medaka embryos diverge dramatically from this ideal embryo. Considering cycle 2 (2 to 4 cells), it was detected that only about one quarter of the observed embryos represented the idealized embryo by showing homogenous morphology after highly symmetric cell divisions. Instead, half of the embryos showed slightly shifted cleavage furrows with reduced symmetry at the interception point. Based on the relative frequency of 55% of those embryos, it can be assumed that they represent the normal situation in medaka. However, the remaining quarter of the investigated medaka embryos showed higher levels of asymmetric cell arrangements and embryonic morphology.

Asymmetric cleavages also occurred during other cell divisions and not only during cycle 2, but those were only sensed, but not documented in detail during this thesis since they only had a minor influence on normal development, or it was not possible to measure them with confidence.

Asymmetric cell divisions from the 1-cell stage to the 2-cell stage would have the largest impact on embryogenesis. At the 1-cell stage, the embryos consist of only one cell and the orientation of the cleavage furrow has no influence on an equal distribution of cell volume. The determining factor during this first cleavage is the correct positioning of the mitotic spindle in the center of the cell since asymmetric cell divisions are caused by contractile rings that are not located in the middle of the cell [89]. The orientation of the contractile ring itself is determined by the orientation of the mitotic spindle during anaphase of mitosis as the cleavage plane is established on the preceding metaphase plane and bisects the mitotic spindle [90][91][92][93].

Clearly asymmetric cleavage furrows were also observed at cycle 3 (4 to 8 cells, data not shown), but the unequal distribution of cellular volumes by sporadic asymmetric cell divisions at this cycle have a smaller impact on the embryo than during the division from 2 to 4 cell.

As it has also been shown, the orientations of the two cleavage furrows during cycle 2 mainly determinate the basic embryonic shape and morphology for the next couple of cell divisions before embryos have finally established the typical multilayered disc of the pre-blastula stage. This kind of influence of asymmetric cell cleavages is reduced further by each new cell cycle due to the increasing number of cells within a single embryo. The further the embryo has progressed, the smaller is the number of affected cells by isolated asymmetric divisions.

Still, a critical step might be cycle 5 (16 to 32 cells), when the homogenous blastomeres of the 16-cell stage are separated into two layers, forming an inner layer surrounded by an outer layer, which results in a more roundish and disk-like embryo and determining the embryos morphology during the next divisions [2].

However, asymmetric cell divisions during cleavage phase have been reported for other species like leech [37], sea urchin [94], *C.elegans* [95][96], zebrafish [87], mouse [89][97]. At least for leech, *C.elegans* and sea urchin they are used for cell fate determination. Here, the orientations of the cleavage furrows dictate the segregation of cellular components between

daughter cells [98][99][100]. This mechanism for example determines germ cells in C.elegans [101][98]. But this does not apply for medaka because not all embryos divide asymmetrically. The observed asymmetries at the 4-cell stage in medaka embryos are most likely the direct results of asymmetrical cleavage furrows that progressed with eccentric orientation during the previous cell division [102][103]. But as this work has shown, the asymmetric cleavages at cycle 2 still can have remarkable influence on the following developmental processes by interfering with the equal distribution of cell volume and cellular compounds and they can also heavily impair the early embryonic morphology and division pattern. Furthermore, the grade of asymmetry and the resulting imbalance in cell volume distribution are neither a rare phenomenon, nor do they have a seemingly negative effect on the proper completion of development of medaka. In fact, highly symmetric cleavages, as they were described for the ideal medaka embryo by Iwamatsu [2], show almost the identical survival frequency as highly asymmetric.

3.2.2. MBT control by the nuclear-cytoplasmic-ratio

In my thesis I could demonstrate by confocal imaging that some medaka embryos showed large volume differences at the 4-cell. Although different regulatory models have been introduced and proven at different levels, the hypothesis that the nucleo-cytoplasmic ratio is the major control mechanism for midblastula regulation has been established as the best proven and most reliable one [13][43][25][20][58]. It proposes that a regulatory factor is already present in high concentrations in the cytoplasm of the unfertilized egg. It is supposed that this factor binds to chromatin factor and represses RNA transcription [13]. Also, its high dosage in the egg is capable to maintain the repressing effect until MBT while it is titrated out by the increasing amount of DNA, which is duplicated with every cell cycle [50].

However, as this study shows, cells usually differ in volumes in single medaka embryos at the 4-cell stage. More precisely, only very few embryos (15%) contained cells with volumes that can be taken as “even”, whereas other embryos showed significant differences in cell volumes. In the most extreme case, the biggest cell contained 2.7 times more volume than the smallest cell of the same embryo. Several publications have demonstrated that manipulated cell volumes or different amounts of DNA resulted in late or early MBT onset, respectively [23][25][44][13][20][43][45].

So, if cells in medaka embryos differ in cell volumes at least by the factor 2, the only logical consequence is that those cells should enter MBT at different time points. Since large volume differences already appeared at the 4-cell stage, it is a logical consequence that the subsequent cell divisions will produce large clusters of cells of different volumes. Consequently, this could mean that about one quarter of all cells in those embryos enter MBT one cell division earlier than normal, a second quarter enters MBT one cell division later than normal, and only half of all cells, enters MBT at the correct time point. In return, cell volume differences at later cell divisions would have smaller consequences, as the percentage of affected cells from

the total embryo would be lower and accordingly the number of cells that enter MBT at a diverging time point would be lower as well.

With the available technology it was not possible to confirm this hypothesis by monitoring the cell volume progression of single cells in living embryos throughout the entire cleavage phase. Hence, it can only be assumed that the observed cell volume differences at the 4-cell stage truly lead to shifted MBT activation times. The attempt to monitor cell volumes with a high enough accuracy in a dividing embryo represents an enormous technical challenge. Although conventional confocal laser scanning microscopy is sufficient to investigate fixed embryos, it is not fast enough for live-imaging complete cleavage phases with high-enough resolution. However, several more advanced imaging techniques have emerged and some of them show the potential to allow this task in future studies.

First, there are variations of the selective plane illumination microscopy (SPIM) or other fluorescence microscopy techniques that illuminate the sample with a focused light sheet instead of a light-beam. They allow time lapse scanning at very high frequency and resolutions, but still produce image data with the confocal effect [104]. Thereby they have become increasingly popular in developmental time lapse studies [105][85][106][107].

Furthermore, the third harmonic generation (THG) imaging technique, a noninvasive technique that works with laser-wavelengths near the biological penetration window and hence produces no optical damage, has been recently introduced into the field of developmental studies. Another great advantage of this technique is that no fluorescent labeling is required and thus overcomes the usual problem of dye availability, stability and toxicity.

So far, THG imaging was successfully used to monitor developmental processes in different species like *C.elegans* [108][109], *Drosophila* [110], *Xenopus* [111], zebrafish [112][87] and mouse [113]. For example, this technique made it possible to monitor the cell cycle

lengthening and the establishment of a metasynchronous division pattern in zebrafish embryos. Furthermore, cell volume variability between cell siblings was also reported [87].

3.3. Asymmetric MBT activation

The results in this thesis have demonstrated that cells in medaka embryos at the 4-cell stage can differ in cell volume by noteworthy scale, which has a putative effect on the synchronous MBT activation.

The cell cycle lengthens at the end of cleavage phase before MBT. This could be of benefit for the "slow" cells that need one additional cycle to reach the MBT-required nucleo-cytoplasmic ratio. Also, at the MBT, the metasynchronous cell division is lost and cells develop their own cell cycle duration independently of the other cells [13][20]. This additionally argues for a low importance of the total embryo to enter MBT synchronously.

Moreover, it has already been assumed that cell volume fluctuations during early cleavage phase could lead to local fluctuations of MBT initiation rather than the rapid transition of the total embryo from synchrony to asynchrony and from pre-MBT to MBT [87]. Those fluctuations of asynchronous cell cycle lengthening have been reported for zebrafish and it was suggested that those result from unequal cell volume distributions during early cleavages [20]. Thereby, it can be reasoned that the diverging cell volumes in medaka embryos at the 4-cell stage also results in fluctuated MBT initiation. Furthermore, since higher cell cleavage asymmetry resulted in higher cell volume differences, this indicates that fluctuated MBT initiations should be more likely in more asymmetrically cleaved embryos.

3.4. Transcriptional activity in medaka embryos before MBT

3.4.1. RNAPII phosphorylation in pre-MBT medaka embryos

In my work I could show that RNA polymerase II (RNAPII) becomes phosphorylated in medaka embryos already with the 16-cell-stage, which is a strong indicator for active transcription.

So far, the earliest time reported point for active transcription in medaka was stage 11[114].

For investigating transcriptional activity in pre-MBT medaka, embryos were investigated for RNA polymerase II phosphorylation by immunofluorescence staining. For this, a primary antibody targeting the phosphorylation site in YSPTSpPS-repeats in the carboxyterminal domain (CTD) of human RNA polymerase II (http://www.scbt.com/datasheet-13583-p-pol-ii-8a7-antibody.html; 06.17.2011) was used. Although this antibody was originally generated to target the CTD of RNAPII of human origin, it is also suitable for other species including medaka, since the YSPTSPPS-repeats of the CTD are highly conserved in fungi, plants and animals and the only interspecific differences found regard the number of tandem repeats [115].

The CTD of RNAPII was investigated for phosphorylation because it has been shown that the initiation of RNA transcription only takes place when RNA polymerase II is hypophosphorylated at its carboxy-terminal domain, while elongation only takes place when RNAPII is highly phosphorylated at the CTD [68][67][66]. Thereby, CTD-phosphorylation of RNA polymerase II was taken as a clear marker for an active transcription machinery and unphosphorylated CTDs have been shown to be a reliable marker for inactive transcription [66][67][68][69] [116][117].

By investigating the RNAPII-CTD phosphorylation, I found the first indications for transcriptional activity in pre-MBT medaka embryos as early as at the 16-cell stage (stage 6). Interestingly, the phosphorylation occurred only in a small fraction of cells. The percentage of phosphorylation positive cells increased with reaching the 64-cell stage (stage 8) to high

levels. The reason, why only a small amount of cells at the 16- and 32-cell stages and later a large amount at the 64-cell stage and later stages showed RNAPII phosphorylation remains unclear. The strong increase of cells with phosphorylated RNAPII at 64 cells argues for a specific activation of transcription at this stage. Otherwise the percentage of positive cells would just show a smooth increase with every cell division. The appearance of phosphorylation in cells before the 64-cell stage could be the result of a leaky mechanism that regulates the transcriptional repression. Alternatively this may indicate a so far unnoticed zygotic transcription potential importance for very early embryonic development.

Furthermore, p-RNAPII positive cells were located mainly at and near the embryonic center and almost never at the rim. A possible explanation for this pattern could be that embryos showing this phenomenon were at a very late stage of cell cycle with more central cells already fully in transcriptional active cell stages, whereas peripheral cells were delayed and still in a transcriptional inactive cell stage. Later, in embryos at the 128-cell stage, embryos were found in which several cells in central localization were observed that were negative for RNAPII phosphorylation. This could indicate the beginning of the next round of metasynchronous cell division and central cells have already stopped RNA transcription and RNAPII was dephosphorylated. This theory is supported by a study which reports that the first transcription of genes occurs in *Drosophila* embryos in patterns that mimic the wave-like cell cycle progression. Here, transcription was detected in nuclei at the prophase, metaphase, and anaphase, whereas telophase and interphase nuclei seemed to be transcriptional inactive [15].

However, against this theory argues the fact that no embryos at the 64-cell stage were found that showed only RNAPII phosphorylation in non-central cells, which would represent the beginning metasynchronous cell division to the 128-cell stage. It is stochastically unlikely that all investigated embryos at the 64-cell stage were fixed at time points that did not involve a pre-mitotic stage to 128-cells. Furthermore, phosphorylation in very peripheral cells was still

rare, even in embryos that also showed unphosphorylated cells in the center. Either one of those two positions should be phosphorylated since metasynchronous cell divisions occurred not at that rate that a new cycle started while the previous one was not completely finished.

This question can only be answered in the future by real time observations in dividing embryos.

3.4.2. Increase of transcripts before MBT

This thesis has demonstrated that mRNA transcription of specific genes is active at distinct time points before the midblastula transition.

So far, the earliest time point of zygotic transcription in medaka was only determined by the first appearance of paternal transcripts in embryos. For this, two inbred strains, which were generated from two naturally occurring population and feature polymorphisms for certain ESTs, were crossed together and the embryos were monitored for expression of paternal ESTs. This has determined the beginning of zygotic transcription and MBT initiation to stage 11, an early blastula stage of about 2000-4000 cells [62].

While the phosphorylation of the RNAPII-CTD alone is already a strong indicator for active transcription, the amplification of mRNAs was also verified directly by RT-PCR on cDNAs from different time phases during cleavage phase.

These periods spanned the stages 0 to 2, 8 to 10, and also the single stages 11 and 14. Embryonic stage 14 is a pre-mid gastrula stage and should represent a transcriptional active stage whereas stage 11 was the hitherto earliest time point of detectable zygotic transcription [114]. Pooled stages 8-10 contained the embryonic stages 64 to 1000 cells during which RNAPII shows enhanced CTD-phosphorylation. This mixed pool of cell stages was not suitable to give information about transcriptional initiation specifically for the 64-cell stage, but still covers only pre-MBT stages. Nevertheless, a detectable increase of mRNA levels for this pool of cell stages still is at least 2-3 cell divisions earlier to the hitherto earliest time point of transcription initiation at stage 11 [114]. The target genes for this investigation were chosen from a study in which the transcriptional upregulation for 125 out of over 16.000 genes in a mixed pool of 64-/128-cell stage zebrafish embryos was demonstrated [49].

Nevertheless, the proof of a detectable increase of transcripts for the period from 64 to 1000 cells together with the RNA polymerase II phosphorylation after the 64-ecll stage demonstrates that transcription is active in medaka embryos prior to the assumed midblastula

transition. Furthermore, the fact that CTD-phosphorylation of RNAPII appears never in all cells of medaka embryos at pre-MBT stages strongly speaks for a “soft” activation of transcription and not for an all-or-nothing event at a specific stage, although the strong increase in phosphorylation at the 64-cell stage argues for a certain role of this embryonic stage.

The here described transcription at early stages is contradictory to the only study so far that has investigated zygotic transcription initiation in medaka

3.5. STAT3 signaling in pre-MBT medaka embryos

In my thesis I could show that mutated STAT3 proteins are able to cause developmental defects if injected as DNA, but lack this ability if injected as mRNA.

STAT3 has been in the focus of embryological and stem cell research because it has been shown that the maintenance of the stemness-status in murine embryonic stem (ES) cells and self-renewal of ES cells is strongly depending on the activation of STAT3 via the Leukemia Inhibitory Factor (LIF) [118]. Inhibition of STAT3-activation consequently blocks self-renewal and promotes ES cell differentiation [119]. Additionally, STAT3-/- mouse embryos die at embryonic day 7 at the beginning of gastrulation [120].

However, these findings could not be confirmed in other ES cell lines from other species, especially not for human ES cell lines that do not require STAT3 signaling for ES self-renewal and in which STAT3 phosphorylation is not sufficient to prevent differentiation [121][122][123].

Another species that differs from mouse in this respect is the medaka. In this context strong hints were discovered that STAT3 signals to the nucleus in medaka embryos before the midblastula transition. More precisely, medaka embryos show an even distribution for STAT3 between the nucleus and cytoplasm until the 32-cell stage and a strongly enhanced nuclear localization beginning with the 64-cell stage (see Diploma thesis “Analysis of STAT3-activity

during early development of *Oryzias latipes*"; M.Kräußling) [124], which is several cell stages before the blastula stage from which medaka ES cells were obtained [125]. Interestingly, no STAT3 accumulation was detected neither at the later blastula stage nor in ES cells from this stage [75].

For the context of the dissertation work this was interesting because STAT3 is a transcription factor and this special type of proteins control the level of mRNA transcription by binding to specific DNA sequences in enhancer or promoter regions after target sequence recognizing which is mediated by DNA-binding domains [126]. Transcription itself is regulated by interaction with components of the basal transcription complex that assembles at the gene promoter region. Enhanced transcription is the result of a direct influence on the rate of transcription factor complex assembly or by stimulating the complex's activity [126][127][128]. Transcriptional repression on the other hand is achieved by negatively acting transcription factors that block promoting factors from binding to DNA or even by factors that can inhibit transcription by direct or indirect interactions with the basal transcription complex [126]. In this context STAT3 can function either as an activator or repressor for transcription.

Thereby, a clear nuclear enrichment of STAT3 specifically at the 64-cell stage argues for a functional transcriptional regulation, especially the activation of certain genes by this transcription factor.

The injection with plasmids for a constitutively active MF-STAT3 into medaka embryos led in the majority of embryos to a developmental arrest at the onset of gastrulation. Similar results were found in Xenopus eggs that arrested at gastrulation after inhibition of protein synthesis [129][80]. The effects in medaka embryos after injection with the dominant negative MF-STAT3 were less distinct and showed several kinds of phenotypes that could not clearly assigned to a specific developmental process. However, the phenotypes for the malformed heads argue for different affected tissues like forebrain, hindbrain and midbrain [130][131].

Both phenotypes however were most probably caused by mutated STAT3 proteins that were translated from plasmids at a large scale only after the activation of zygotic transcription near the MBT and thereby may only represent post-MBT effects. The exact timing of transcription start from CMV promoters has never been determined in embryos, but the first appearance of CMV driven transcripts were detected in zebrafish at 2h after injection [132], which corresponds to a developmental stage of about 128 cells for developing at 28.5°C [1]. Although this observation correlates with the first wave of transcription in zebrafish [49] and with the observed activation of the transcription machinery in this study, it remains unlikely that the limited number of produced mutated STAT3 proteins during the fast cell cycles would be sufficient to cause detectable defects. Only after cleavage phase has ended it seems plausible that the slowed cell cycle facilitates the production of sufficient amounts of protein and its interaction with the wild type protein.

In order to target at pre-MBT function of STAT3 shortly after the 64-cell stage, mRNAs coding for the mutated STAT3s were injected, but unfortunately without a significant effect.

Only injecting a very high dosage of mRNA, about 800ng/µl, resulted in detectable developmental defects, but those occurred also in the control embryos and thereby represent effects that were caused by the high injection dosage and rather not by the STAT3 proteins. Perhaps the effects of low dosages injections were inhibited or diminished by the maternal STAT3 mRNAs and proteins, as well as by the fast progressing cell divisions during cleavage phase.

Support for a transcriptional regulatory activity of medaka STAT3 come from a recent study that showed that a *Drosophila* STAT (STAT92E) works together with the transcription factor ZELDA as a transcriptional activator of a large number of zygotic genes which are transcribed at early MBT [133]. In this combination, STAT works as a general transcriptional activator, while ZELDA controls the spatial pattern and the level of transcription.

Unfortunately, the data from the injected embryos were not clear enough to allow assumptions why STAT3 is translocated to the nucleus in pre-MBT medaka embryos.

4. Outlook

The results described in this thesis represent a basis for new approaches in the field of embryogenesis, especially for studies concerning the MBT regulation and zygotic genome activation. The identification of asymmetric cell cleavages at early developmental stages and their impact on the homogeneous distribution of cellular materials implies that this has a putative effect on the synchronous MBT activation. This finding promises the potential for future investigations to answer long standing and unexplained observations by new time-laps techniques that will allow the embryo-wide and simultaneous determination of cell volume modifications and individual MBT activation on a single cell resolution.

The detection of the pre-MBT transcription at specific stages and in distinct cell populations represents a new point of view for the problem when and how transcription is activated during early embryogenesis. Pre-MBT activation of transcription has already been reported for other species, but only as a global, embryo-wide event. The here presented data, which indicate that transcription is initiated in specific temporal and spatial patterns, open up new perspectives on this old mindset. These findings represent a new and promising starting-point for further experiments, with the possibility for new and instructive insights into a still only poorly understood, but highly important developmental period.

5. Summary

The study of animal development is one of the oldest disciplines in the field of biology and the collected data from countless investigations on numerous species have formed a general understanding of the animal life-cycle.

Almost one century ago, one consequence of these intense investigations was the discovery of specific morphological changes that occur during the cleavage phase, a period that follows fertilization and egg activation at the very beginning of animal embryogenesis. These observations resulted into the formulation of the concept of a midblastula transition (MBT).

So far, the mechanism of the nucleo-cytoplasmic ratio model is the only one that explains MBT regulation in a satisfying way. It suggests that the MBT is controlled by several maternal repressive factors in the egg, which are titrated out by every cell division until they lose their repressing potential.

Although this regulatory mechanism was proven for several species and in different approaches, it is still only a rudimentary model for MBT control and leaves numerous questions unanswered.

On this conceptual background, this thesis has shown that embryos from the medaka fish (*Oryzias latipes*) lose their cell cycle synchrony already after the fourth or fifth round of cell divisions, and replace it by a metasynchronous divisions pattern, in which cell division occurs in clear waves beginning in the embryo's center. The reason for this change in division mode is still unknown, although several hypotheses were put forward, most notable a difference in yolk-access between cells. However, this theory was weakened by division waves that progressed from one embryonic pole to the opposing one, which were occasionally observed in deformed embryos, leaving the mechanism for this phenomenon furthermore unclear.

Those deformed embryos were most likely the result of asymmetric cell divisions at very early stages, a phenomenon which occurred in a significant percentage of medaka embryos and which directly influenced the equal distribution of cytoplasmic material. It could not be

uncovered what kind of effects this unequal distribution of cytoplasm exerted on the progression of embryonic development, but it can be argued that relevant differences in cell volumes could result in cell clusters that will enter MBT at different time points. Comparable observations were already made in other species and it was hypothesized that they were the direct results of early unequal cell cleavages.

Finally, it was demonstrated that zygotic transcription in medaka embryos is activated prior to the hitherto assumed time of the first transcriptional initiation. Moreover, indications were found that strongly speak for a transcriptional activation that occurs in two steps; a first step at the 16-cell stage when first cells were identified positive for RNAPII phosphorylation, and a second step at the 64-cell stage, when the number of p-RNAPII positive cells significantly increased. A stepwise activation of zygotic transcription was already observed in other species, but only for the overall increasing amount of mRNAs and irrespective of the actual number of transcriptionally active cells within the embryos.

A model that summarizes the here presented processes during the medaka cleavage is shown in Figure 22.

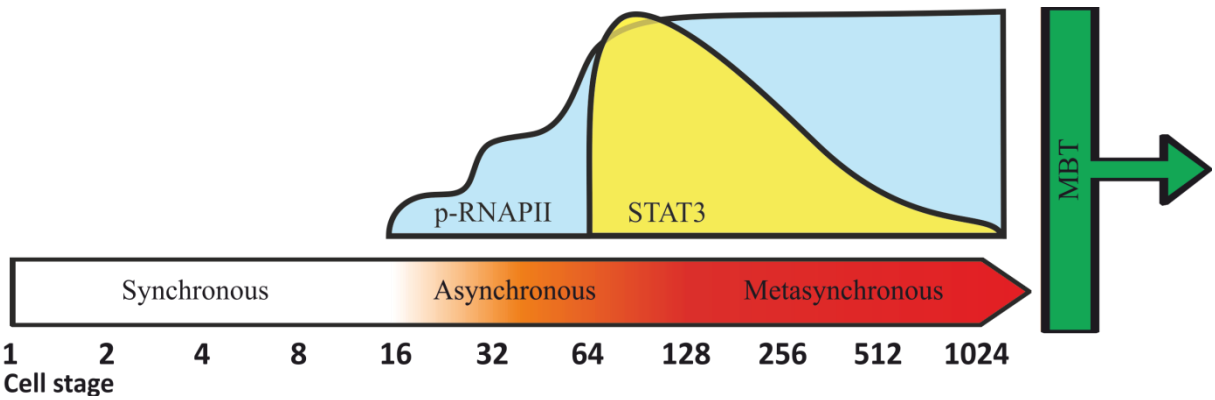

Figure 22: Illustrated is the time line of the transition from a synchronous to a metasynchronous division pattern. The stepwise increase of RNA PolymeraseII phosphorylation after the developmental stage 16-cells is demonstrated by the blue box. The strong nuclear localization of STAT3 a the 64-cell stage and the decline during the following stages is illustrated by the yellow box. MBT starts shortly after (green box).

Overall, these data confirm and expand the basic knowledge of pre-MBT embryos and about the MBT itself. Furthermore, they also suggest that many early processes in pre-MBT embryos are only rudimentarily understood or still totally unknown.

6. Zusammenfassung

Das Studium der Entwicklung von Tieren ist eine der ältesten Disziplinen in der Biologie. Die gesammelten Daten von unzähligen Untersuchungen an den verschiedensten Spezies wurden dazu benutzt, um ein generelles Verständnis des tierischen Lebenszykluses zu formulieren.

Ein wichtiges Ergebnis der intensiven Untersuchungen war vor etwa einem Jahrhundert die Entdeckung spezifischer morphologischer Veränderungen, die sich während der Teilungsphase, der Zeitperiode die der Befruchtung und Aktivierung des Eies am Anfang der Embryogenese folgt, vollziehen. Diese Befunde führten schlussendlich zur Formulierung des Konzepts einer „Mid-Blastula Transition“ (MBT).

Bisher gibt es nur eine Theorie die die Regulierung der MBT in befriedigender Weise erklärt. Dies ist das Model des Kern/Plasma-Verhältnis, welches sich aus dem Verhältnis DNA-Menge zu Zytoplasmavolumen ableitet. Es erklärt die MBT-Aktivierung durch bisher unbekannte, maternal deponierte Faktoren im Ei, welche die MBT Aktivierung kontrollieren, deren Konzentration allerdings mit jeder Zellteilung verdünnt wird, bis sie schließlich ihre blockierende Funktion verloren haben.

Zwar wurde die Existenz dieses Mechanismuses schon in zahlreichen Spezies experimentell bewiesen, allerdings bleibt er nur eine ungenaue Beschreibung der ablaufenden Prozesse und lässt weiterhin viele Fragen unbeantwortet.

Vor diesem Hintergrund hat diese Arbeit gezeigt, dass die Zellzyklen in Embryonen von Medaka (*Oryzias latipes*) ihre Synchronität schon nach dem vierten oder fünften Teilung verlieren, und diese durch ein Teilungsmuster ersetzt wird, das als „metasynchron“ bezeichnet wird. In diesem Teilungsmuster verlaufen die Zellteilungen in Wellen, die im Zentrum des Embryos beginnen und sich von dort nach außen hin radial ausbreiten. Noch ist der Sinn einer auf diese Art verlaufenden Zellteilung unbekannt, auch wenn es verschiedene Theorien gibt die versuchen den zugrunde liegenden Mechanismus zu erklären. Allen voran steht die Theorie eines unterschiedlichen Zugangs zu Faktoren innerhalb des Dotters. Allerdings wird

diese Theorie durch die Beobachtungen in verformten Embryonen wiederlegt, in denen sich die Teilungswellen von einer Seite des Embryos zur gegenüberliegenden Seite ausgebreitet haben. Somit bleibt der Mechanismus für diese Art der Zellteilung weiterhin unklar.

Nicht zu vergessen ist, dass diese deformierten Embryonen eine der möglichen Konsequenzen asymmetrischer Furchung während einer frühen Zellteilung sind. Asymmetrische Teilungen treten in Medaka in einer erheblichen Anzahl von Embryonen auf und haben einen direkten Einfluss auf die gleichmäßige Verteilung des Zytoplasma. Leider war es nicht möglich die Auswirkungen einer solchen ungleichmäßigen Verteilung aufzudecken, auch wenn man davon ausgehen kann, dass ein ausreichend großes Ungleichgewicht zu unterschiedlichen Zeitpunkten der MBT-Aktivierung in verschiedenen Zellgruppen führen müsste. Ähnliche Beobachtungen wurden bereits in anderen Spezies gemacht, und es wurde vermutet, dass diese in ungleichmäßigen Zellteilungen begründet lagen.

Weiterhin wurde bewiesen, dass die zygotische Transkription schon wesentlich vor dem bisher angenommenen frühesten Zeitpunkt aktiv ist. Darüber hinaus wurden Hinweise gefunden, die darauf hindeuten, dass die Transkription in Embryonen von Medaka in zwei Schritten einsetzt. Der erste Zeitpunkt ist das 16-Zellen-Stadium, in dem die ersten Zellen identifiziert wurden, die Phosphorylierung für RNAPII zeigten, und der zweite das64-Zellen Stadium, in dem der Anteil an p-RNAPII positiven Zellen signifikant anstieg. Ein schrittweiser Anstieg der Transkription wurde bereits in anderen Spezies beobachtet, auch wenn in diesen Fällen nur eine Erhöhung der mRNA-Menge festgestellt wurde, und nicht die unterschiedliche Anzahl an transkriptionell aktiven Zellen untersucht wurde.

Eine Zusammenfassung der hier präsentierten Prozesse während der Teilungsphase in Embryonen von Medaka ist in Abbildung 23 gezeigt.

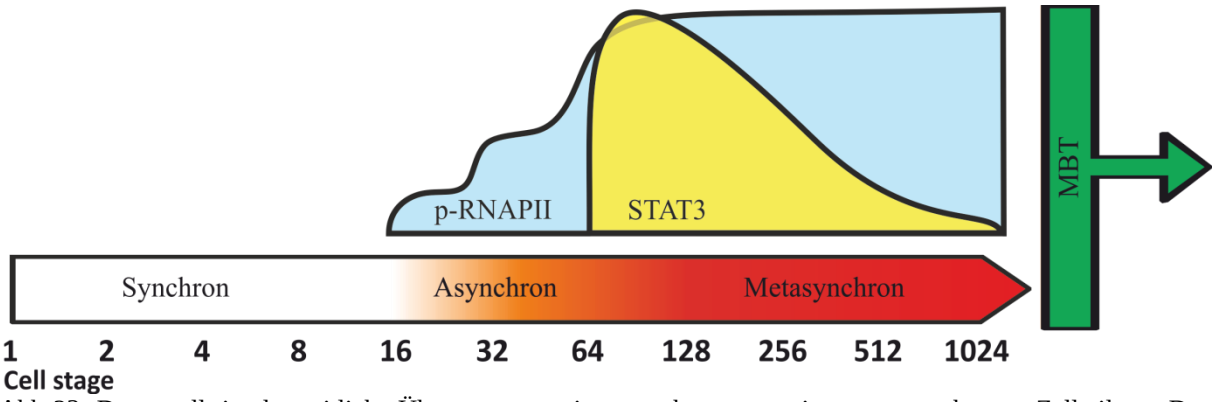

Abb 23: Dargestellt ist der zeitliche Übergang von einer synchronen zu einer metasynchronen Zellteilung. Der schrittweise Anstieg der RNA Polymerase II phosphorylierung ab dem Erreichen des 16-Zellstadiums wird durch die blaue Box gezeigt. Die gelbe Box illustriert die Lokalization von STAT3-Protein im Zellkern. Die Midblastula Transition beginnt kurz danach.

Zusammenfassend bestätigen und erweitern die hier gezeigten Daten die grundliegenden Kenntnisse über die Prozesse vor und währen der MBT, liefern darüber hinaus aber auch Anzeichen für viele Prozesse vor und während der MBT, die nur wenig oder gar nicht verstanden sind.

7. Material & Methods

7.1. Software used

- Microsoft Word 10: http://office.microsoft.com/de-de/word/
- Microsoft Excel 10: http://office.microsoft.com/de-de/excel/
- Mendeley (1.0.1): http://www.mendeley.com/
- ImageJ (1.44): http://rsbweb.nih.gov/ij/download.html
- Volocity (5.4.2): http://cellularimaging.perkinelmer.com
- CoralDrawX5: http://www.corel.com
- GATC viewer: http://www.gatc-biotech.com/de/info-center/downloadlinks.html
- V-NTI_10: http://www.invitrogen.com
- STATISZICA_9: http://www.statsoft.de
- Leica Application Suite (LAS):
- http://cifweb.unil.ch/index.php?option=com_docman&task=doc_download&gid=48&Itemid=57

7.2. Special technical devices

- Fluorescent microscopes: M205FA (Leica) and software (LAS V3.4.0); DMI6000 (Leica) and software (LAS V2.2.0)
- Confocal Microscopes: TCS SP5 (Leica) and software; C1 (Nikon) and software
- cDNA-quantification: Quibt Fluorometer - (Invitrogen; Q32871)
- DNA/RNA quantification: NanoDrop 1000 - (Thermo Scientific)
- PCR cycler: T3000 Thermocycler - (Biometra)
- PCR gradient cycler: TPersonal Thermocycler - (Biometra)
- RealTime PCR: reaplex^2 Mastercycler - (Eppendorf); and Software

7.3. Online tools used

- NEBcutter V2.0: http://tools.neb.com/NEBcutter2/ (Assessed: 22.08.2011)
- Calculating primer melting temperatures http://www.iit-biotech.de/iit-cgi/oligo-tm.pl (Assessed: 22.08.2011)
- Ensembl genome browser http://www.ensembl.org/index.html (Assessed: 22.08.2011)
- Multiple sequence alignment http://multalin.toulouse.inra.fr/multalin/multalin.html (Assessed: 22.08.2011)
- Primer3Plus http://www.bioinformatics.nl/cgi-bin/primer3plus/primer3plus.cgi (Assessed: 22.08.2011)
- Chi-Square-Test calculator http://www.people.ku.edu/~preacher/chisq/chisq.htm (Assessed: 22.08.2011)

7.4. Kits

Kit	Manufacturer	Catalog number
peqGOLD TriFast 100 ml	PEQLAB	30210
PureYield Plasmid Midiprep System	Promega	A2495
PureYield Plasmid Miniprep System	Promega	A1223
Wizzard SV Gel & PCR Clean-Up System	Promega	A9282
GenElute™ HP Plasmid Miniprep Kit	Sigma-Aldrich	NA0160-1KT
GenElute PCR Clean-Up Kit	Sigma-Aldrich	NA1020-1KT
mMessage mMachine SP6	Ambion	AM 1340
mScript mRNA T7 Production	EPICENTRE	MSC11625
RevertAid First Strand cDNA Kit	Fermentas	K1622

7.5. Primer sequences

Primer name	5‘-Sequence-3‘
MF_CCNF_RT_F01	ACTGGAGTGAAGCAGCGATT
MF_CCNF_RT_R01	TCAGGCTCCACTTCAGGAAT
MF_Ccnb1_RT_F01	TTCTGCGAGTGCTGAAGTTT
MF_Ccnb1_RT_R01	TGGAGAGCTCCAGCAGGTAT
MF_HER9_RT_F01	GGAGAGCGAGAATCAACGAA
MF_HER9_RT_R01	GCTTTTTCCAGCTTGGAGTG
MF_PSMD10_RT_F01	AAAACACTCGCCTGCAAAAC
MF_PSMD10_RT_R01	GATCGAGGAGGAACTCCACA
MF_Psmb8_RT_F01	GTACCTGCTGGGTTCCATGT
MF_Psmb8_RT_R01	CGGTGGTTGTTCCTCAGTCT
MF_Psmc1_RT_F01	GGAGCGCATCAAAGACTACC
MF_Psmc1_RT_R01	TCGTCCACCTTTGACCTCTC
MF_RPS12_RT_F01	CTGCGCTGAGCATCAAATTA
MF_RPS12_RT_R01	CAACTACAGCCGACCACCTT
MF_Rpl19_RT_F01	GAATCCTGCGTCGTCTTCTC
MF_Rpl19_RT_R01	ATCAGGATGCGCTTGTTCTT
MF_UBA1_RT_F01	GTACTTTGACGCGCTGGAGT
MF_UBA1_RT_R01	CTGCCCATCATACCGAGAGT
MF_mespA_RT_F01	ACCTCCAAGGTCAGCAGAGA
MF_mespA_RT_R01	GCTGCTGAATCCAGAACTGA
cmv_AseI_f01	TAGTTATTAATAGTAATCAATTA
ClonTechX1-Sp6-f01	AGCTATTTAGGTGACACTATAGAAGTCAG ATCCGCTAGC
ClonTech-r01	GGACAAACCACAACTAGAATGCAGTGA
cmv_t7_Kozak_XhoI_r01	AGCCATCTCGAGCTGTCTCCCTATAGTGAG TCGTATTAGGATCTGACGGTTCAC
Nhel-FLAG-mCherry-f02	ATCCTCGCTAGCATGGACTACAAGGACGAC GATGACAAGATGGTGAGCAAGGGCGAGG
mf_stat3-f04	AGGACTCGAGATGGCTCAGTGGAACCAGTT ACAGCA
mf_stat3-r04	CTGCAGAATTCGCTTGTCATCGTCGTCCTTG TAGTCCATGGGGGAAGCGACGTCCATGT
STAT3_Seq_f01	GCGTTCAGGACATGGAACAG
STAT3_Seq_f02	TCAGCACCGGCCCGCCCTAG
STAT3_seq_r01	ACCAGGATATTGGTGGC
MF-S3_exc_f01	CAGCAAATTCTGGAGCACAA

MF-S3_exc_r01	CAACAGGCAGGGAATGAGTT
MF-S3_exc_r02	CAGGAGGCTTGGTGAAGAAG
MFSTAT3_5UTR_f01	GAGACCAAACTGCTCCGGATCCAACG
MFSTAT3_3UTR_r01	CTGTACAGGCAGATGATGTACACTC
mk_mus-STAT3-r01	GCAGAATTCGCTTGTCATCGTCGTCCTTGTA GTCTTTCCAAACTGCATCAAT
MF-STAT3_short_f02	GTGACCCCCACAAACTCTGGAAA
MF-STAT3_short_r01	AGTTTGTGGGGGTCACGCAGATG
MF-STAT3_short_r02	TGCAGAATTCTCACATGGGGGAAGCGAC
MF-STAT3_short_screen_r01	TTGTGGGGGGTCAC
mf_stat3_f05	CCTGGTGTTCCACAATCTCC
mf_stat3_f06	CGTTCAGGACATGGAACAGA
mf_stat3_f07	CTGGCAGATTGGAAGAGAAGA
mf_stat3_f08	CAGGAGTGCAGTTCACAAACA
mf_stat3_r05	TCTGTTCCATGTCCTGAACG
mf_stat3_r06	AGGCGATTTGCTGTCTTCTC
mf_stat3_r07	CCAGCAACCTGACTTTGTTTG
S3_CA_f01	GTTACTGAGGAGCTCCATCTG
S3_CA_f02	TGTACATGCATTCTCGTCTCCCCCCTGGTGT ACCTCTACCCTGACATC
S3_CA_r01	TCCCGAAAGCTTCCTCTTTGGGGATGTCAG GGTAGAGGTAAACAAGAGGCGACACCAG GATACAGGTGCAATCCATAAT
S3_CA_r02	CACCAGGGGGGAGACGAGAATGCATGTA CAATCCATAATCTTGTAACC
S3_CAscreen_r01	ACCAGGATACAGGTGCA
S3_CAscreen_r02	CACCAGGGGGGAGAC
S3_DN_f01	GGCGACTCCGCCAGTATTACACAACCCTTC TTGAAGACAAAGTTC
S3_DN_f02	GCACCACGGACACTGGAATCTCTCATGCA CAATGAGCCA
S3_DN_r01	GAAGGGTTGTGTAATACTGGCGGAGTCG CCTCCTGCCTCGGGTTC
S3_DN_r02	GAGAGATTCCAGTGTCCGTGGTGCCATCA TAGGAAACAG
S3_DNscreen_f01	GGCGACTCCGCCAGT
S3_DNscreen_f02	GCACCACGGACACTG

7.6. Fluorescent dyes

Dye	Manufacturer	Catalog number
Hoechst 34580	Invitrogen	H21486
Topro3	Invitrogen	T3605
Bodipy FL C_5-ceramide (green)	Invitrogen	D3521
Bodipy 558/568 C_{12} (red)	Invitrogen	D3835
CellMask Orange	Invitrogen	C10045
CellMask Deep Red	Invitrogen	C10046

7.7. Antibodies

Primary antibody	Manufacturer	Catalog number
STAT3 (C-20)	Santa Cruz	Sc-482
p-STAT3 (Tyr 705)	Santa Cruz	Sc-7993
p-STAT3 (Ser727)	Acris	AP02345PU-N
p-Pol II (8A7)	Santa Cruz	Sc-13583
Anti-dimethyl-Histone H3	upstate	07-441
Anti-acetyl-Histone H3	upstate	06-599
Anti-acetyl-Histone H4	upstate	06-866

Secondary antibody	Manufacturer	Catalog number
Alexa Fluor 488 chicken a-rabbit	Invitrogen	A21441
Alexa Fluor 488 goat a-mouse	Invitrogen	A11001
Alexa Fluor 488 goat a-chicken	Invitrogen	A11039
Alexa Fluor 488 chicken a-mouse	Invitrogen	A21200
Alexa Fluor 568 donkey a-mouse	Invitrogen	A10037
Alexa Fluor 568 donkey a-rabbit	Invitrogen	A10042
Alexa Fluor 594 donkey a-goat	Invitrogen	A11058
Alexa Fluor 594 goat a-mouse	Invitrogen	A11032
Alexa Fluor 594 goat a-rabbit	Invitrogen	A11037
Alexa Fluor 594 goat a-chicken	Invitrogen	A11042

7.8. Fishes

Medaka fishes (*Oryzias latipes)* of the Carbio strain (Carolina Biological Supplies, USA) were kept as a large random-mating colony under standard conditions at a 14h light-cycle and 24°C room temperature. Mating occurs as soon as lights turn on and eggs were collected from female fishes about 30minutes after fertilization. After detaching from the egg-filaments they were raised in de-ionized water in a petri dish on a shaker until hatching.

7.9. Injection of medaka embryos

Eggs were collected from female medakas 10minutes after fertilization. The egg-filaments were gently removed using forceps and the eggs were mounted in a 10cm dish containing 2% agarose in water containing angular grooves for egg-clamping. Subsequently, eggs were injected as previously described [134].

7.10. Fluorescent staining of medaka embryos

7.10.1. Embryo preparation for fluorescent staining

Embryos were raised in a shaking petri dish until the respective stage of interest was reached. Embryos were staged according Iwamatsu [2]. Embryos were then transferred into ice-cold water for 5’ to arrest the cell cycle. Afterwards, they were fixed o/n in 4%PFA/PBS in a 2ml Eppendorf tube at room temperature (RT). On the next day, the eggs were transferred into fresh PBS and stored at 4°C for 2days. Afterwards, the eggs were transferred into a 5cm glass dish containing fresh PBS. The chorion was removed using forceps and the embryo was detached from the yolk. Fluorescent staining followed directly.

7.10.2. DNA staining with Hoechst 34580

Chromosomes of prepared embryos were stained according to the following protocol

(1) Transfer embryos into a Ø 2cm glass dish containing PBS

(2) Add Hoechst 34580 to a concentration of 1:2000

(3) Incubate for 2’ at RT

(4) Wash twice in PBS for 5’ at RT

(5) Wash o/n in PBS at 4°C

(6) Store embryos at 4°C until imaging

7.10.3. Cell staining with CellMask DeepRed

Cells of prepared embryos were stained according to the following protocol:

(1) Transfer embryos into a Ø 2cm glass dish containing PBS

(2) Add CellMask DeepRed to a concentration of 1:1000 and incubate for 1h at RT

(3) (Optional: for DNA staining, add Hoechst 34580 to a concentration of 1:2000 for the last 2’ of incubation)

(4) Wash embryos 4 times in PBS for 20’ at RT

(5) Wash embryos in PBS o/n at 4°C

(6) Store embryos at 4°C until imaging

(7) Image embryos within 2-3 days

7.10.4. Immunofluorescent staining

Immunofluorescent staining was performed on previously fixed and prepared embryos according to the following protocol in an Ø 2cm glass dish:

(1) Incubate in 0.1% TritonX in PBS for 30’ at RT

(2) Wash twice in PBS for 5’ for 10’ at RT

(3) Block with 5%BSA in PBS for 1h at RT

(4) Incubate in fresh 5%BSA/PBS containing primary antibody (usually 1:1000) o/n at 4°C

(5) Wash twice for 5’ and twice for 20’ in PBS at RT

(6) Incubate in 5%BSA for 10’ at RT

(7) Incubate in fresh 5%BSA/PBSA containing corresponding secondary antibody (usually 1:1000) o/n at 4°C.

(8) (Optional: for DNA staining, add Hoechst 34580 to a concentration of 1:2000 for the last 2’ of incubation)

(9) Wash twice for 5’ and twice for 20’ in PBS at RT

(10) Wash o/n in fresh PBS at 4°C

(11) Scan embryos within 2-3 days

7.10.5. Embryo mounting

Embryos were stored in PBS until imaging. Right before imaging, embryos were transferred into a 30µl drop of PBS on a microscope slide using forceps. Subsequently, they were covered with a cover slip.

7.11. RNA isolation from embryos

RNA isolation from total embryos was performed according to the following protocol:

(1) Collect about 200eggs per stage in a 2ml Eppendorf tube; store at -80°C

(2) Thaw embryos in 500µl peqGold TriFast

(3) Incubate for 5’ at RT

(4) Homogenize

(5) Add 500µl peqGold TriFast and vortex

(6) Centrifuge for 10’ at 14kRPM at 4°C

Proceed only with the liquid (upper) phase

(7) Pipet the liquid into a new 2ml tube

(8) Add 200µl ice-cold chloroform and mix well

(9) Centrifuge for 10’ at 14kRPM at 4°C

(10) Transfer upper phase into a fresh 2ml tube

(11) Add 500µl isopropanol

(12) Precipitate at -20°C o/n

(13) Centrifuge 45’ at max-speed at 4°C

(14) Wash pellet with 70% ice-cold ethanol for 5’

(15) Remove liquid

(16) Centrifuge again briefly and remove remaining liquid with a pipet

(17) Briefly air-dry pellet (10’)

(18) Resuspend pellet in RNase-free water, keep on ice for 3’ and heat to 65°C for 3’

(19) Quantify RNA

7.12. In-vitro cDNA transcription

In-vitro transcription of cDNA from isolated mRNAs from medaka embryos was performed with the RevertAid First Strand cDNA Kit (Fermentas) according to the manufacturer´s manual.

7.13. PCR

Polymerase chain reaction was used for bacterial colony screening, amplification of templates for mRNA production and for amplifying DNA fragments for cloning into expression vectors.

A standard reaction was prepared as follows:

- 1µl dNTP Mix (2.5mM each)
- 2µl 10xReaction Buffer
- 0.2µl Polymerase
- 1µl Forward primer (10pmol/µl)
- 1µl Reverse primer (10pmol/µl)
- 1µl Template
- 14µl H_2O

A standard cycling program was performed as follows:

Step	Temp.	Time	
1	95°C	pause (preheating)	
2	95°C	5’	
3	95°C	30’’	
4	52°C	30’’	
5	72°C	1’ per 1kb DNA	Repeat from step 3 for 34 times
6	72°C	5’	

7	10°C	pause (storing)

Annealing temperature (step 4) and elongation time (step 5) were adjusted to the needs of the used primers or DNA templates.

7.14. Sewing PCR

PCR sewing was performed to introduce point mutations into DNA sequences from plasmid-templates. First, two standard PCR reactions were performed to amplify two DNA fragments that overlapped at the 5' and 3' end, respectively. The point mutation was introduced into the overlapping region by overhang sequences contained within the amplification primers. Next, both DNA fragments were sewed together in a third PCR reaction by using both fragments as templates and only the two external primers of the original PCR reactions.

A sewing PCR reaction was performed as follows:

Step	Temp.	Time	
1	95°C	pause (preheating)	
2	95°C	5'	
3	95°C	30''	
4	56°C	30''	
5	72°C	1' per 1kb DNA	Repeat from step 3 for 4times
6	95°C	30''	
7	52°C	30''	
8	72°C	1' per 1kb DNA	Repeat from step 6 for 30times
9	72°C	5'	
10	10°C	pause (storing)	

7.15. Endonuclease digestion

Endonulcease digestion was used for colony screens, the linearization of plasmids for mRNA transcription or the preparation of plasmids and DNA fragments from PCR for ligation.

A standard reaction was performed as follows:

(1) 1-5µl DNA

(2) 1µl 10x Reaction Buffer

(3) 1µl Restriction Enzyme (10U/µl)

(4) Add H_2O to 10µl

(5) Incubate at 37°C for 1h

(6) Heat inactivation (Temperature and duration depended on the used enzyme)

(7) Clean up

Restriction enzymes and corresponding buffers were obtained from New England Biolabs (NEB), Promega or Fermentas.

DNA purification after digestion was usually performed with kits from Promega (A9282) or Sigma (NA1020-1KT), following the instruction manual.

7.16. Ligation

Ligations were performed to introduce endonulcease digested DNA fragments into target plasmids (which were previously linearized to present matching DNA overhangs).

A standard reaction was performed as followed:

(1) 1µl linearized vector

(2) 1µl DNA-insert

(3) 1µl 10x-Reaction Buffer

(4) 1µl T4-Ligase (Fermentas)

(5) 6µl H_2O

(6) Incubate at 37°C for 1h

(7) Transform into competent bacteria or store at -20°C until use

The concentration of insert and vector were estimated by running 1µl insert and vector in an agarose gel. Concentrations of the DNA fragments were adjusted to obtain equal molarities for all fragments. Then, multiple reactions were set up with different molar ratios between insert and vector.

7.17. DNA-Transformation into bacteria

7.17.1. Preparation of chemically competent bacterial cells

(1) Grow in 5 ml LB media a o/n culture of the strain DH5α of *Escherichia coli*

(2) Dilute the o/n-culture by 1/10 - 1/20 to fresh 200 ml of LB

(3) Grow about 90-180' to early log phase (OD600 = 0.2 - 0.4)

(4) Transfer the cells on ice for 15'; all further steps are performed at 4°C

(5) Collect cells by centrifugation (2g for 5') at 4°C.

(6) Resuspend the cells in 1/2 culture volume of 0.1 M ice-cold $CaCl_2$.

(7) Hold on ice for at least 30', better 1 - 2 h.

(8) Collect cells as before and gently resuspend them in 1/10 of 0.1 M $CaCl_2$ + 20% Glycerin of the starting culture volume.

(9) Aliquot the bacterial cells and store them until use at -80°C

7.17.2. Heat-shock transformation of chemically competent bacterial cells

(1) Thaw competent bacteria on ice

(2) Add 50µl of the competent bacteria cells to the plasmid/ ligation mix

(3) Keep the mix on ice for 20-30'

(4) Heat-shock at 42°C for 90''

(5) Put on ice for 2'

(6) Add 1ml LB medium

(7) Shake for 1h at 37°C

(8) Slowly centrifuge for 5’

(9) Waste 90% of the liquid phase

(10) Resuspend bacteria in the remaining liquid

(11) Plate

7.18. Plasmid preparation

For isolation of plasmids from bacteria kits from Promega or Sigma were used. The procedures were performed according the respective protocols provided by the kit manufacturers.

7.19. In-vitro transcription of mRNA

MRNAs for injection into medaka embryos were produced with the mMessage mMachine SP6 kit (Ambion; AM 1340), or with the mScript mRNA T7 kit (EPICENTRE; MSC11625) according the provided protocols.

7.20. RealTime PCR

RealTime PCR was used to quantify mRNA levels in different cDNAs.

A standard reaction was prepared as follows:

(1) 18µl H_2O

(2) 2.5µl 10xBuffer

(3) 0.2µl Polymerase

(4) 0.7µl dNTPs (10mM)

(5) 0.75µl SYBR-GREEN 1:2000

(6) 0.75µl 5'Primer (10pmol/µl)

(7) 0.75µl 3'Primer (10pmol/µl)

(8) 2µl Template

A standard cycling program was performed as follows:

Step	Temp.	Time	
1	90°C	pause (preheating)	
2	90°C	2'	
3	95°C	15''	
4	60°C	15''	
5	72°C	15''	Repeat from step 3 for 39 times
6	95°C	15''	
7	60°C	15''	
8		20'	Melting curve
9	95°C	15''	

7. Bibliography

[1] C. B. Kimmel, W. W. Ballard, S. R. Kimmel, B. Ullmann, and T. F. Schilling, "Stages of embryonic development of the zebrafish.," *Developmental dynamics : an official publication of the American Association of Anatomists*, vol. 203, no. 3, pp. 253-310, Jul. 1995.

[2] T. Iwamatsu, "Stages of normal development in the medaka Oryzias latipes.," *Mechanisms of development*, vol. 121, no. 7-8, pp. 605-18, 2004.

[3] J. Wittbrodt, A. Shima, and M. Schartl, "Medaka—a model organism from the far East," *Nature Reviews Genetics*, vol. 143, no. 96, pp. 267-276, 2002.

[4] J. Wittbrodt, A. Shima, and M. Schartl, "Medaka--a model organism from the far East.," *Nature reviews. Genetics*, vol. 3, no. 1, pp. 53-64, Jan. 2002.

[5] S. F. Gilbert, *Developmental Biology*. 2000, p. 26.

[6] P. H. O. Farrell, "HOW METAZOANS REACH THEIR FULL SIZE : THE NATURAL HISTORY OF BIGNESS," *Cell Growth*, 2003.

[7] P. H. O'Farrell, J. Stumpff, and T. T. Su, "Embryonic cleavage cycles: how is a mouse like a fly?," *Current biology : CB*, vol. 14, no. 1, pp. R35-45, Jan. 2004.

[8] J. Mitchison, *The Biology of the Cell Cycle*. 1971, pp. 8-9.

[9] A. Spradling and T. Orr-Weaver, "Regulation of DNA replication during Drosophila development.," *Annual review of genetics*, vol. 21, pp. 373-403, Jan. 1987.

[10] J. Walter and J. W. Newport, "Regulation of replicon size in Xenopus egg extracts.," *Science (New York, N.Y.)*, vol. 275, no. 5302, pp. 993-5, Feb. 1997.

[11] S. L. McKnight and O. L. Miller, "Electron microscopic analysis of chromatin replication in the cellular blastoderm Drosophila melanogaster embryo.," *Cell*, vol. 12, no. 3, pp. 795-804, Nov. 1977.

[12] C. F. Graham and R. W. Morgan, "Changes in the cell cycle during early amphibian development," *Developmental Biology*, vol. 14, no. 3, pp. 439-460, 1966.

[13] J. Newport and M. Kirschner, "A major developmental transition in early Xenopus embryos: I. characterization and timing of cellular changes at the midblastula stage.," *Cell*, vol. 30, no. 3, pp. 675-86, Oct. 1982.

[14] J. E. Ferrell, M. Wu, J. C. Gerhart, and G. S. Martin, "Cell cycle tyrosine phosphorylation of p34cdc2 and a microtubule-associated protein kinase homolog in Xenopus oocytes and eggs.," *Molecular and cellular biology*, vol. 11, no. 4, pp. 1965-71, Apr. 1991.

[15] D. K. Pritchard and G. Schubiger, “Activation of transcription in Drosophila embryos is a gradual process mediated by the nucleocytoplasmic ratio.,” *Genes & development*, vol. 10, no. 9, pp. 1131-42, May. 1996.

[16] A. Murray, “Cell cycle checkpoints.,” *Current Opinion in Cell Biology*, vol. 6, no. 6, pp. 872-6, Dec. 1994.

[17] J. W. Raff and D. M. Glover, “Nuclear and cytoplasmic mitotic cycles continue in Drosophila embryos in which DNA synthesis is inhibited with aphidicolin.,” *The Journal of cell biology*, vol. 107, no. 6 Pt 1, pp. 2009-19, Dec. 1988.

[18] D. M. Glover et al., “Mitosis in Drosophila development.,” *Journal of cell science. Supplement*, vol. 12, pp. 277-91, Jan. 1989.

[19] J. Newport and M. Dasso, “On the coupling between DNA replication and mitosis.,” *Journal of cell science. Supplement*, vol. 12, pp. 149-60, Jan. 1989.

[20] D. A. Kane and C. B. Kimmel, “The zebrafish midblastula transition.,” *Development (Cambridge, England)*, vol. 119, no. 2, pp. 447-56, Oct. 1993.

[21] V. E. Foe and B. M. Alberts, “Studies of nuclear and cytoplasmic behaviour during the five mitotic cycles that precede gastrulation in Drosophila embryogenesis.,” *Journal of cell science*, vol. 61, pp. 31-70, May. 1983.

[22] B. a Edgar and G. Schubiger, “Parameters controlling transcriptional activation during early Drosophila development.,” *Cell*, vol. 44, no. 6, pp. 871-7, Mar. 1986.

[23] B. a Edgar, C. P. Kiehle, and G. Schubiger, “Cell cycle control by the nucleo-cytoplasmic ratio in early Drosophila development.,” *Cell*, vol. 44, no. 2, pp. 365-72, Jan. 1986.

[24] D. Kimelman, M. Kirschner, and T. Scherson, “The events of the midblastula transition in Xenopus are regulated by changes in the cell cycle.,” *Cell*, vol. 48, no. 3, pp. 399-407, Mar. 1987.

[25] P. Clute and Y. Masui, “Regulation of the appearance of division asynchrony and microtubule-dependent chromosome cycles in Xenopus laevis embryos.,” *Developmental biology*, vol. 171, no. 2, pp. 273-85, Oct. 1995.

[26] J. Signoret, J. & Lefresne, “Contribution a l’etude de la segmentation de l’oeuf d’Axolotl. II. Influence de modifications du noyau et de cytoplasme sur les modalités de la segmentation,” *Ann. Embryol. Morphol*, vol. 6, pp. 200-307, 1973.

[27] G. K. Yasuda and G. Schubiger, “Temporal regulation in the early embryo: is MBT too good to be true?,” *Trends in genetics : TIG*, vol. 8, no. 4, pp. 124-7, Apr. 1992.

[28] E. Syngayewslaya, “Desynchronization of cell divisions in the course of egg cleavage and an attempt at experimental shift of its on,” *Wilhelm Roux Arch. EntwMech. Org.*, vol. 125, pp. 176-88, 1931.

[29] B. I. Balinsky, “Über den Teilungsrhythmus bei der Entwicklung des Eies der Ascidie Ciona intestinalis,” *Wilhelm Roux Arch. EntwMech. Org.*, vol. 125, pp. 155-75, 1931.

[30] K.-I. Sirakami, “On the cleavage of isolated blastomeres from morulae of Bufo vulgaris,” *Mem. Fac. lib. Arts Educat. Jamanshi Univ.*, vol. 9, p. 182, 1985.

[31] N. N. Neyfakh, A. A. & Rott, “Synchronization of cell-divisions in early embryos of Misgurnus fossilis, induced by low temperature treatment,” *Dokl. Akad. Nauk. S.S.S.R.*, vol. 125, pp. 432-4, 1959.

[32] N. V. Pankova, “Changes in the cell nucleus at early developmental stages of the loach,” *Cytology*, vol. 5, pp. 36-42, 1963.

[33] I. P. S. Agrell, “Membrane formation and membrane contacts during the development of the sea urchin embryo,” *Cell and Tissue Research*, vol. 72, no. 1, pp. 21-72, 1966.

[34] M. N. Skoblina, “Dimensionless description of the length of mitotic phases of first cleavage divisions in axolotl,” *Dokl. Akad. Nauk. S.S.S.R.*, vol. 160, pp. 700-3, 1965.

[35] E. V. Chulitskaia, “The occurrence of desynchronism and change in the rhythm of nuclear division in the period of blastulation,” *Dokl. Akad. Nauk. S.S.S.R.*, vol. 173, pp. 1473-6.

[36] N. N. Rott and G. a Sheveleva, “Changes in the rate of cell divisions in the course of early development of diploid and haploid loach embryos.,” *Journal of embryology and experimental morphology*, vol. 20, no. 2, pp. 141-50, Sep. 1968.

[37] S. T. Bissen and D. A. Weisblat, “The durations and compositions of cell cycles in embryos of the leech, Helobdella triserialis.,” *Development (Cambridge, England)*, vol. 106, no. 1, pp. 105-18, May. 1989.

[38] A. W. Shermoen and P. H. O’Farrell, “Progression of the cell cycle through mitosis leads to abortion of nascent transcripts.,” *Cell*, vol. 67, no. 2, pp. 303-10, Oct. 1991.

[39] B. a Edgar and G. Schubiger, “Parameters controlling transcriptional activation during early Drosophila development.,” *Cell*, vol. 44, no. 6, pp. 871-7, Mar. 1986.

[40] J. Mata, S. Curado, a Ephrussi, and P. Rørth, “Tribbles coordinates mitosis and morphogenesis in Drosophila by regulating string/CDC25 proteolysis.,” *Cell*, vol. 101, no. 5, pp. 511-22, May. 2000.

[41] T. C. Seher and M. Leptin, “Tribbles, a cell-cycle brake that coordinates proliferation and morphogenesis during Drosophila gastrulation.,” *Current biology : CB*, vol. 10, no. 11, pp. 623-9, Jun. 2000.

[42] W. Tadros and H. D. Lipshitz, “The maternal-to-zygotic transition: a play in two acts.,” *Development (Cambridge, England)*, vol. 136, no. 18, pp. 3033-42, Sep. 2009.

[43] Y. Kobayakawa and H. Y. Kubota, “Temporal pattern of cleavage and the onset of gastrulation in amphibian embryos developed from eggs with the reduced cytoplasm.,” *Journal of embryology and experimental morphology*, vol. 62, pp. 83-94, Apr. 1981.

[44] Y. Masui and P. Wang, “Cell cycle transition in early embryonic development of Xenopus laevis.,” *Biology of the cell / under the auspices of the European Cell Biology Organization*, vol. 90, no. 8, pp. 537-48, Nov. 1998.

[45] I. Mita and C. Obata, “Timing of early morphogenetic events in tetraploid starfish embryos,” *Journal of Experimental Zoology*, vol. 222, no. 2, pp. 215-222, 1984.

[46] W. Tadros et al., “SMAUG is a major regulator of maternal mRNA destabilization in Drosophila and its translation is activated by the PAN GU kinase.,” *Developmental cell*, vol. 12, no. 1, pp. 143-55, Jan. 2007.

[47] A. J. Giraldez et al., “MicroRNAs regulate brain morphogenesis in zebrafish.,” *Science (New York, N.Y.)*, vol. 308, no. 5723. pp. 833-8, 06-May-2005.

[48] A. J. Giraldez et al., “Zebrafish MiR-430 promotes deadenylation and clearance of maternal mRNAs.,” *Science (New York, N.Y.)*, vol. 312, no. 5770, pp. 75-9, 2006.

[49] S. Mathavan et al., “Transcriptome analysis of zebrafish embryogenesis using microarrays.,” *PLoS genetics*, vol. 1, no. 2, pp. 260-76, 2005.

[50] J. Newport and M. Kirschner, “A major developmental transition in early Xenopus embryos: II. Control of the onset of transcription.,” *Cell*, vol. 30, no. 3, pp. 687-96, Oct. 1982.

[51] M. P. S. Dekens, F. J. Pelegri, H.-M. Maischein, and C. Nüsslein-Volhard, “The maternal-effect gene futile cycle is essential for pronuclear congression and mitotic spindle assembly in the zebrafish zygote.,” *Development (Cambridge, England)*, vol. 130, no. 17, pp. 3907-16, Sep. 2003.

[52] A. Bird, “The essentials of DNA methylation.,” *Cell*, vol. 70, no. 1, pp. 5-8, Jul. 1992.

[53] S. U. Kass, N. Landsberger, and a P. Wolffe, “DNA methylation directs a time-dependent repression of transcription initiation.,” *Current biology : CB*, vol. 7, no. 3, pp. 157-65, Mar. 1997.

[54] S. U. Kass, D. Pruss, and a P. Wolffe, “How does DNA methylation repress transcription?,” *Trends in genetics : TIG*, vol. 13, no. 11, pp. 444-9, Nov. 1997.

[55] T. H. Bestor, “The DNA methyltransferases of mammals.,” *Human molecular genetics*, vol. 9, no. 16, pp. 2395-402, Oct. 2000.

[56] D. S. Dunican, A. Ruzov, J. a Hackett, and R. R. Meehan, “xDnmt1 regulates transcriptional silencing in pre-MBT Xenopus embryos independently of its catalytic function.,” *Development (Cambridge, England)*, vol. 135, no. 7, pp. 1295-302, Apr. 2008.

[57] D. Read, M. Levine, and J. L. Manley, “Ectopic expression of the Drosophila tramtrack gene results in multiple embryonic defects, including repression of even-skipped and fushi tarazu.,” *Mechanisms of development*, vol. 38, no. 3, pp. 183-95, Sep. 1992.

[58] X. Lu, J. M. Li, O. Elemento, S. Tavazoie, and E. F. Wieschaus, "Coupling of zygotic transcription to mitotic control at the Drosophila mid-blastula transition.," *Development (Cambridge, England)*, vol. 136, no. 12, pp. 2101-10, Jun. 2009.

[59] B. Benoit et al., "An essential role for the RNA-binding protein Smaug during the Drosophila maternal-to-zygotic transition.," *Development (Cambridge, England)*, vol. 136, no. 6, pp. 923-32, Mar. 2009.

[60] D. Kimelman, M. Kirschner, and T. Scherson, "The events of the midblastula transition in Xenopus are regulated by changes in the cell cycle.," *Cell*, vol. 48, no. 3, pp. 399-407, Feb. 1987.

[61] S. De Renzis, O. Elemento, S. Tavazoie, and E. F. Wieschaus, "Unmasking activation of the zygotic genome using chromosomal deletions in the Drosophila embryo.," *PLoS biology*, vol. 5, no. 5, p. e117, May. 2007.

[62] K. Aizawa, A. Shimada, K. Naruse, H. Mitani, and A. Shima, "The medaka midblastula transition as revealed by the expression of the paternal genome.," *Gene expression patterns : GEP*, vol. 3, no. 1, pp. 43-7, Mar. 2003.

[63] N. Satoh, "'Metachronous' Cleavage and Initiation of Gastrulation in Amphibian Embryos," *Development, Growth and Differentiation*, vol. 19, no. 2, pp. 111-117, Jun. 1977.

[64] M. Kraeussling, T. U. Wagner, and M. Schartl, "Highly asynchronous and asymmetric cleavage divisions accompany early transcriptional activity in pre-blastula medaka embryos.," *PloS one*, vol. 6, no. 7, p. e21741, Jan. 2011.

[65] R. Ashworth et al., "Molecular and functional characterization of inositol trisphosphate receptors during early zebrafish development.," *The Journal of biological chemistry*, vol. 282, no. 19, pp. 13984-93, May. 2007.

[66] T. O'Brien, S. Hardin, a Greenleaf, and J. T. Lis, "Phosphorylation of RNA polymerase II C-terminal domain and transcriptional elongation.," *Nature*, vol. 370, no. 6484. pp. 75-7, Jul-1994.

[67] J. M. Payne, P. J. Laybourn, and M. E. Dahmus, "The transition of RNA polymerase II from initiation to elongation is associated with phosphorylation of the carboxyl-terminal domain of subunit IIa.," *The Journal of biological chemistry*, vol. 264, no. 33, pp. 19621-9, Nov. 1989.

[68] D. L. Cadena and M. E. Dahmus, "Messenger RNA synthesis in mammalian cells is catalyzed by the phosphorylated form of RNA polymerase II.," *The Journal of biological chemistry*, vol. 262, no. 26, pp. 12468-74, Sep. 1987.

[69] J. G. Valay, M. Simon, M. F. Dubois, O. Bensaude, C. Facca, and G. Faye, "The KIN28 gene is required both for RNA polymerase II mediated transcription and phosphorylation of the Rpb1p CTD.," *Journal of molecular biology*, vol. 249, no. 3, pp. 535-44, Jun. 1995.

[70] J. F. Bromberg et al., “Stat3 as an oncogene.,” *Cell*, vol. 98, no. 3, pp. 295-303, Aug. 1999.

[71] A. N. Mathur et al., “Stat3 and Stat4 direct development of IL-17-secreting Th cells.,” *Journal of immunology (Baltimore, Md. : 1950)*, vol. 178, no. 8, pp. 4901-7, Apr. 2007.

[72] A. Kaptein, V. Paillard, and M. Saunders, “Dominant negative stat3 mutant inhibits interleukin-6-induced Jak-STAT signal transduction.,” *The Journal of biological chemistry*, vol. 271, no. 11, pp. 5961-4, Mar. 1996.

[73] D. M. Wrighting and N. C. Andrews, “Interleukin-6 induces hepcidin expression through STAT3.,” *Blood*, vol. 108, no. 9, pp. 3204-9, Nov. 2006.

[74] Z. Wen, Z. Zhong, and J. E. Darnell, “Maximal activation of transcription by Stat1 and Stat3 requires both tyrosine and serine phosphorylation.,” *Cell*, vol. 82, no. 2, pp. 241-50, Jul. 1995.

[75] T. U. Wagner, M. Kraeussling, L. M. Fedorov, C. Reiss, B. Kneitz, and M. Schartl, “STAT3 and SMAD1 signaling in Medaka embryonic stem-like cells and blastula embryos.,” *Stem cells and development*, vol. 18, no. 1, pp. 151-60, 2009.

[76] J. Turkson, T. Bowman, R. Garcia, E. Caldenhoven, R. P. De Groot, and R. Jove, “Stat3 activation by Src induces specific gene regulation and is required for cell transformation.,” *Molecular and cellular biology*, vol. 18, no. 5, pp. 2545-52, May. 1998.

[77] J. Turkson et al., “Requirement for Ras/Rac1-mediated p38 and c-Jun N-terminal kinase signaling in Stat3 transcriptional activity induced by the Src oncoprotein.,” *Molecular and cellular biology*, vol. 19, no. 11, pp. 7519-28, Nov. 1999.

[78] Y. Shen et al., “Essential role of STAT3 in postnatal survival and growth revealed by mice lacking STAT3 serine 727 phosphorylation.,” *Molecular and cellular biology*, vol. 24, no. 1, pp. 407-19, Jan. 2004.

[79] S. Becker, B. Groner, and C. W. Müller, “Three-dimensional structure of the Stat3beta homodimer bound to DNA.,” *Nature*, vol. 394, no. 6689, pp. 145-51, Jul. 1998.

[80] C. Hensey and J. Gautier, “A developmental timer that regulates apoptosis at the onset of gastrulation.,” *Mechanisms of development*, vol. 69, no. 1-2, pp. 183-95, Dec. 1997.

[81] R. Rappaport, “Cytokinesis in animal cells,” in *Cytokinesis in animal cells*, 1966, pp. 154-155.

[82] E. V. Chulitskaia, “Desynchronization of cell divisions in the course of egg cleavage and an attempt at experimental shift of its onset.,” *Journal of embryology and experimental morphology*, vol. 23, no. 2, pp. 359-74, Apr. 1970.

[83] Broterenbrood, “Duration of cleavage cycles and asymmetry in the direction of cleavage waves prior to gastrulation,” *Development, Genes and Evolutio*, vol. 192, no. 5, pp. 216-221, 1983.

[84] A. W. Marrable, “Variations in early cleavage of the zebrafish,” *Nature*, vol. 184, pp. 1160-1161, 1959.

[85] P. J. Keller, A. D. Schmidt, J. Wittbrodt, and E. H. K. Stelzer, “Reconstruction of zebrafish early embryonic development by scanned light sheet microscopy.,” *Science (New York, N.Y.)*, vol. 322, no. 5904, pp. 1065-9, Nov. 2008.

[86] A. W. Marrable, “Cell numbers during cleavage of the zebra fish egg.,” *Journal of embryology and experimental morphology*, vol. 14, no. 1, pp. 15-24, Aug. 1965.

[87] N. Olivier et al., “Cell lineage reconstruction of early zebrafish embryos using label-free nonlinear microscopy.,” *Science (New York, N.Y.)*, vol. 329, no. 5994, pp. 967-71, Aug. 2010.

[88] R. Winklbauer, “Cell proliferation in the ectoderm of the Xenopus embryo: development of substratum requirements for cytokinesis.,” *Developmental biology*, vol. 118, no. 1, pp. 70-81, Nov. 1986.

[89] W. J. Reeve and F. P. Kelly, “Nuclear position in the cells of the mouse early embryo.,” *Journal of embryology and experimental morphology*, vol. 75, pp. 117-39, Jul. 1983.

[90] E. D. Salmon, “Cytokinesis in animal cells.,” *Current opinion in cell biology*, vol. 1, no. 3, pp. 541-7, Jul. 1989.

[91] L. Wolpert, “The mechanisc and mechanism of cleavage,” *Int.Rev.Cytol*, vol. 10, pp. 163-216, 1960.

[92] R. Rappaport, “Cleavage,” *Concepts of Development (eds J. Lash & J. R. Whittaker)*, pp. 76-100. Sinauer Associates, Stamford, Connecticut., 1974.

[93] M. Glotzer, “Cleavage furrow positioning.,” *The Journal of cell biology*, vol. 164, no. 3, pp. 347-51, Feb. 2004.

[94] K. Okazaki, “Normal development to metamorphosis,” *The Sea Urchin Embryo*, pp. 177-232, 1975.

[95] J. E. Sulston, E. Schierenberg, J. G. White, and J. N. Thomson, “The embryonic cell lineage of the nematode Caenorhabditis elegans.,” *Developmental biology*, vol. 100, no. 1, pp. 64-119, Nov. 1983.

[96] P. Gönczy and L. S. Rose, “Asymmetric cell division and axis formation in the embryo.,” *WormBook : the online review of C. elegans biology*, pp. 1-20, Jan. 2005.

[97] M. H. Johnson and C. A. Ziomek, “The foundation of two distinct cell lineages within the mouse morula.,” *Cell*, vol. 24, no. 1, pp. 71-80, May. 1981.

[98] S. Strome and W. B. Wood, “Generation of asymmetry and segregation of germ-line granules in early C. elegans embryos.,” *Cell*, vol. 35, no. 1, pp. 15-25, Dec. 1983.

[99] A. Chenn and S. K. McConnell, “Cleavage orientation and the asymmetric inheritance of Notch1 immunoreactivity in mammalian neurogenesis.,” *Cell*, vol. 82, no. 4, pp. 631-41, Aug. 1995.

[100] R. Kraut, W. Chia, L. Y. Jan, Y. N. Jan, and J. A. Knoblich, “Role of inscuteable in orienting asymmetric cell divisions in Drosophila.,” *Nature*, vol. 383, no. 6595, pp. 50-5, Sep. 1996.

[101] S. Strome and W. B. Wood, “Immunofluorescence visualization of germ-line-specific cytoplasmic granules in embryos, larvae, and adults of Caenorhabditis elegans.,” *Proceedings of the National Academy of Sciences of the United States of America*, vol. 79, no. 5, pp. 1558-62, Mar. 1982.

[102] B. I. Balinsky, *An introduction to embryology*, Fourth., vol. Fourth edi. 1975.

[103] G. Berrill, N. J. & Karp, “Development,” *New York: McGraw-Hill*, p. 566, 1976.

[104] J. Huisken and D. Y. R. Stainier, “Selective plane illumination microscopy techniques in developmental biology.,” *Development (Cambridge, England)*, vol. 136, no. 12, pp. 1963-75, Jun. 2009.

[105] J. Huisken, J. Swoger, F. Del Bene, J. Wittbrodt, and E. H. K. Stelzer, “Optical sectioning deep inside live embryos by selective plane illumination microscopy.,” *Science (New York, N.Y.)*, vol. 305, no. 5686, pp. 1007-9, Aug. 2004.

[106] J. R. Martinez-Morales et al., “Ojoplano-Mediated Basal Constriction Is Essential for Optic Cup Morphogenesis.,” *Development (Cambridge, England)*, vol. 136, no. 13, pp. 2165-75, Jul. 2009.

[107] P. J. Keller et al., “Fast, high-contrast imaging of animal development with scanned light sheet-based structured-illumination microscopy.,” *Nature methods*, vol. 7, no. 8, pp. 637-642, Jul. 2010.

[108] R. Aviles-Espinosa et al., “Third-harmonic generation for the study of Caenorhabditis elegans embryogenesis.,” *Journal of biomedical optics*, vol. 15, no. 4, p. 046020, 2011.

[109] G. J. Tserevelakis, G. Filippidis, a J. Krmpot, M. Vlachos, C. Fotakis, and N. Tavernarakis, “Imaging Caenorhabditis elegans embryogenesis by third-harmonic generation microscopy.,” *Micron (Oxford, England : 1993)*, vol. 41, no. 5, pp. 444-7, Jul. 2010.

[110] W. Supatto et al., “In vivo modulation of morphogenetic movements in Drosophila embryos with femtosecond laser pulses.,” *Proceedings of the National Academy of Sciences of the United States of America*, vol. 102, no. 4, pp. 1047-52, Jan. 2005.

[111] D. Oron, D. Yelin, E. Tal, S. Raz, R. Fachima, and Y. Silberberg, “Depth-resolved structural imaging by third-harmonic generation microscopy.,” *Journal of structural biology*, vol. 147, no. 1, pp. 3-11, Jul. 2004.

[112] C.-K. Sun et al., “Higher harmonic generation microscopy for developmental biology.,” *Journal of structural biology*, vol. 147, no. 1, pp. 19-30, Jul. 2004.

[113] T. Watanabe et al., "Characterisation of the dynamic behaviour of lipid droplets in the early mouse embryo using adaptive harmonic generation microscopy.," *BMC cell biology*, vol. 11, p. 38, Jan. 2010.

[114] K. Aizawa, "The medaka midblastula transition as revealed by the expression of the paternal genome," *Gene Expression Patterns*, vol. 3, no. 1, pp. 43-47, Mar. 2003.

[115] H. P. Phatnani and A. L. Greenleaf, "Phosphorylation and functions of the RNA polymerase II CTD.," *Genes & development*, vol. 20, no. 21, pp. 2922-36, Nov. 2006.

[116] R. W. & S. S. Dirks, "Dynamics of RNA polymerase II localization during the cell cycle," *Histochemistry and cell biology*, vol. 111, no. 5, pp. 405-410, 1999.

[117] J. M. Gottesfeld, V. J. Wolf, T. Dang, D. J. Forbes, and P. Hartl, "Mitotic repression of RNA polymerase III transcription in vitro mediated by phosphorylation of a TFIIIB component.," *Science (New York, N.Y.)*, vol. 263, no. 5143, pp. 81-4, Jan. 1994.

[118] I. Chambers, "The molecular basis of pluripotency in mouse embryonic stem cells.," *Cloning and stem cells*, vol. 6, no. 4, pp. 386-91, Jan. 2004.

[119] H. Niwa, T. Burdon, I. Chambers, and a Smith, "Self-renewal of pluripotent embryonic stem cells is mediated via activation of STAT3.," *Genes & development*, vol. 12, no. 13, pp. 2048-60, Jul. 1998.

[120] K. Takeda et al., "Targeted disruption of the mouse Stat3 gene leads to early embryonic lethality.," *Proceedings of the National Academy of Sciences of the United States of America*, vol. 94, no. 8, pp. 3801-4, Apr. 1997.

[121] B. E. Reubinoff, M. F. Pera, C. Y. Fong, a Trounson, and a Bongso, "Embryonic stem cell lines from human blastocysts: somatic differentiation in vitro.," *Nature biotechnology*, vol. 18, no. 4, pp. 399-404, Apr. 2000.

[122] J. a Thomson et al., "Embryonic stem cell lines derived from human blastocysts.," *Science (New York, N.Y.)*, vol. 282, no. 5391, pp. 1145-7, Nov. 1998.

[123] R. K. Humphrey et al., "Maintenance of pluripotency in human embryonic stem cells is STAT3 independent.," *Stem cells (Dayton, Ohio)*, vol. 22, no. 4, pp. 522-30, Jan. 2004.

[124] Y. Hong, C. Winkler, and M. Schartl, "Pluripotency and differentiation of embryonic stem cell lines from the medakafish (Oryzias latipes).," *Mechanisms of development*, vol. 60, no. 1, pp. 33-44, Nov. 1996.

[125] Y. Hong and M. Schartl, "Isolation and differentiation of medaka embryonic stem cells.," *Methods in molecular biology (Clifton, N.J.)*, vol. 329, pp. 3-16, Jan. 2006.

[126] D. S. Latchman, "Transcription factors: an overview.," *The international journal of biochemistry & cell biology*, vol. 29, no. 12, pp. 1305-12, Dec. 1997.

[127] R. G. Roeder, "The role of general initiation factors in transcription by RNA polymerase II.," *Trends in biochemical sciences*, vol. 21, no. 9. pp. 327-35, Sep-1996.

[128] D. B. Nikolov and S. K. Burley, “RNA polymerase II transcription initiation: a structural view.,” *Proceedings of the National Academy of Sciences of the United States of America*, vol. 94, no. 1, pp. 15-22, Jan. 1997.

[129] T. S. Tanaka, F. Nishiumi, T. Komiya, and K. Ikenishi, “Characterization of the 38 kDa protein lacking in gastrula-arrested mutant Xenopus embryos.,” *The International journal of developmental biology*, vol. 54, no. 8-9, pp. 1347-53, Jan. 2010.

[130] L. Solnica-Krezel et al., “Mutations affecting cell fates and cellular rearrangements during gastrulation in zebrafish.,” *Development (Cambridge, England)*, vol. 123, pp. 67-80, Dec. 1996.

[131] A. F. Schier et al., “Mutations affecting the development of the embryonic zebrafish brain.,” *Development (Cambridge, England)*, vol. 123, pp. 165-78, Dec. 1996.

[132] P. Collas, “Modulation of plasmid DNA methylation and expression in zebrafish embryos.,” *Nucleic acids research*, vol. 26, no. 19, pp. 4454-61, Oct. 1998.

[133] A. Tsurumi, F. Xia, J. Li, K. Larson, R. Lafrance, and W. X. Li, “STAT Is an Essential Activator of the Zygotic Genome in the Early Drosophila Embryo.,” *PLoS genetics*, vol. 7, no. 5, p. e1002086, May. 2011.

[134] S. R. Porazinski, H. Wang, and M. Furutani-Seiki, “Microinjection of medaka embryos for use as a model genetic organism.,” *Journal of visualized experiments : JoVE*, no. 46, p. e1937, Jan. 2010.

8. Acknowledgements

Foremost, for his advice, help and support, his patience and of course the amusing tales in the evenings I want to thank my supervisor Prof. Manfred Schartl. He made all this possible.

A general "Thank you" goes to every member of the lab I have ever med during the last years. However you contributed to this work, if it was support with an experiment, or just by candy and a joke to the right time, it helped a lot.

Not to forget Toni Wagner who introduced me into the lab and somehow made me stick to it.

Also my two other colleagues in the lab, Eva and Dani, thank you for suffering by my side.

Max and Hannes simply for being guys in a female-dominated environment.

Greetings to my friend Qiang Gan, who made the endless hours in the Virchow-center bearable. Hang on Bro´!

All the other people I med throughout the last years and who gave me a memorable moment. Of course those who I lost to mention, but deserve it by any means.

For the constant support and her unfailing confidence in me I really have to thank my mother

Last, but least, I have to thank my little sister for giving me a nephew and niece who are easy to love, even if you are not related to them.